JAN. - APR. 1996
Volume II Number I

ISSN 0859 144X

THE ASEAN JOURNAL OF RADIOLOGY

Published by The Radiological Society and
the College of Radiologists of Thailand,
Bangkok, Thailand

Supported through an educational grant from

Have you really considered the importance of open MRI on patient comfort?

- for your patients who will return to you?
- for your technicians, who will improve throughput?
- for your radiologists, who will not have to read patient movement artifacts?
- for your administrator, who will see better return on investment?

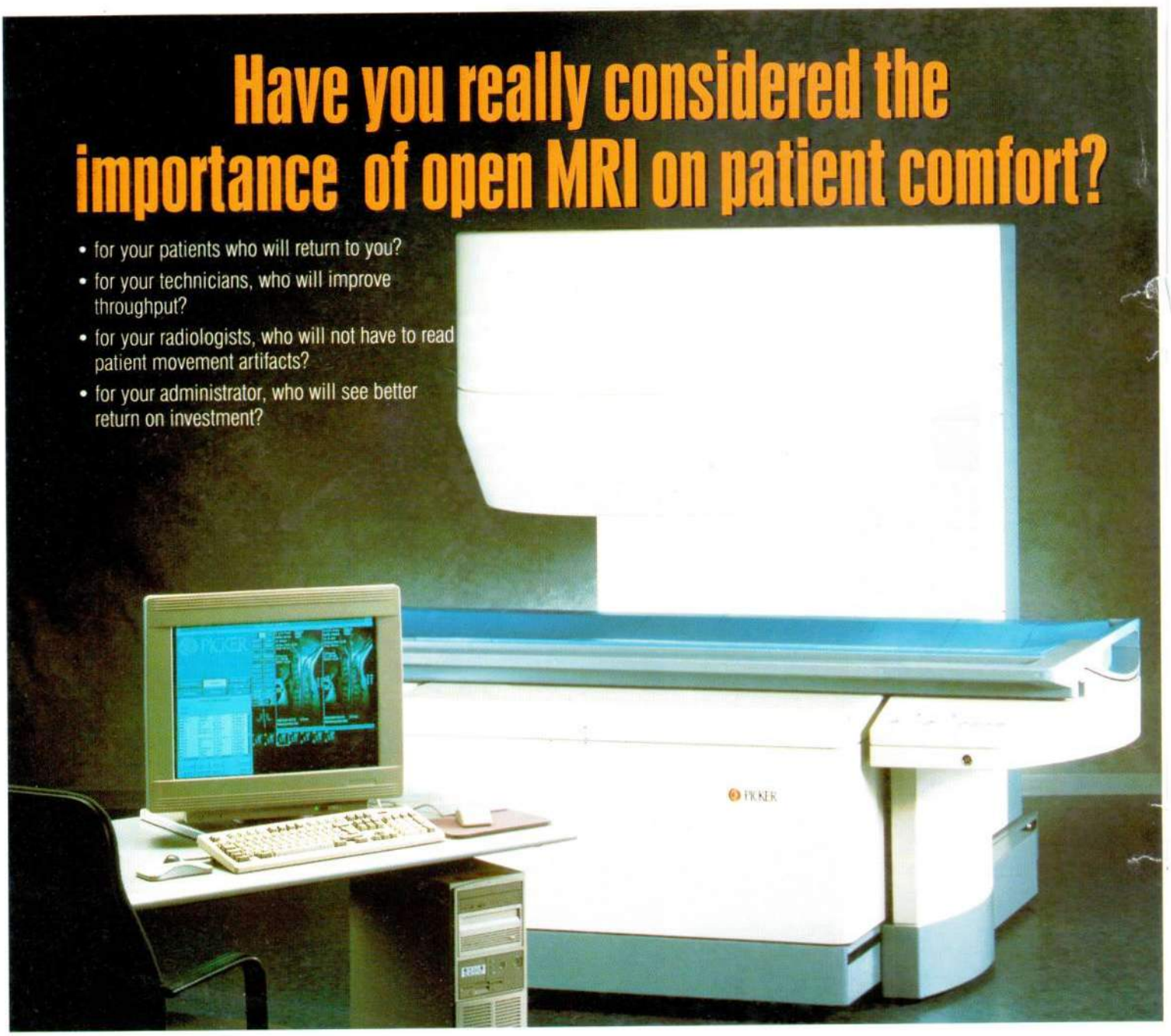

The new OUTLOOK™ in MRI...

Picker's new, really open, state-of-the-art, whole body MRI scanner.

Features include: 46 cm free vertical opening, freedom of patient handling in horizontal plane, easy access to the patient, CP phased array coils, powerful and fast gradients, high quality MR angio with MT, integrated MPR and MIP, and very fast 233 MHz Digital AlphaStation™ 400 console. The most modern open MRI scanner available.

OUTLOOK™ is Picker's newest addition to its impressive line of MRI scanners.
For more information, please contact your nearest Picker representative.

PICKER

Picker International, Inc.
World Headquarters
595 Miner Road
Cleveland, Ohio 44143
U.S.A.
Tel: 1-216-473-3000
Fax: 1-216-473-2413

Picker International, France
GEC S.A.
2, rue Henri Bergson
92600 Asnières
France
Tel: 33-1-46-13-52-54
Fax: 33-1-47-33-11-31

Picker International GmbH
Robert-Bosch-Strasse 11
6238 Hofheim 4 Wallau
Germany
Tel: 49-6122-9140
Fax: 49-6122-8536

Picker International Canada, Inc.
7956 Torbram Road
Brampton, Ontario L6T 5A2
Canada
Tel: 1-950-791-1494
Fax: 1-950-791-7297

Picker International, Inc.
Room 1303
C C Wu Building
302-308 Hennessy Road
G.P.O. Box 15
Wanchai, Hong Kong
Tel: 852-892-1238
Fax: 852-838-4302

Picker International Latin America
110 Merrick Way
Suite 3A
Coral Gables, Florida
33134 U.S.A.
Tel: 1-305-444-9993
Fax: 1-305-445-0545

Picker International GmbH
Mosettigasse 1,
4th floor, A-1232 Vienna
Austria
Tel: (43) 1-6610
Fax: (43) 1-6610760

Picker International Ltd.
Kemble House
Kemble Street
London, WC2B 4 AJ
England
Tel: +44-71-489-4044
Fax: +44-71-489-4043

Picker Singapore
101 Thomson Road,
#10-01 United Square,
Singapore 1130
Tel: (65) 250-9866
Fax: (65) 254-0020

Picker International GmbH
European/Middle East Distribution
Headquarters
Robert-Bosch-Str. 11,
6519 Hofheim
Tel: +49-6122-9140
Fax: +49-6122-914-460

Picker Italia SpA
Vicolo Carloni, 4
I-22055 Merate (Lecco)
Tel: (39)39-9900169
Fax: (39)39-9901016

JAN. - APR. 1996
Volume II Number I

ISSN 0859 144X

THE ASEAN JOURNAL OF RADIOLOGY

Published by The Radiological Society and the College of Radiologists of Thailand, Bangkok, Thailand

Supported through an educational grant from

1. The AAR Journal of Radiology publishes the papers on Radiological Sciences, such as research work, review articles, case reports, innovations in Medical Sciences related to all branches of Radiology, and letters to the editor. The aforementioned materials can be written in English only.

2. The authors have to submit 2 copies of the manuscript and a diskette: **to Prof. Dr. Kawee Tungsubutra,** 318 Kaweevej Hospital, Tarksin Road, Dhonburi, Bangkok 10600, Thailand.
or to the Associate Editors at the Radiological Society of Malaysia, Indonesia, Phillippine, Singapore and Brunei. The names and addresses of the Associate Editors in each country were published in the front page of this Journal.

3. The original copy to be submitted must be typed in a double space on one side of the page of 8″ × 11″ paper.

4. The format of the article must include:

   a. Title page and address of the author (s)

   b. Abstract

   c. Introduction (Background)

   d. Material and Method

   e. Results and discussion (Tables and Illustrations)

   f. Acknowledgement (it any)

   g. References (Follow the Vancouver style developed by ICMJE)

5. We will provide 25 copies of reprints for the author (s) who submit (s) and article for publication in the AAR Journal.

6. The illustrations and tables must be clearly prepared with legends in English as they are the art works to be reproduced.

7. The authors are responsible for the contents of the article as to its facts and findings.

8. Ethics.

Paper reporting studies which might be interpreated as human experimentation (e.g. controlled trials) should conform to the standards of the Declaration of Helsinki (see British Medical Journal 1964:2:177) and should indicate that approval that such studies may proceed has been granted by the local or hospital Ethics Committee.

When reporting experiments on animals indicate whether the institution's or the National Research Council's guide for, or any national law on, the care and use of laboratory animals was followed.

Message from

Prof. Dr. Kawee Tungsubutra

Editor-in-Chief, The Asean Journal of Radiology.

This is the first No of Vol II or the second year of our Asean Journal of Radiology. In this issue the first article is very valuable for the Asean to assess the bone mineral density of the patients whether it is the normal loss due to old age or intercurrent diseases, not only for the Thais but also to all the Asian people in comparison with the Japanese.

The theme of this first number of the second volume is devoted to the diagnoses and treatment of tumours at different parts of the body.It is the mixtures of different methods or techniques in diagnosis and treatment using ionizing radiation including ultrasound and chemotherapy using radiomimetic drugs. Interventional radiology, the rapidly growing specialty in radiology was also presented.

In this issue there are two papers from Malaysia and one paper from Singapore. This is very encouraging for me and the board of editors to have participation from the Asean Countries. We hope to have papers from Philippines, Indonesia and Brunei in the next issue.

With best wishes and happy New Year 1996.

Kawee Tungsubutra

Kawee Tungsubutra
January 1, 1996.

THE ASEAN JOURNAL OF RADIOLOGY

Volume II Number I JAN.-APR. 1996

CONTENTS

		Page
1.	**ASSESSMENT OF BONE MINERAL DENSITY IN NORMAL THAIS** Makumkrong POSHYACHINDA, Tawatchai CHAIWATANARAT.	1-12
2.	**OSTEOSARCOMA WITH HIGH SERUM ALKALINE PHOSPHATASE OVER 500 U/L** Lucksana POCHANUGOOL, Ratana PIRABUL, Daungjai SANGTHAWAN, Supon ONSANIT.	13-17
3.	**COMPARISON OF SURVIVAL OF POST-OPERATIVE IRRADIATION BETWEEN LOW-GRADE GLIOMA, ANAPLASTIC GLIOMA AND GLIOBLASTOMA MULTIFORM** Saipin TANGKARATT.	19-23
4.	**ANGIOSARCOMA OF THE LIVER – A CASE REPORT** Associate Professor C.R. JAYAKUMAR, Dr. Lilius CHUA KIM LIAN.	25-29
5.	**IFOSFAMIDE INDUCED RICKETS WHICH IS REVERSIBLE FOLLOWING TREATMENT** Dr. Chong Aun KEE, Associate Professor C.R. JAYAKUMAR, Dr. Saw LWIN.	31-35
6.	**AMNIOTIC BAND SEQUENCE - A REVIEW OF ARTICLES WITH DEMONSTRATION OF A CASE** Patchrin PEKANAN, Boonchuay SATHAPATAYAVONGS.	37-38
7.	**LYMPHEDEMA (NONNE-MILROY TYPE) - A CASE DEMONSTRATION** Patchrin PEKANAN, Boonchuay SATHAPATHAYAVONGS.	39-40
8.	**PARASPINAL HEMORRHAGE FROM WHOOPING COUGH A CASE DEMONSTRATION** Patchrin PEKANAN, Boonchuay SATHAPATAYAWONGS, Siripan VONGSHABSHI.	41-42
9.	**MAGNETIC RESONANCE IMAGING IN SOFT TISSUES MASSES OF THE MUSCULOSKELETAL SYSTEM** Dr. M A Png, Dr. T S G Chee.	43-50
10.	**THE PREOPERATIVE DIAGNOSIS OF PRIMARY ALDOSTERONISM BY THIN-SECTION COMPUTED TOMOGRAPHY** Malai MUTTARAK, Saowalak DEEWIJIT.	51-53
11.	**AGGRESSIVE FIBROMATOSIS OF THE EXTREMITIES** Patchrin PEKANAN, Sopon KUMPOLPUNTH, Boonchuay SATHAPATAYAVONGS, Pimjai SIRIWONGPAITRAT, Sirikan WONGSRISOONTORN.	55-61

ASSESSMENT OF BONE MINERAL DENSITY IN NORMAL THAIS

Makumkrong POSHYACHINDA[1], Tawatchai CHAIWATANARAT[1]

ABSTRACT

Bone mineral density (BMD) of anterior and lateral lumbar spine and femoral neck were studied in 301 normal healthy subjects (205 women and 96 men; age range, 20-84 years) utilizing dual energy x-ray absorptiometer (DEXA). In normal women, bone mass was increased with age and peaked around age 35 at all three scanning sites. Bone diminution began about the age of 40 and the loss was accelerated after age 50. The average rate of loss upto age 75 was 0.8% per year at all sites. In normal men, the pattern of bone diminution with age was different from women. Bone diminution from vertebrae and femoral neck began in young adulthood and were linear. The rate of decrease in BMD was two-thirds of that in women for femoral neck but was only one-fifth of that in women for anterior lumbar spine. Mean BMD in women was less than men at all three scanning sites.

Key Words : Bone mineral density, Bone mass, Bone densitometer, Dual energy x-ray absorbtiometer.

INTRODUCTION

Bone mineral density (BMD) and bone strength change throughout life. Density increases during growth, especially in adolescence, continue to increase in young adulthood and peaks around age 30. After skeletal maturity is reached, bone loss begins and persists until age 85 to 90 years. The loss is attributed to an imbalance in skeletal remodeling, in which the rate of bone formation is less than that of bone resorption. The influences of heredity, race and sex on incidence of osteoporosis appear to reflect their effects on peak bone density. Differences in peak bone density at skeletal maturity also may account for racial and sex differences in the incidence of osteoporosis. Therefore osteoporosis varies widely among ethnic groups, regions and nations (1).

Osteoporosis is a major community health problem affecting upto half of the elderly female population in most western countries (2-5). Osteoporosis reflects the inadequate accumulation of bone tissue during growth and maturation, excessive losses thereafter or both. When bone tissue is reduced in amount, the likelihood of fracture is increased.

[1] Division of Nuclear Medicine, Department of Radiology, Faculty of Medicine, Chulalongkorn University, Rama IV Road, Bangkok 10330 Thailand.

For correspondance :
M. POSHYACHINDA
Division of Nuclear Medicine, Department of Radiology, Faculty of Medicine, Chulalongkorn University, Rama IV Road, Bangkok 10330 Thailand.

Currently the available data indicate a significant inverse relationship between bone mass and fracture incidence and it is no longer meaningful to require the presence of fracture to diagnose osteoporosis since an osteoporotic patient was at risk of fracture long before the fracture event, therefore measurement of bone mass provide the single best test for assessing the risk of subsequent fracture (6).

A variety of techniques have been developed to quantify bone density, among these, Quantitative digital radiography (QDR), also known as Dual-energy x-ray absorptiometry (DEXA) has the ideal properties of obtaining precise measurements in a short time with very low radiation exposure (5,7-10).

The objective of the present study is to establish a range of bone density from normal healthy Thais which will be served as normal reference for our clinical services.

MATERIALS AND METHODS

Subjects

Healthy volunteers with the age of 20 and above were studied. A detailed social history was obtained from all volunteers in order to analyse risk factors. The inclusion and exclusion criteria for selection of studied population were as follows:

Inclusion criteria

Thais who were born and live in Thailand, healthy and fully mobile. Body mass index (BMI) are between 18-28. Non smoking.

Exclusion criteria

History of prolonged bed rest (over 4 weeks).

Current medication including contraceptive pill or stop medication less than on month.

On calcium, vitamin D supplement.

On hormone replacement therapy at any time.

Presence of chronic illness including diabetes mellitus, hypertension, Thyroid disease, hyperparathyroidism.

History of steroid administration.

Daily alcohol intake.

History of x-ray contrast media administration or radionuclide study one week prior to present study.

In addition to the above criteria, pregnant, or lactating women, women with history of amenorrhea, premature ovarian failure, hysterectomy, öovarectomy or other ailment likely to affect bone metabolism were also excluded.

Method

Boty weight and height were recorded in all subjects and BMI were calculated.

Serum calcium, phosphate, haematocrit and MCV were determined whenever possible.

BMD of anterior lumbar spine at L_1 to L_4, lateral lumbar spine at L_2 to L_4 and left hip of all subjects were measured using a DEXA system (Hologic QDR-2000). The results of BMD at each site was expressed as $g/cm.^2$ For the hip, only BMD of femoral neck was analysed. The precision of these measurements in our laboratory is 0.41% for anterior lumbar, 0.76% for lateral lumbar and 0.89% for femoral neck.

Statistical analysis

The relation between BMD and age of male and female volunteers were separately analysed by using linear regression. The independent variables (height, weight) in relation to the dependent variable (BMD) was assessed by multiple linear regression analysis.

For establishing normal limits, the lower 5th percentile and upper 95th percential from appropriate regression equation was estimated.

The study was approved by the Chulalongkorn hospital Research ethics committee.

RESULTS

A total of 301 healthy volunteers, 205 women and 96 men, with the age range from 20-84 year-old were studied. The haematocrit, MCV, serum calcium and serum phosphate were determined in 140 subjects (84 women, 56 men) and they were within normal limits (Table 1).

The mean BMI for females and males was 22.5 and 23.2 respectively. There is significant effect of weight on BMD of anterior lumbar spine and femoral neck in both sexes but significant effect of height was only on femoral neck in both males and females (Table 2).

Table 1 Results of and blood examination

	Hct		MCV		Calcium		Phosphate	
	Female	Male	Female	Male	Female	Male	Female	Male
Mean	38.8	44.7	87.0	90.1	9.3	9.4	3.4	3.1
SD	2.7	2.8	7.2	6.5	0.6	1.1	0.5	0.5
Range	31-50	38-50	68-100	71-100	7.4-11	7.8-11	2.4-4.6	2.4-4.6

Table 2 Assessment of independent variable on BMD

	Women		Men	
	Lumbar	Femoral neck	Lumbar	Femoral neck
Weight	P<0.01	P<0.001	P<0.03	P<0.000
Height	P=0.056	P<0.005	P=0.056	P<0.000

The results of BMD determination at anterior and leteral lumbar spines and femoral neck in 205 women and 96 men are shown in Figs. 1-6. In normal women, BMD increase from age 20 and peaking around age 35 years at both anterior and lateral lumbar spines and femoral neck (Figs. 1-3). After age 40 years, bone diminution with aging occurred at all three scanning sites. Accelerated bone loss was observed between age 50 to 65 years, after that the diminution of bone mass wass less at all sites.

In normal men, bone diminution were observed at the age of 20 onward at all 3 scanning sites and the decline in BMD with aging was linear at all sites. The bone diminution was more rapid at the femoral neck (Fig. 4), less so at lateral lumbar spine (Fig. 5) and minimal at anterior lumbar spine (Fig. 6). There are certain different pattern of age regression of BMD between both sexes, bone loss in women was more accelerated than men at all sites (Fig. 7-9). The BMD of the femoral neck in women was lower than men throughout life but the BMD at the vertebrae in women during age 30-50 years was somewhat similar to men of the same age, after that bone loss in women was much more rapid. The mean of peak bone mass at each site for women and men is shown in Table 3.

Table 3 Peak BMD of lumbar spine and femoral neck

Site	BMD (g/cm^2)	
	Women (Mean + SD)	Men (Mean + SD)
Lumbar spine		
Anterior	0.987 + 0.089	1.030 + 0.081
Lateral	0.807 + 0.076	0.933 + 0.062
Femoral neck	0.810 + 0.087	0.973 + 0.097

In order to set a cutoff value for the purpose of diagnosis of osteoporosis, the value of BMD that is more than 2.5 SD below the young adult mean value was adopted (11) as shown in Table 4.

Table 4 Cutoff value for diagnosis of osteoporosis

	BMD (g/cm^2)	
	Women	Men
Lumbar spine		
Anterior	0.765	0.828
Lateral	0.617	0.778
Femoral neck	0.593	0.732

Comparison of BMD between our studied population, and Japanese population which was used as normal reference by the manufacture of our DEXA (Hologic) was attempted. We found slightly lower BMD in Thai women as compared to Japanese women at both lumbar spine and femoral neck and the bone mass was peaked earlier in Japanese women (Fig. 10-11). The BMD of Thai men was also slightly lower than Japanese men at lumbar spine (Fig. 12-13).

DISCUSSION

From our study, bone mass at axial and appendicular skeleton in normal women was similarly peaked at age 35 years, started to loss at age 40 years and the loss was accelerated at age 50 years which corresponded to the average menopausal age of 49.5 ± 3.6 years in Thai women (12). The age at peak bone mass and at the beginning of bone deminution in our study is somewhat similar to British women (13) but unlike Japanese population where the bone mass was peaked around 30 years old. The average peak bone mass in our study was 0.987 g/cm^2 which is slightly lower than the value of 1.06 g/cm^2 found in British women by Hall el al (13). The BMD of lumbar spine and femoral neck were also slightly lower than Japanese women.

A biphasic pattern of bone loss has been identified for both cortical and trabecular bone : a protracted slow phase that occur in both sexes and a transient accelerated phase that occurs in women after menopause (4). Our study also revealed similar pattern of bone loss for both cortical and trabecular bones in normal women. However data on trabecular bone loss from the axial skeleton are conflicting, some shows a linear decrease bone loss begining in young adulthood (14,15) and some have found evidence of an accelerated phase of bone loss following menopause (16,17).

For men, the peak BMD at anterior lumbar spine in our study is slightly less than Japanese populations. Bone diminution with aging at the femoral neck and the vertebrae was linear which is similar to Japanese men and other reports (18,19). However the BMD at the vertebrae fell much less rapid than the femoral neck which is in agreement to one report (18) but in contrast to other report (19).

By age 70 years, the age regression for BMD of anterior and lateral lumbar spine and femoral neck in women had decreased to a level below 2SD of peak bone mass. Similar findings were found in normal men except the anterior lumbar spine which had much less bone diminution with advancing age. The rate of decrease in BMD of anterior and lateral lumbar spine and femoral neck in women at age 75 years was 23%, 27% and 23% respectively or in average of 0.8% per year at all sites while in men the decrease rate at the same age was 8%, 21% and 26% or in average of 0.15% per year for anterior lumbar spine, 0.4% per year for lateral lumbar and 0.5% per year for femoral neck, Thus the rate of decrease in BMD for men was two-thirds of that in women for femoral neck, one-

half for lateral lumbar spine but was only one-fifth of that in women for anterior lumbar spine. These findings ar somewhat similar to other report which explained that why the female/male ratio is 2:1 for hip fractures but 8:1 for vertebral fractures (18).

In conclusion, the bone mass was peaked around age 35 years old for both trabecular and cortical bones in normal women and began tc loss bone mass at age 40 with accelerated loss after age 50 For normal men, the pattern of bone loss with age was different from women and the mean BMD was higher. Bone diminution with aging was linear for both vertebral and cortical bones and the rates of loss were less than women at all sites especially at lumbar spine where bone diminution with aging was minimal.

REFERENCE

1. Peck WA, Riggs BL and Bell NH. The biology of bone. In Physician's resource manual on osteoporosis. A decision-making guide. Published by National Osteoporosis Foundation. USA 1987, P. 2-5.
2. Stevenson JC and MI Whitehead. Post menopausal osteoporosis. Br. Med J 1982; 285: 585-588.
3. Nordin BEC, Horsman A, Crilly RG, Marshall DH and Sympson M. Treatment of spinal osteoporosis in postmenopausal women. Br. Med J 1980; 280: 451-454.
4. Spector TD, Cooper C and Fenton Lewis. Trends in admission for hip fracture 1968-1985 in the U.K. Brit Med J 1990; 300: 1173-1174.
5. WHO Technical Report Series : 843, WHO Study group on assessment of fracture risk and its application to screening for postmenopausal osteoporosis, Rome, 22-25 June 1992.
6. Wasnich RD. Bone mass measurements in diagnosis and assessment of therapy. Amer J Medicine 1991; 91 (suppl 5B): 54s-58s.
7. Siberstein EB. Update on the diagnosis and therapy of osteoporosis. Nucl Med Annual. New York. Raven Press 1988; 209-243.
8. Fogelman I. Bone scanning in osteoporosis : The role of radionuclide bone scan and photon absorptiometry. Nucl Med Annual. New York. Raven Press 1990; 1-37.
9. Genant HK, Faulkner KG and Gluer CC. Mesurement of bone mineral density : Current status. Proceedings of a Symposium on osteoporosis. Am J Med 1991; 91 (5B): 49-53.
10. Svendsen OL, Marslew U, Hassagar C and Christiansen C. Measurement of bone mineral density of the proximal femur by two commercially available dual energy x-ray absorptiometric system. Eur J Nucl Med 1992; 19: 41-46.
11. Kanis JA, Melton LJ, Christiansen C, Johnston CC, Khaltabv N. Perspective. The diagnosis of osteoporosis. J Bone Min Res 1994; 9 (3): 1137-1141.
12. Chompootweep S, Tankeyoon M, Yamarat K, Pumsuwan P, Dusitsin N. The menopausal age and climateric complaints in Thai women in Bangkok. Maturitas 1993; 17: 63-71.
13. Hall ML, Heavens J, Cullum ID, Ell PJ. The range of bone density in normal British women. Brit J Radiol 1990; 63: 266-269.
14. Riggs BL, Wahner HW, Dunn WL, Mazess RB, Offord KP, Melton LJ. Differential changes in bone mineral density of the appendicular and axial skeleton with aging. Relationship to spinal osteoporosis. J Clin Invest 1981; 67: 328-335.
15. Riggs BL, Wahner HW, Melton LJ III, Richelson LS, Judd HL, Offord KP. Rates of bone loss in the axial and appendicular skeletons of women : evidence of substantial vertebral bone loss prior to menopause. J Clin Invest 1986; 77: 1487-1491.
16. Krolner B, Pors Nielsen S. Bone mineral content of lumbar spine in normal and osteoporotic women : cross sectional and longitudinal studies. Clin Sci 1982; 62: 326-329.
17. Genant HK, Cann CE, Ettinger B, Gordon GS. Quantitative computed tomography of vertebral spongiosa : a sensitive method for detecting early bone loss after oophorectomy. Ann Intern Med 1982; 97: 699-705.
18. Riggs BL, Wahner HW, Seeman E, et al. Changes in bone mineral density of the proximal femur and spine with aging. Differences between the postmenopausal and senile osteoporosis syndromes. J Clin Invest 1982; 70: 716-723.
19. Meier DE, Orwoll ES, Jones JM. Marked disparity between trabecular and cortical bone loss with age in healthy men : measurement by vertebral computed tomography and radial photon absorptiometry. Ann Intern Med 1984; 101: 605-612.

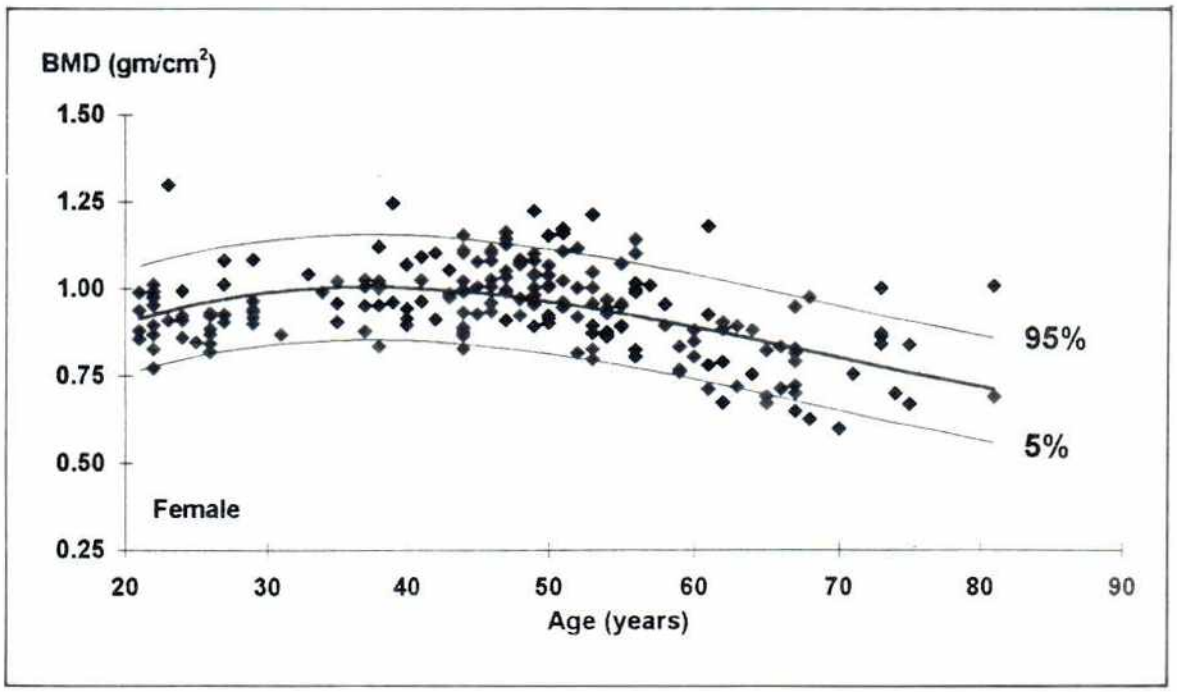

Fig. 1 Regression of BMD of anterior lumbar spine on age in 205 normal women (◆). The upper and lower lines represent 90% confidence limits.

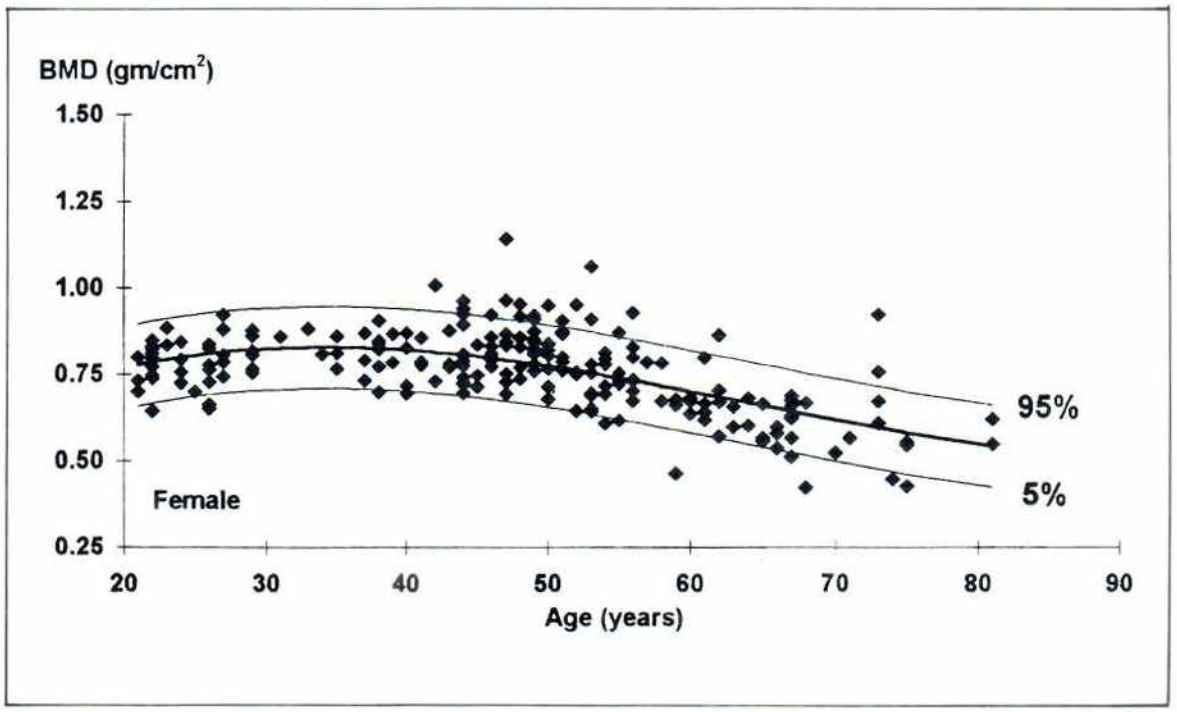

Fig. 2 Regression of BMD of lateral lumbar spine on age in 205 normal women (◆). The upper and lower lines represent 90% confidence limits.

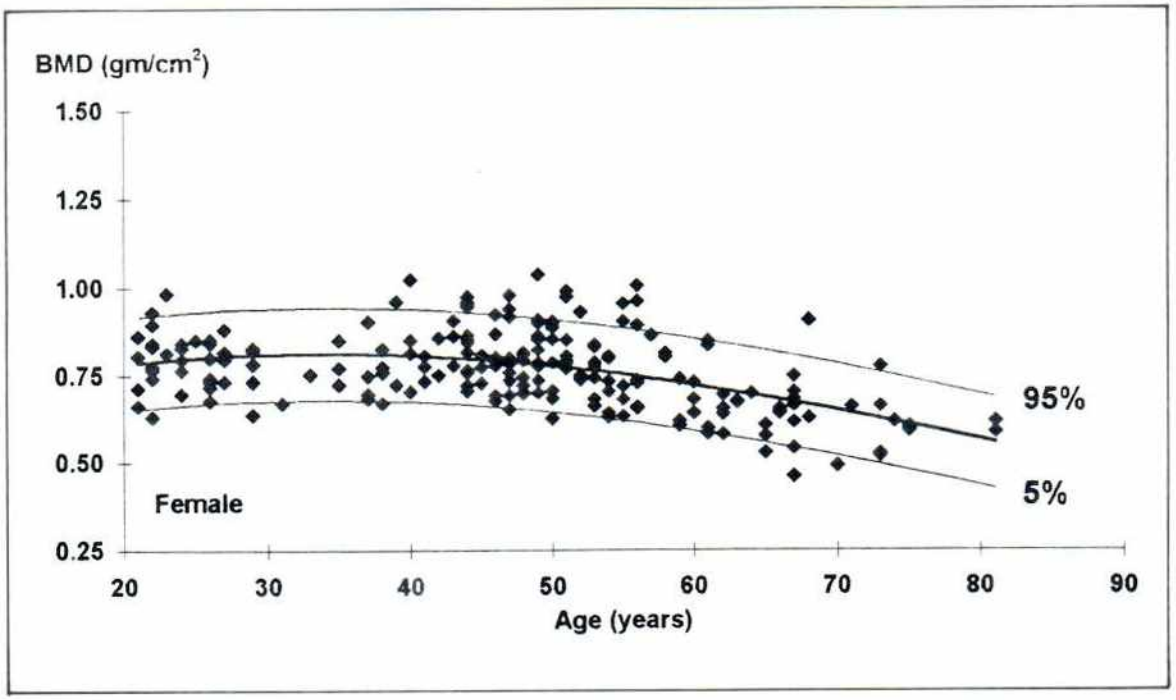

Fig. 3 Regression of BMD of femoral neck on age in 205 normal women (◆). The upper and lower lines represent 90% confidence limits.

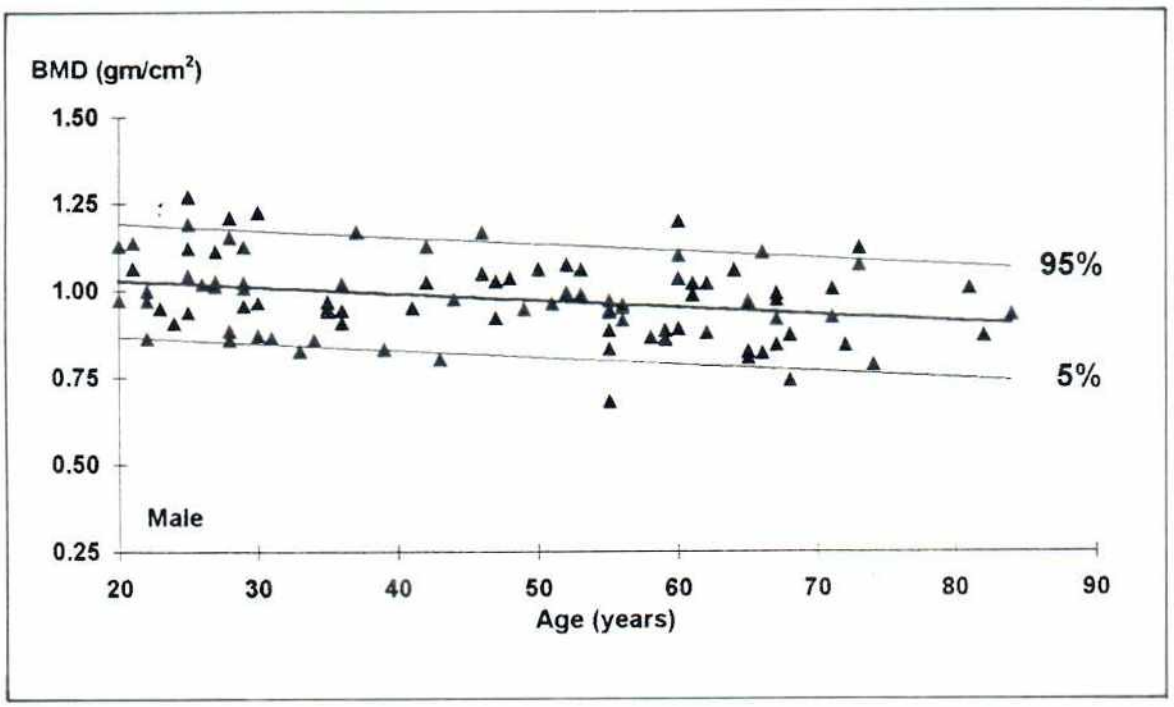

Fig. 4 Regression of BMD of anterior lumbar spine on age in 96 normal men (▲). The upper and lower lines represent 90% confidence limits.

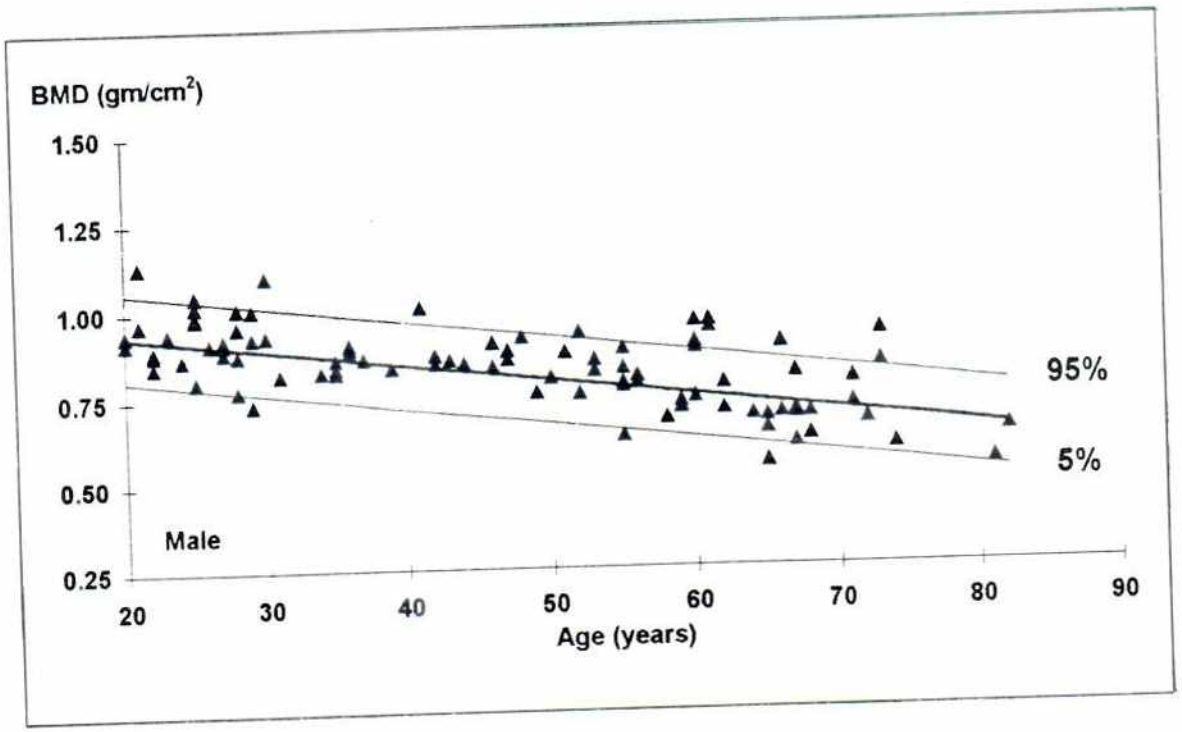

Fig. 5 Regression of BMD of lateral lumbar spine on age in 96 normal men (▲). The upper and lower lines represent 90% confidence limits.

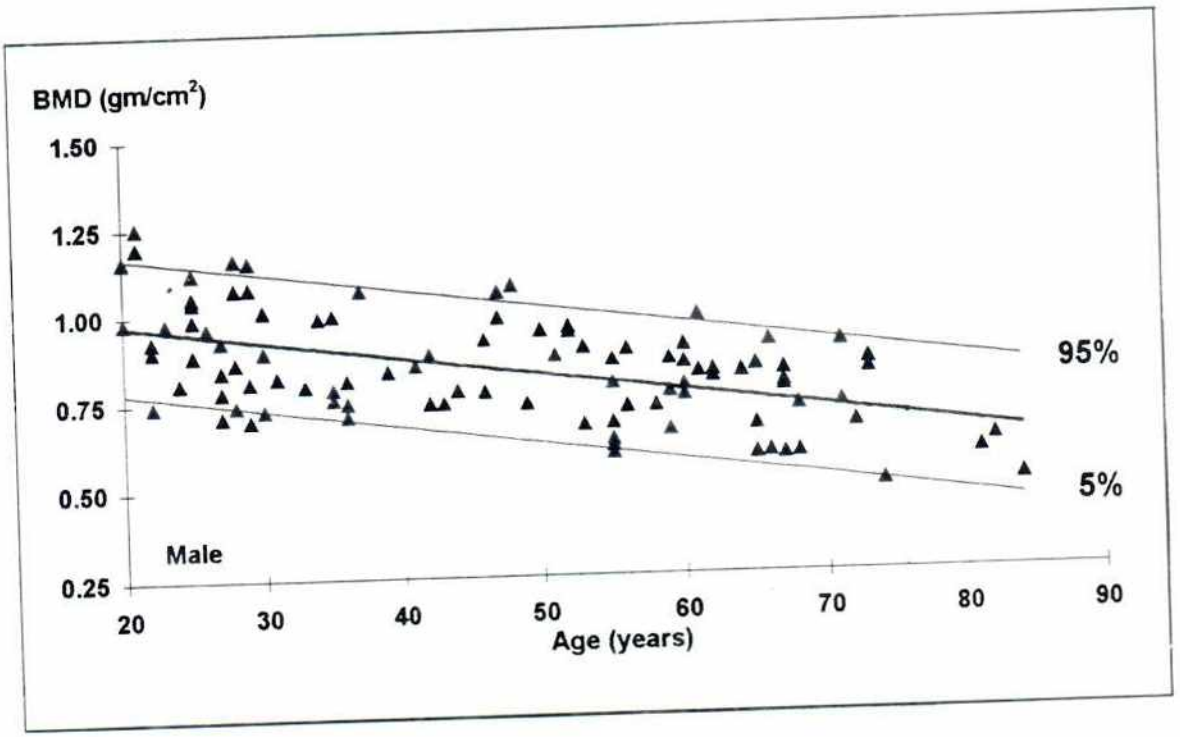

Fig. 6 Regression of BMD of femoral neck on age in 96 normal men (▲). The upper and lower lines represent 90% confidence limits.

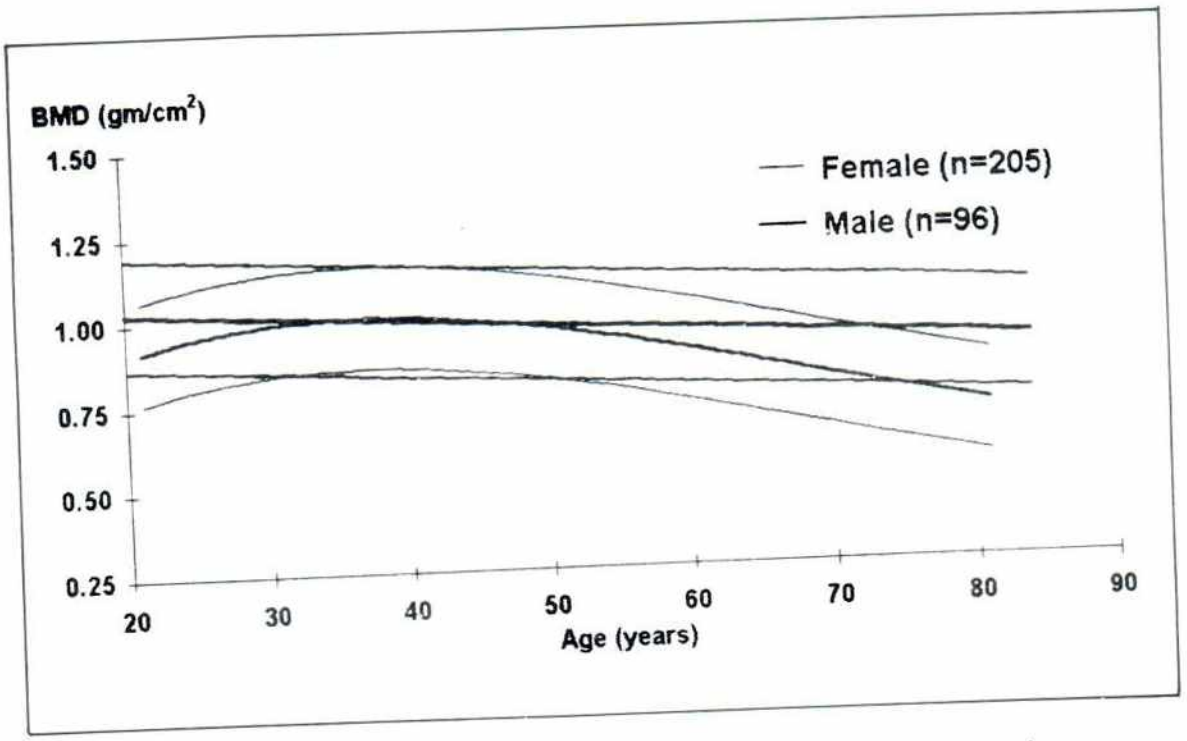

Fig. 7 Age regression of BMD of anterior lumbar spine in normal men and women. Central lines of each group is age regression and upper and lower lines represent 90% confidence limits.

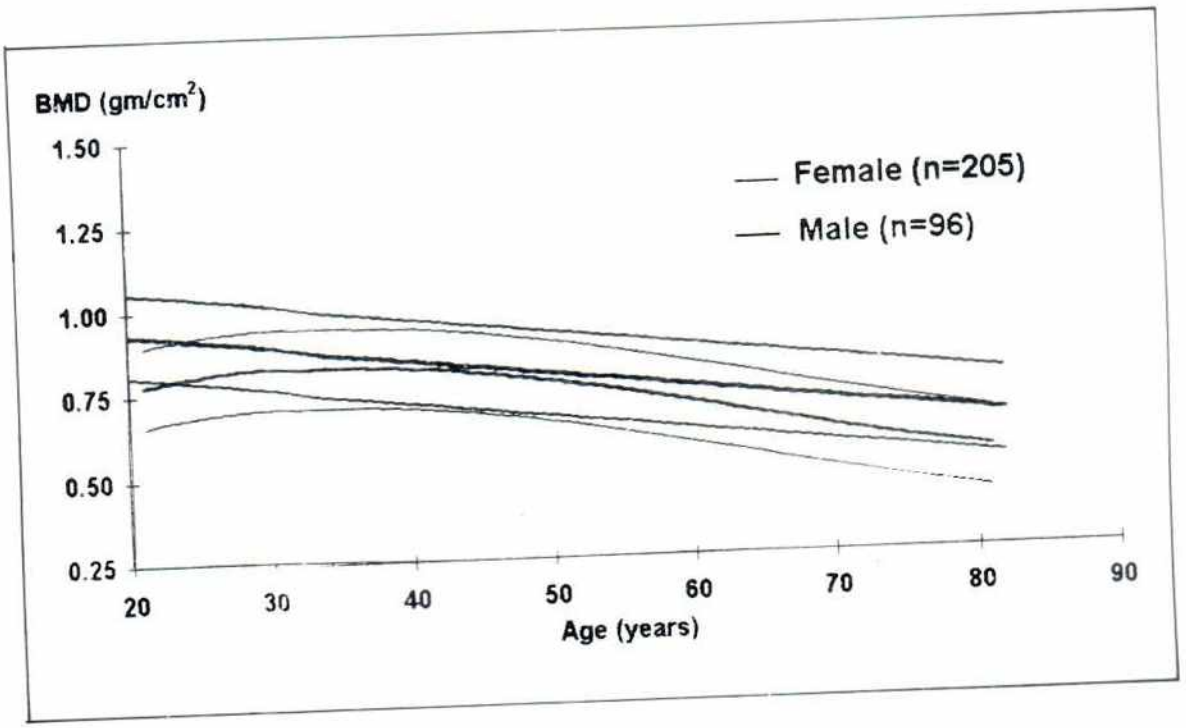

Fig. 8 Age regression of BMD of lateral lumbar spine in normal men and women. Central lines of each group is age regression and upper and lower lines represent 90% confidence limits.

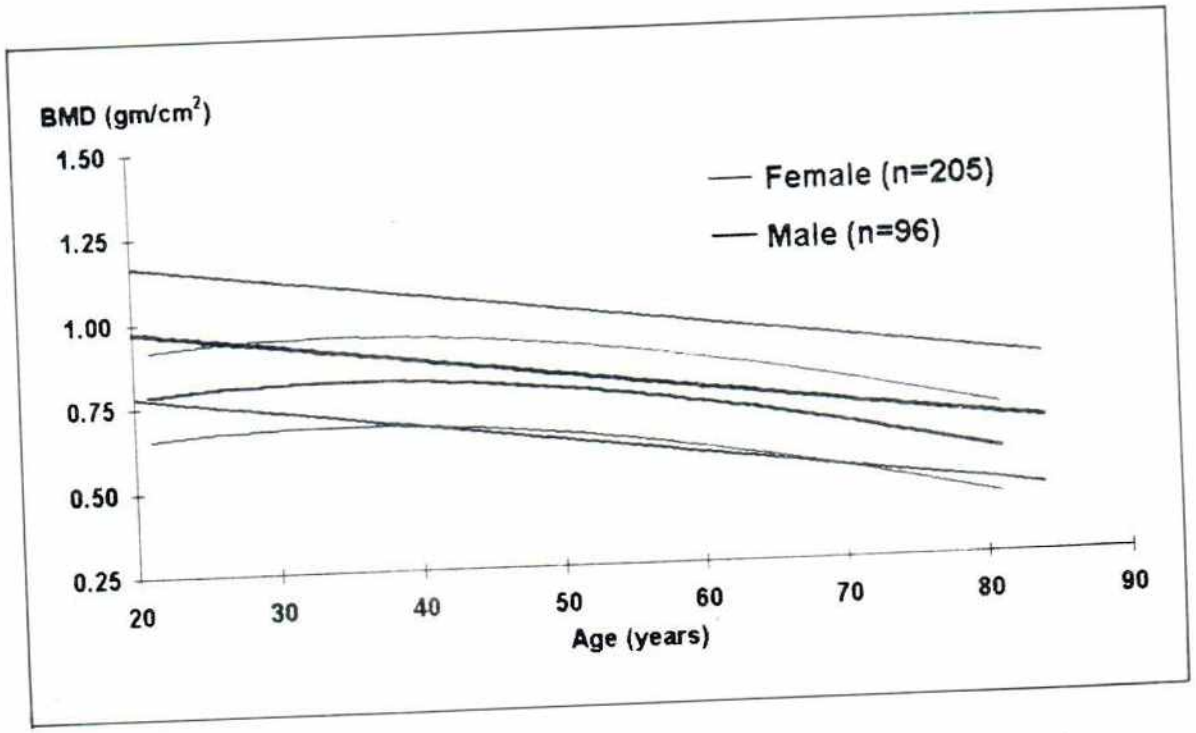

Fig. 9 Age regression of BMD of femoral neck in normal men and women. Central lines of each group is age regression and upper and lower lines represent 90% confidence limits.

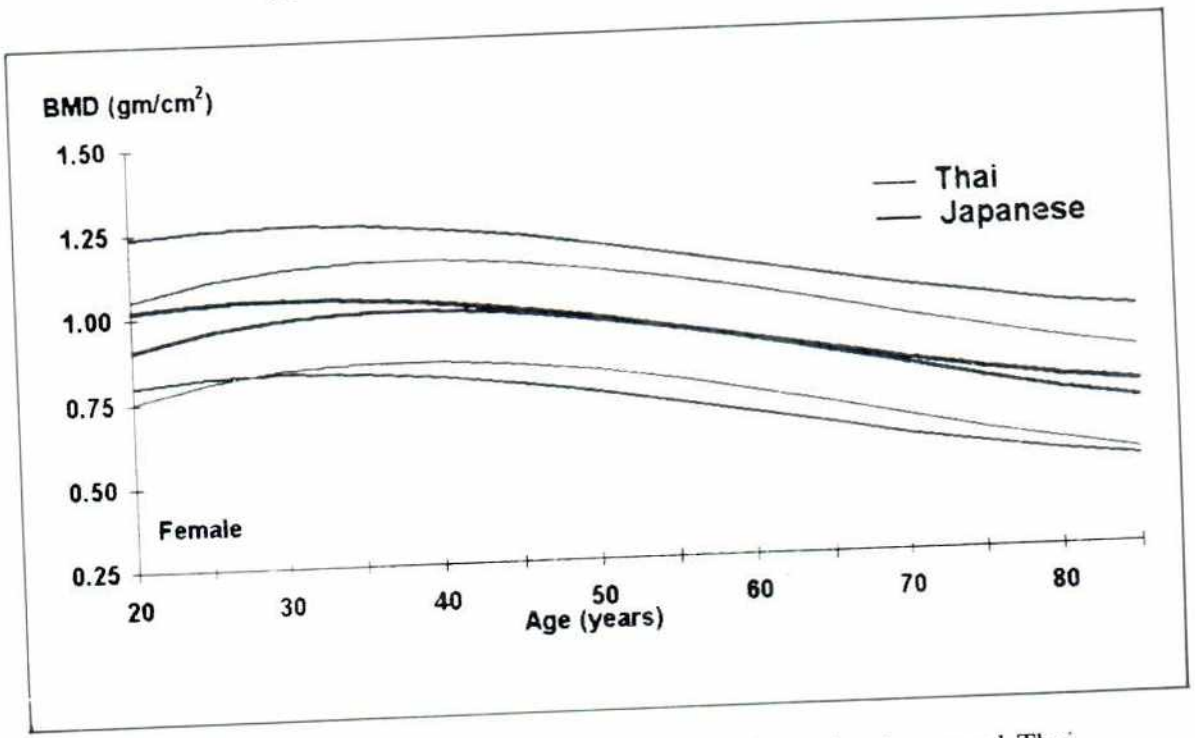

Fig. 10 Age regression of BMD of anterior lumbar spine in normal Thai and Japanese women. Central lines of each group is age regression and upper and lower lines represent 90% confidence limits.

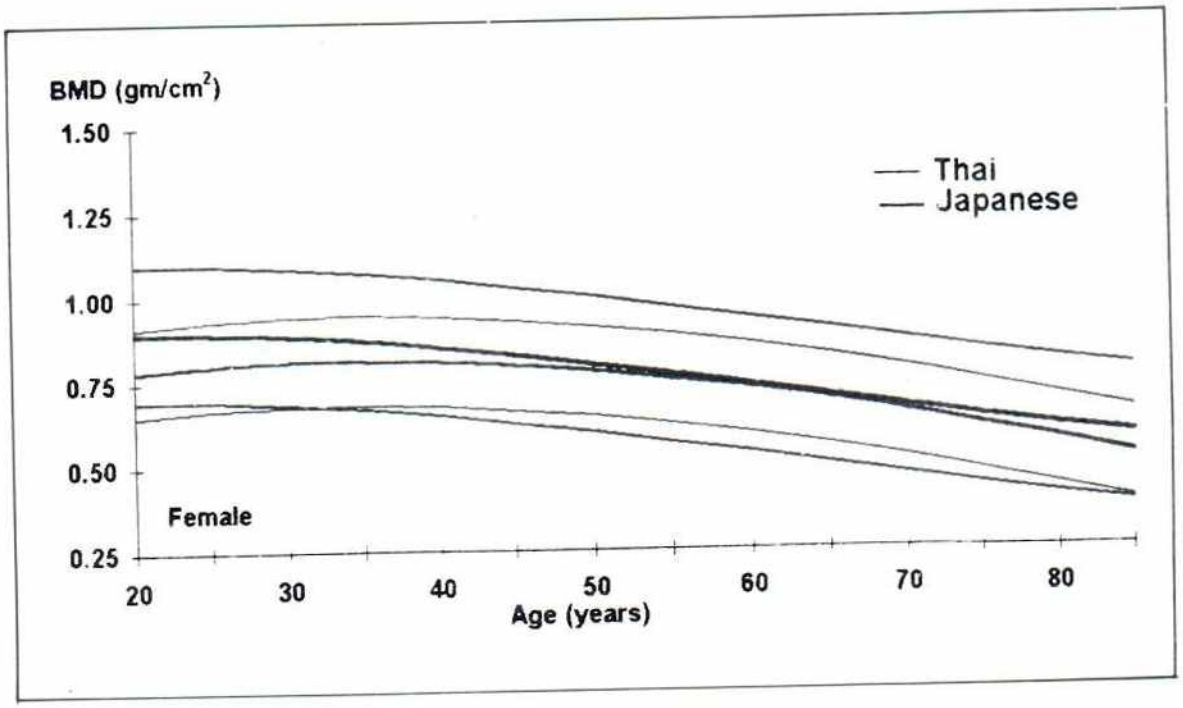

Fig. 11 Age regression of BMD of femoral neck in normal Thai and Japanese women. Central lines of each group is age regression and upper and lower lines represent 90% confidence limits.

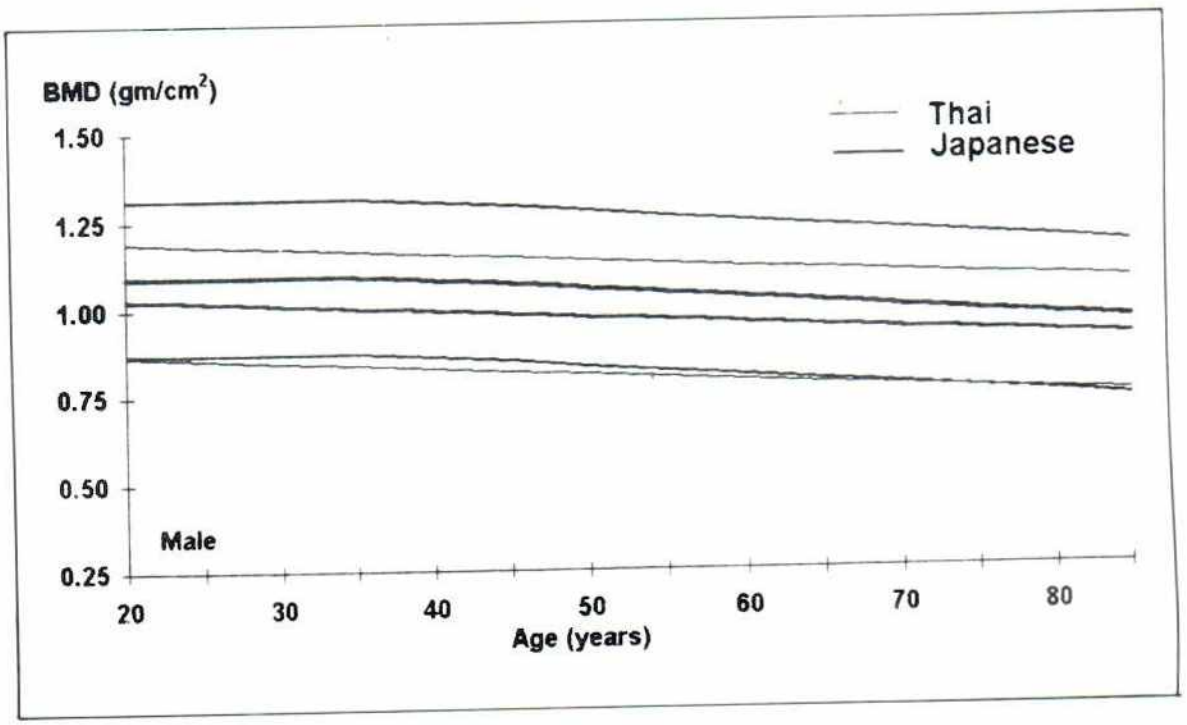

Fig. 12 Age regression of BMD of anterior lumbar spine in normal Thai and Japanese men. Central lines of each group is age regression and upper and lower lines represent 90% confidence limits.

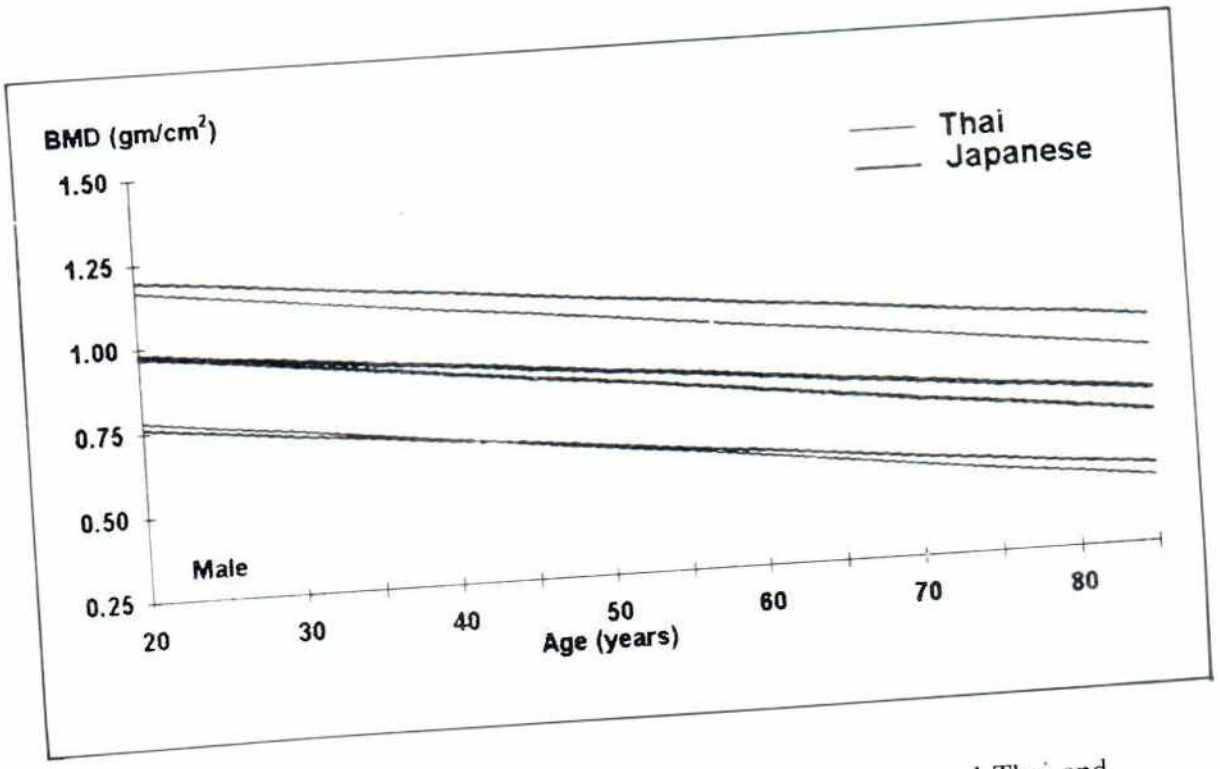

Fig. 13 Age regression of BMD of femoral neck in normal Thai and Japanese men. Central lines of each group is age regression and upper and lower lines represent 90% confidence limits.

OSTEOSARCOMA WITH HIGH SERUM ALKALINE PHOSPHATASE OVER 500 U/L

Lucksana POCHANUGOOL, Ratana PIRABUL,
Daungjai SANGTHAWAN, Supon ONSANIT

ABSTRACT

Twenty two cases of primary osteosarcoma of the bone out of 125 total cases (17.6%) were detected to have over 500 U/L of serum alkaline phosphatase level (AP), which was a very high level as compared to the normal range of 40-105 U/L. There were 13 cases (59.09%) with metastatic disease or terminated by other courses. Only two patients in this group still survive more than 86 and 17 months. Their initial AP were not the highest. The level gradually increased after intraarterial chemotherapy and suddenly turned to normal level after radiation and surgery of the primary bone tumor. In the group of 32 long term survivors among the 125 cases, 13 cases had normal range of AP, only 2 cases had AP over 400 IU. This study, we concluded that if initial serum alkaline phosphatase was over 500 U/L, the disease was more aggressive and tended to metastasize. So different approaches in this group of patients may lead to longer survival.

INTRODUCTION

Elevation of serum alkaline phosphatase in patients with primary osteosarcoma of the bone was observed in less than 50 to 56.4 percent. (1-2) The serum alkaline phosphatase value generally reflects a tendency to new bone formation. The significantly increased level tends to decline to normal level following removal of the primary tumor, or radiation therapy, due to the devitalization of the tumor osteoblast producing the enzyme and a physiological detoxification of circulating enzyme by the liver. (3) The serum AP level always increases when either bone or lung metastasis is detected. There were no previous report mentioned about the information of the patient with the very high serum AP levels. This study reported the nine years experience about the status and the course of disease in 22 osteosarcoma cases who had serum AP level of more than 500 U/L.

MATERIAL AND METHOD

From March 1986 to March 1995, a 125 cases of primary osteosarcoma of the bone were admitted to the Faculty of Medicine, Ramathibodi Hospital. Of these, one hundred and twenty patients had serum alkaline phosphatase levels (AP) recorded. All valued were in International unit with the follow up AP levels except in 16 cases, the values were recorded only once during treatment. All these 16 patients either refused any treatment or lost to follow up after incomplete treatment. Thirty four out of 120 patients (28.3%) had normal or borderline levels of serum AP. The remaining 86 cases had elevated levels, only 22 cases who had the level of serum AP higher than 500 International units, (ranging from 531-5400 U/L) were recruited for this study. Treatment consisted of preoperative intraarterial infusion of cisplatin combined with intravenous chemotherapy, with or without

Department of Radiology, Faculty of Medicine, Ramathibodi Hospital.

local irradiation, surgery and prophylactic whole lung irradiation, treatment details were given elsewhere. (4-9)

RESULTS

Among these 22 cases, high initial serum AP was observed in 15 cases. One woman with 143 U/L of AP at the beginning, the level increased to 1140 U/L when she developed lung metastasis 16 months after initial diagnosis. She refused to have her limb amputated and was lost to follow up after 3 courses of intraarterial chemotherapy. She was hospitalized again with lung metastasis with high AP level (case No 5). Other 6 cases had increasing AP level during the course of treatment, all after chemotherapy. Among these patients, all except two, the serum AP level returned to normal after radiotherapy or surgery or combined treatment. Among the two, one had the AP level decreased after another course of chemotherapy (case No 12) while the level of the other is still high after another course of chemotherapy and lost to follow up probably because of dead due to poor general condition and having a very advanced disease (case No 19). Other 4 cases, metastatic disease were detected when the serum AP level increased, 2 metastasized to the lung and 2 to the bone (Table 1 & 2).

For the status of these 22 cases, only 2 patients survived more than 86 and 17 months with a very good health and performance. The first patient, with scapula osteoblastic osteosarcoma, had 90 percent residual tumor after 6 courses of intraarterial cisplatin. He still survives without local recurrence or distance metastasis after 86 months, his serum AP level increased from 2300 IU to 5400 IU after chemotherapy and dropped to 102 U/L after surgery, the level at last follow up was 29 U/L. His erythrocyte sedimentation rate (ESR) dropped from 65 mm/hr. in the past 7 years to 29 mm/hr. in the last visit (case No 1). The other girl with high grade osteosarcoma of distal femur, had her AP level dropped from 1083 IU to 57 IU after radiation and surgery (case No 2). One patients (case No 6) with pelvic chondroblastic osteosarcoma had dramatically decreased in the level of serum alkaline phosphatase after 30 Gy local irradiation (1390 unit to 282 unit)

After treatment, 4 patients had lung metastasis, one also had bone metastasis in addition, the others had local recurrence. In 4 cases, the AP level decreased when intraarterial chemotherapy was started and returned to normal level but increase again when lung metastasis or local recurrence developed. Another female patient during the course of treatment, her AP level was just 66-143 U/L but rose to 1140 U/L when she had lung metastasis. While the patient developed bony metastasis, the AP level tended to increase as well. In one patient, the AP level was 3965 U/L initially but decreased to a level of 270 U/L after treatment, the level had raised up to 1775 U/L when bony metastasis was detected.

Two patients did not survive even their AP level dramatically droped from 1056 to 106 and 531 to 63 after treatment respectively.

For the overall results, there were a total of 6 lung and 4 bony metastases. One patient had both lung and bone metastases and the other had lung, bone and cord metastases, while one had local recurrence (Table 2). Eight out of 22 cases had already terminated. One had stable lung lesion after treatment. There were 9 cases which were lost to follow up, 5 with metastatic diseases either only lung lesion or combined with bone metastases, so all of these may be already dead. The other two with high AP level refused treatment after diagnosis.

DISCUSSION

For the total of 120 cases whose serum AP was measured the elevation of serum AP was observed in 86 cases (71.67%). There were only 22 cases with very high level over than 500 U/L. Eight cases (36.36%) in this group had already died. Other 5 cases were suspected to be dead due to metastatic diseases. In the 125 cases of osteosarcoma with AP level studies, 49 cases had lung metastases, 5 bony metastases and 11 multiple metastases with 4 local recurrences.

The reason we set the high level of AP to be over 500 U/L is due to the fact that in normal adolescent during the "growth spurt" with increased osteoblastic activity the serum AP level may also increase by as much as two to threefold that of the normal range, but not over fivefold. (2) Again in condition of bony fracture, serum AP level can also increase to as much as double or triple for a period of several months but not over fivefold. (10)

After surgical removal of markedly bone forming osteosarcoma, the serum AP value returns to normal in a few days. Unless the patient is in a "growth spurt", a renewed rise in AP level is an ominous sign signifying probable recurrence or metastasis. (11) In 1966, McKenna et al described a study of 48 patients in which 79% showed an elevation in the serum AP level 3 months before recurrence or metastasis became

clinically obvious. Serum AP level can be a valuable prognostic indicator of the outcome as well as of effective modes of therapy, such as when switching from one set of chemotherapeutic agents to another (2), although serum AP is not a specific tumor marker for metastatic osteosarcoma and relatively insensitive index of bone turnover owing to the presence of other isoenzyme from hepatobiliary, intestinal and other tissue sources. (10, 12-13) Serum specific bone AP isoenzyme and bone AP are more accurate index of osteoblastic activity but these tests are not yet available in Thailand. However, it might be expected that serum AP higher than 500 U/L which is in a very high level will be correlated with the amount of bony cellular activity especially when the primary tumor is removed, the re-elevation means metastasis. The level of ESR and LDH will be further evaluated to find any possible correlation.

REFERENCES

1. Ohno T, Abe M, Tateishi A. Osteogenic sarcoma. A Study of one hundred and thirty cases. J Bone Joint Surg Am 1975; 57A: 397-404.
2. Mirra JM. Primary, high grade intramedullary variants. In : Mirra JM, Picci P, Gold RH. eds. Bone tumors, clinical, radiologic, and pathologic correlations. Volume one. Philadelphia : Lea & Febiger 1989: 262-3.
3. O' hara JM, Hunter RVP, Foote FW, Miller T, Woodard HO. An analysis of 30 patients surviving longer than 10 years. J Bone Joint Surg Am 1968; 50A: 335-54.
4. Pochanugool L, Nontasut S, Subhadharaphandou T et al. Multidisciplinary "Limb salvage" treatment of osteosarcoma. J Med Assoc Thai 1991; 74: 404-11.
5. Pochanugool L, Nontasut S, Keorochana S, Sirikulchayanonta V, Ratanatharathorn V, Subhadhraphandou T. Multidisciplinary preoperative therapy for bone and soft tissue sarcoma. Intern Med 1988; 4: 5-8.
6. Subhadraphandhu T, Kearochana S, Prichasuk S. Limb salvage procedure for the treatment of osteosarcoma : a preliminary report. Rama Med J 1988; 11: 104-10.
7. Subhadraphandhu T, Nontasut S, Pochanugool L, Sirikulchayananta V. Limb salvage for extremities sarcoma in Ramathibodi Hospital, Thailand. In Limb salvage, current trends. Proceeding 7th international symposium. Singapore 1993: 101.
8. Sirikulchayanonta V, Pochanugool L, Subhadrabandhu T. Update of osteosarcoma in Ramathibodi, Thailand In Humphrey GB, Koops HS, Molenaar WM, Postma A, eds. Osteosarcoma in adolescents and young adults : new developments and controversies. Massachusetts : Kluwer Academic Publishers 1993: 371-4.
9. Subhadrabandhu T, Nontasut S, Pochanugool L, Sirikulchayanonta V. Limb salvage for extremity sarcoma in Ramathibodi Hospital. J Med Assoc Thai 1992; 75 (suppl 1): 112-8.
10. Galasko CSB. Detection of skeletal metastasis. In : Galasko CSB. Skeletal metastases. London : Butterworth & Co Ltd. 1986: 52-4.
11. Mirra JM. Primary, high grade intramedullary variants. In : Mirra JM, Picci P, Gold RH. eds. Bone tumors, clinical, radiologic, and pathologic correlations. Volume one. Philadelphia : Lea & Febiger 1989: 73.
12. Imai K, Tomaru Y, Ohnuki T, et al. Significance of a new stratification of alkaline phosphatase and extent of disease in patients with prostate carcinoma with bone metastasis. Cancer 1992; 69; 2983-9.
13. Hannisdal E, Engan T. Blood analyses and survival in symptom and survery detected lung cancer patients. J Int Med 1991; 229: 337-41.

Table 1 The serum AP level and the status of 22 cases

No	Serum AP Level			Cause of change		Metastasis	Status	survival (mos.)
	initial	maxinum	mininum	increased	decreased			
1	2300	5400	29	after CT	after SX.	No	very well	86+
2	474	1083	57	after CT	after RT & SX	No	very well	17+
3	784	804	55	after CT	after SX	lung	stable	6+
4	531	531	63	-	after CT	unknown	dead	43
5	143	1140	66	lung metastas	-	lung	dead	27
6	1271	1390	94	after CT	after RT	bone	dead	17
7	516	516	-	-	-	bone	dead	17
8	1231	1231	198	-	after CT & SX	lung bone	loss	15
9	3965	3965	270	-	after RT & SX	bone progressed	dead	14
10	700	700	82	-	after CT, RT, SX	bone	dead	14
11	964	964	86	local recur	after SX	local recur	dead	14
12	888	1265	60	after CT	after 2nd CT	unknown	loss	13
13	564	564	40	-	after CT	lung	loss	12
14	597	597	190	-	after CT	lung	loss	12
15	1415	1415	-	-	-	lung, bone spinal cord	dead	6
16	3040	3040	1830	-	after CT	unknown	loss	3
17	773	773	196	-	after CT	lung	loss	3
18	1056	1056	106	-	after CT	unknown	loss	3
19	970	1350	970	after CT	-	unknown	loss	3
20	595	595	-	-	-	lung	loss	1
21	865	865	-	-	-	unknown	No Rx	-
22	555	555	-	-	-	unknown	No Rx	-

CT = chemotherapy, SX = surgery, RT = irradiation

Table 2 End results of 22 cases of high AP level

Survived	2
lung metastases	6
bony metastases	4
lung, bone metastases	1
lung, bone, spinal cord metastases	1
local recurrence	1
unknown condition	7
Total	22 cases

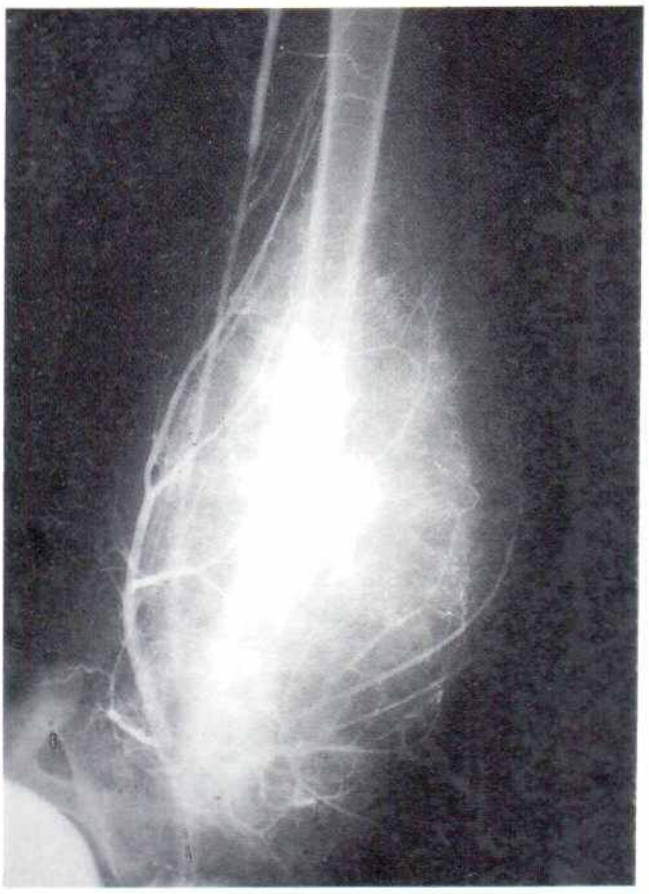

Fig. 1. Angiography of a 10 years boy, with chondroblastic osteosarcoma of his right femur. His initial serum AP was 3040 U/L and decreased to 1830 U/L after 100 mg IA cisplatin and 50 mg epirubicin IV.

COMPARISON OF SURVIVAL OF POST-OPERATIVE IRRADIATION BETWEEN LOW-GRADE GLIOMA, ANAPLASTIC GLIOMA AND GLIOBLASTOMA MULTIFORME

Saipin TANGKARATT, M.D.*

ABSTRACT

One hundred twenty-five patients with glioma were treated with post-operative irradiation between 1983 and 1993. Nineteen patients were excluded from evaluation because of incomplete irradiation schedule. Twenty-eight patients lost to follow up. Only seventy-eight patients (about 62.4 %) were evaluable for survival. Twenty-three patients (about 29.5%) were low-grade gliomas, the median survival of this group was 41 months. Twenty-eight patients were anaplastic gliomas (about 35.9%), the median survival was 19 months. Twenty-seven patients (about 34.6%) were Glioblastomas multiforme, the median survival was 7.6 months. The study showed that histologic grading of glioma was the one significant prognostic factor on survival.

Key Words: Glioma, Histological Grading, Survival, Radiation Therapy.

INTRODUCTION

Glioma is the most common primary tumors in adults, and high grade glioma comprises over 50% of the cases.[1] The outcome in treatment of glioma depend on many factors, such as histological grading, patients status, type of neurosurgical procedures, radiotherapy etc. But the most important factors are age and histological grading.[2] Patients with low grade gliomas have a 5 year survival rate of 28-76% following surgery with post-operative radiation therapy.[3,4,5,6,7] Patients with high grade gliomas had bad prognosis, among the high-grade ones, the presence of tumor necrosis (which had been called glioblastoma multiforme) had the worst prognosis and when compare to another which had absence of tumor necrosis (Astrocytoma with anaplastic foci). Following surgery alone, more than 50% of patients with high grade were dead within 6 months and almost 100% within 2 years.[2,8,9]

The objective of this study was to compare the survival rate of post-operative radiation therapy between low grade glioma, anaplastic glioma, glioblastoma multiforme.

MATERIALS AND METHODS

Gliomatous patients who were refered to this hospital for post-operative irradiaation from January 1983 to December 1993 were included.

ELIGIBILITY

- Eligible patients must have biopsy-proven Gliomas.
- Patients with low grade Gliomas who have complete tumor resection were excluded.
- Age: lesser than 70 years. Older than 18 years. (between 18-70 years.)

* National Cancer Institute, Phaya Thai, Bangkok, Thailand.

- Patients must have adequate renal, bone marrow, pulmonary, cardiac and hepatic function.
- Kasnosfy's performance more than 70.
- Only patients who had completed course of radiation therapy were eligible.
- Feasibility for follow up.

TREATMENT SCHEDULE

Patients with low grade glioma were treated with Co-60 Teletherapy or Linear accelerator 6 MV, localized port technic through lateral parallel fields or wedge fields, both fields each day, 5 days per week, daily dose 180-200 cGy, total tumor dose 5,000-5,500 cGy.

Patients with Anaplastic glioma, or Glioblastoma multiforme were treated with the same machines as above, whole brain irradiation through lateral parallel fields, both fields each day, 5 days per week, daily dose 180-200 cGy, total dose 4,500-5,000 cGy. The tumor bearing areas were boosted with additional 1,500-2,000 cGy.

Symptomatic medications, such as Corticosteroids, anticonvulsants, antiemetics were used depending on patients' symptoms.

Patients were evaluated for neurological signs and performance status weekly during radiotherapy, every 2 months in the first year and every 3 months thereafter.

RESULTS

Between January 1983 and December 1993, 125 patients with Gliomas were refered to Radiation therapy Department for post-operation irradiation. 19/125 patients had not completed radiation courses, 9/19 patients developed uncontrolled increased intracranial pressure, 10/19 had performance status less than 70. Only 106 patients had complete the radiation treatment schedule. 28/106 patients lost to follow up after complete radiation treatment, only 78/106 patients (73.6%) were evaluable for survival. Table 1 shows sex distribution of patient, male: female = 1.2: 1.

Table 1 Sex distribution of patients

		Male	Female
Total Cases	125	68	57
Incomplete XRT	19	11	8
No follow up	28	15	13
Evaluable	78	42	36

High grade gliomas were found more frequent than low grade, about 72.8% of cases.

Table 2 Histological suptypes

	No. of patient		Total	percentage
	Male	Female		
Low grade gliomas	19	15	34	27.2
Anaplastic glioma	21	21	42	33.6
Glioblastoma multiforme	28	21	49	39.2
Total	68	57	125	100.00

In this study, we found that the age distribution of patients was relatively correlated with pathological grading. Patients with younger ages had lower grade of tumor, while the patients with older ages had the more malignant grade. The mean age of patients with low grade was 34.4 years. While the mean age of patients with Glioblastoma Multiforme was 48.5 years.

Table 3 Age distribution

	Age (years)	Mean age (years)
Low grade glioma	22 - 52	34.4
Anaplastic glioma	23 - 51	38.5
Glioblastoma multiforme	35 - 58	48.5

In low grade glioma, only 23 of 34 patients (67.6%) were evaluated for survival, 3 patients developed recurrent tumor at the previous sites, 12 months after complete irradiation. Only 2 of these had re-surgery and the histology of the tumor turned to be malignant glioma. One patient developed severe pulmonary infection and was dead after 8 months of complete radiation. The median survival in this group was 41 months.

In anaplastic gliomas, 28 of 42 patients (59.6%) were evaluated for survival. 8 of 28 patients developed recurrent tumor within 12 months after complete radiation. 6 of 8 patients had histological proven of recurrent tumor by surgery. 2 of 8 cases were presumed by neurosigns and CT scans of brain. Only 4 of 28 patients lived more than 36 months. The median survival of this group was 19 months.

In glioblastoma multiforme, 27 patients of 49 patients (55.1%) were evaluated for survival. Only one patient lived more than 24 months, they developed rapid deterioration of conscious and was dead within few days. 2 of 27 patients had surgical proven of recurrent tumor at 7th and 9th month after irradiation. 13 of 27 patients (about 50%) were dead within 6 months without definite improvement of performance status. Median survival in this group was 7.6 months (Table 4, Fig. 1).

Without autopsy data, late complications were undetected in this study.

Table 4 Survival by pathology

	No. of patient evaluated	Median survival (months)
Low grade glioma	23	41
Anaplastic glioma	28	19
Glioblastoma multiforme	27	7.6

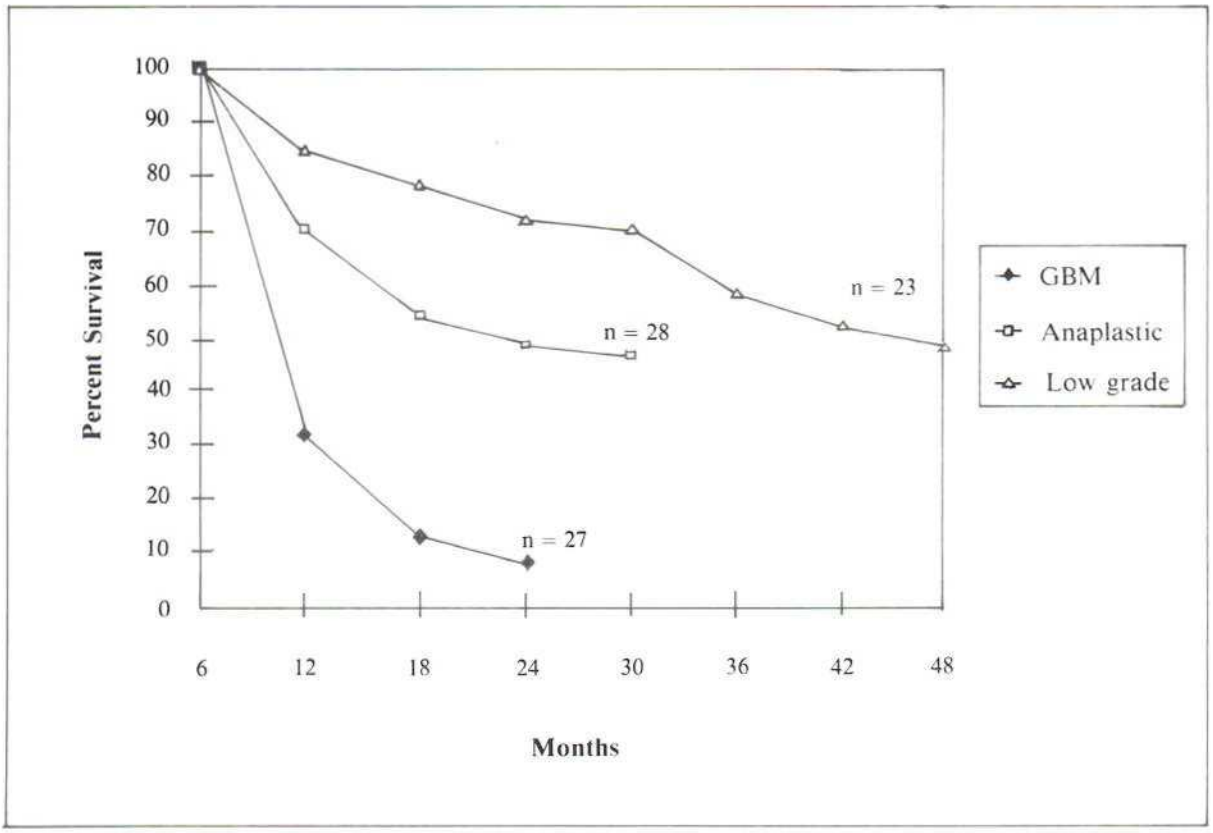

Fig. 1 Survival by pathology

DISCUSSION

The results from our study showed that malignant glioma, both anaplastic glioma and glioblastoma multiforme had bad prognosis with short survival after surgery and radiation, median survival for anaplastic glioma was 19 months, for glioblastoma multiforme was 7.6 months. But only 59.6% of patients with anaplastic gliomas and 55.1% of patients with glioblastoma multiforme were evaluable, so the results for survival may be over estimated, because the patients who dropped out for evaluation may died from tumors. The age distribution in our study was correlated with pathological grade. These results were comparable to tht previous study from RTOG and ECOG. Anaplastic gliomas provided better prognosis than glioblastoma multiforme. Patients with anaplastic gliomas had median survival 27 months and median survival for patients with glioblastoma multiforme was 8 months.[2]

Patients with low grade gliomas developed fewer recurrent tumors with longer disease free interval than malignant gliomas. Anaplastic gliomas developed recurrent tumors more than glioblastoma multiforme, 8 of 28 patients of anaplastic gliomas compare to 2 of 27 patients of glioblastoma multiforme, this may result from the longer survival of anaplastic gliomas than glioblastoma multiforme, who died before development of recurrent tumors.

CONCLUSION

Malignant gliomas, both anaplastic glioms and glioblastoma multiforme, had short survival when treated with post-operative irradiation. Other adjuvant treatment including systemic chemotherapy, heavy particle beam radiation, hyperbaric oxygenation and chemical radiosensitizers, immonotherapy etc, may need to improve survival.

REFERENCES

1. Levin, V.A.; Sheline, GE.; Gutin, PH. Neoplasm of the central nervous system. In: Devita, V.T., Jr.; Hellman, S.; Rosenbug, S.A., eds. Cancer: Principles and Practice of oncology, 3rd ed. Philadelphia: JB. Lippincott Co; 1992: 1417-1441.
2. Chang, C.H.; Hoston, J.; Schoenfeld, D.; Salazas, O.; Perez-Tamayo, R.; Kramer, S.; Weinstein, A.; Nelson, J.S.; Tsukada, Y. Comparison of Postoperative Radiotherapy and Combined Postoperative Radiotherapy and Chemotherapy in the Multidisciplinary Management of Malignant Gliomas: a joint Radiation Therapy Oncology Group and Eastern Cooperative Oncology Group study. Cancer 52: 997-1007; 1983.
3. Fagekas, J.T. Treatment of Grade I and II Brain Astrocytomas. The Role of Radiotherapy. Int.J. Radiat.Oncol.Biol.Phys. 2: 661-666; 1977.
4. Garcia, D.M.; Fulling, K.H.; Masks, J.E. The value of Radiation Therapy in addition to surgery for Astrocytomas of adult cerebrum. Cancer 55: 919-927; 1985.
5. Law, E.R.; Taylor, W.F.; Clifton, M.B.; Okazaki, H. Neurosurgical management of low-grade astrocytoma of cerebral hemisphere. J. Neurosurg. 61: 665-673; 1984.
6. Olmsted. C.M.; Plenk, H. Radiation therapy of astrocytomas grade I-IV. Int. J. Radiat. Oncol. Biol.Phys. 4 (suppl. 2) 229; 1978.
7. Sheline, G.E. Radiation therapy of brain tumors. Cancer 39: 873-881; 1977.
8. Nelson, D.F.; Diener West, M.; Weinstien, A.S.; Schoenfeld, D.; Nelson, J.S.; Sause, W.T., Chang, C.H.; Goodman, R.; Carabell, S. A randomized comparison of Misonidazole sensitized radiotherapy plus BCNU and radiotherapy plus BCNU for treatment of malignant glioma after surgery: final report of an RTOG study. Int. J. Redidt. Oncol. Biol. Phys. 12: 1793-1800; 1986.
9. Nelson, D.F.; Nelson, J.S.; Davis, D.R.; Chang, C.H.; Gritin, T.W.; Pajak, T.F. Survival and Prognosis of patients with astrocytoma with atypical or anaplastic feature. J. Neuro-oncol. 3: 99-103; 1985.

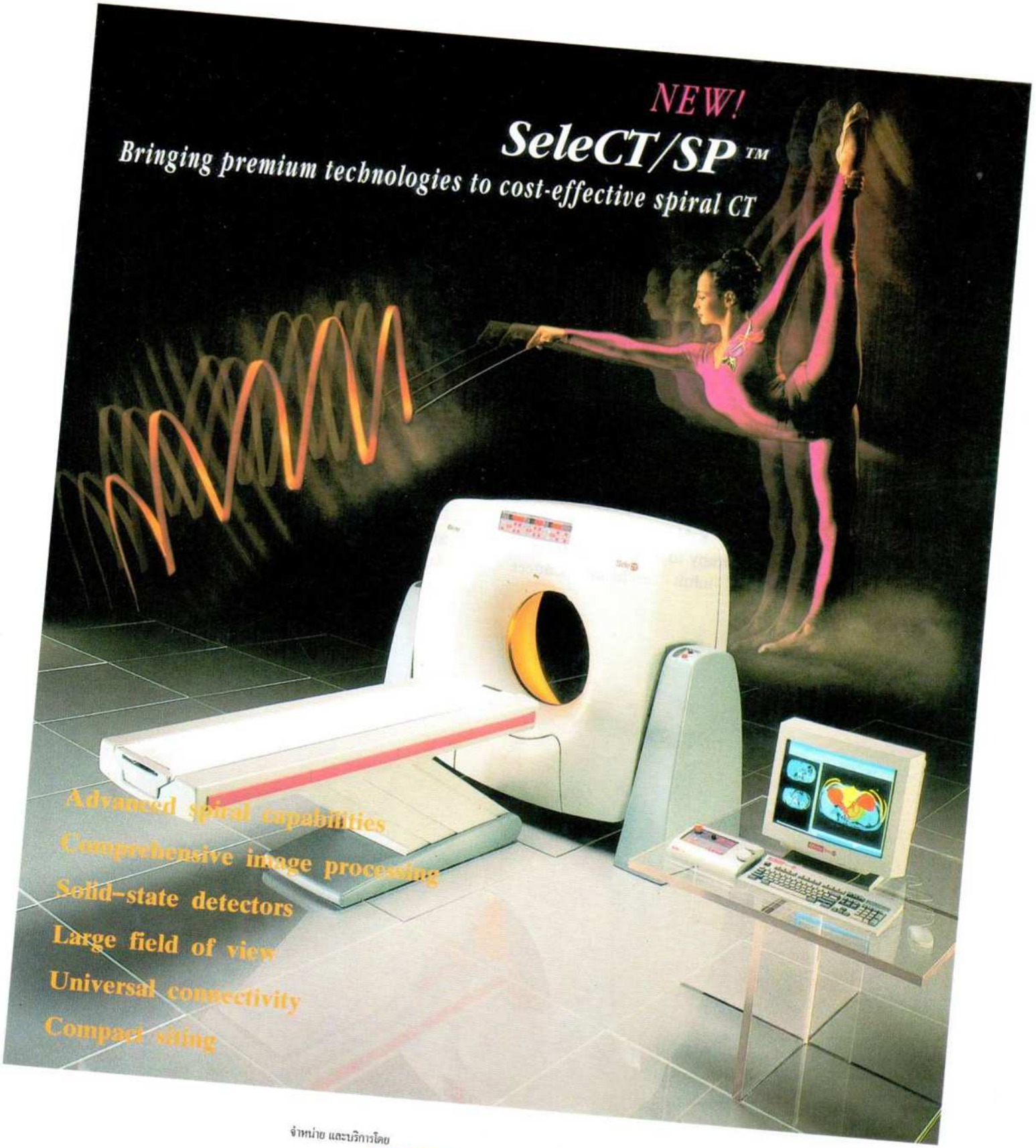

จำหน่าย และบริการโดย

supreme PRODUCTS CO.,LTD.

บริษัท สุพรีม โพรดักส์ จำกัด

163/81-82 ถ.พระปิ่นเกล้า แขวงบางยี่ขัน เขตบางพลัด กรุงเทพฯ 10700 แผนกขาย 434-0040,434-0050 แผนกบริการ 434-0060 โทรสาร 433-3971

ANGIOSARCOMA OF THE LIVER - A CASE REPORT

Assoc. Professor C.R. Jayakumar*
Dr. Lilius Chua Kim Lian**

ABSTRACT

A 42 year old man presented to our hospital with right hypochondrial pain for 6 months. This had increased in severity and frequency over the last one week and was associated with fever. The patient was febrile and had slightly raised total white cell count. Ultrasonography revealed an enlarged liver with an inhomogeneous mass within the right lobe of the liver. In view of the clinical history, a provisional diagnosis of a liver asbcess was made. A percutaneous needle aspiration was performed under ultrasound guidance. There was no pus but blood stained fluid was aspirated instead. This was sent for cytology. Subsequently a CT scan of the abdomen was performed for further evaluation of the liver mass. This showed an ill-defined, predominantly hypodense mass in the right lobe of the liver and medial segment of the left lobe of the liver suggestive of a malignant liver tumour. A tru-cut biosy of the liver tumour was performed under CT guidance. The histopathological examination revealed that the liver tumour was hepatic angiosarcoma.

The patient went on to develop brain metastasis. He was treated with radiotherapy but succumbed to the disease and died 3 months from the time of diagnosis.

The significant aspects of hepatic angiosarcoma and the imaging modalities used are discussed.

Key Words: Angiosarcoma of Liver, Ultrasonography, C.T. Guidance Biopsy

INTRODUCTION

Angiosarcoma of the liver is a rare tumour with a rapidly fatal course. This tumour constitutes only 2% of all primary tumours of the liver. The following report describes a case of hepatic angiosarcoma. The significant aspects of this malignancy are presented. Diagnostic and therapeutic modalities are discussed.

CASE HISTORY

A 42 year old man presented to our hospital with intermittent pain in the right hypochondrium for 6 months which had increased in frequency and severity over the last week and was associated with fever. He was a business man dealing in household goods and had not been exposed to vinyl chloride, thorotrast, arsenicals and radium. He drank alcohol regularly and was a heavy smoker.

Physical examination revealed tenderness in the right hypochondrium with the liver palpable 5cm below the right costal margin. The liver was smooth and firm. The patient was febrile and had temperature of 37.8 degrees C. He was not jaundiced and the rest of the physical examination was unremarkable.

The initial laboratory test revealed a haemoglobin

* Department of Radiology University Hospital Kuala Lumpur
** Correspondence: Assoc. Professor C.R. Jayakumar
Department of Radiology University Hospital 50100 Kuala Lumpur Malaysia.

of 14.4g/dl, a slightly raised total white cell count of 11,500/dl, a normal total bilirubin and alkaline phosphatase. Hepatitis B surface antigen was negative. A provisional diagnosis of liver abscess was made.

An ultrasound of the abdomen revealed an enlarged liver with a large mass in the right lobe of the liver. It appeared inhomogeneous but was predominantly hypoechoic. In view of the clinical history this was thought to be an early liver abscess. The spleen, pancreas and both kidneys appeared normal. Subsequently percutaneous needle aspiration of the focal intrahepatic lesion was performed under ultrasound guidance. A small amount of dark blood stained fluid was obtained. This was sent for cytology. No pus was aspirated. To assess this mass further, a CT scan of the abdomen was performed with intravenous and oral contrast. The intravenous contrast was given during the CT scan. Delayed scans were not performed. The CT scan showed a poorly defined, predominantly hypodense mass in mainly the right lobe and the medial segment of the left lobe of the liver suggestive of a malignant liver tumour. The aspirated fluid from the liver send earlier was inadequate for cytology so a percuteneous tru-cut biopsy was performed under CT guidance. Gel foam was injected during the withdrawal of the needle to prevent bleeding.

The histopathological report of the biopsy specimen was that of a primary hepatic angiosarcoma.

10 days later the patient developed a severe headache and became confused. On examination, apart from an up-going plantar reflex on the left there were no localising signs. A CT scan of the brain showed an enhanching focal lesion of about 3cm in diameter within the right cerebellum, associated with moderate hydrocephalus. This was most likely brain metastasis from the hepatic angiosarcoma. A ventriculo-peritoneal shunt was performed and the patient was nursed in the intensive care unit. He improve over the next 10 days and was discharged. He attended the oncology clinic regularly and was given radiotherapy. Two months later the patient died. An autopsy was not performed.

DISCUSSION

A focal, predominantly hypoechoic intrahepatic lesion on ultrasound has a number of differential diagnoses, namely, metastasis, hepatoma, abscess, lymphoma, cavernous hemangioma, hematoma and cyst. In our patient, who had a history of fever, a liver abscess (pyogenic/amoebic) was thought to be the most likely diagnosis. Liver abscesses have a very variable appearance on both ultrasound and CT and may be indistinguishable from hepatic neoplasms (1).

Metastatic carcinoma is the most common neoplasm of the liver and is responsible for 38% of all tumours in the liver. About 90% of primary carcinomas of the liver are hepatocellular carcinoma and 7% are cholangiocarcinomas. Less common tumours include hepatoblastoma, angiosarcoma and sarcoma (2).

Angiosarcoma, also known as haemangioendothelial sarcoma, constitutes only 2% of all primary tumours of the liver. This neoplasm has been reported in association with exposure to thorotrast, arsenicals, radium and vinyl chloride. This rare neoplasm is also associated with systemic diseases like hemochromatosis and von Recklinghausen's disease. Our patient did not have any history of exposure to the above mentioned chemicals nor did he has any evidence of hemochromatosis or von Recklinghausen's disease. He presented with fever and right hypochondrial pain. Clinically an infective process would be the most likely cause but it is not uncommon for fever to occur in patients with a malignancy.

The ultrasound features of angiosarcoma are nonspecific. It usually appears inhomogeneous and predominantly hypoechoic. The hypoechoic areas probably represent the vascular spaces in this tumour. As already mentioned, these appearances are nonspecific as they are also seen in other benign vascular tumours eg. cavernous hemangioma, primary malignant tumours eg. hepatocellular carcinoma and metastasis.

The computed tomographic appearances of hepatic angiosarcoma have been described in detail in the article written by White P.G. et.al (3). The authors recommended that for accurate assessment of this tumour, non-enhanced scans, dynamic contrast-enhanced scans and delayed post-contrast scans should be obtained.

Prior to intravenous contrast enhancement, angiosarcoma appears hypodense relative to normal liver. The non enhanced scan allows easier recognition of areas of tumour enhancement on subsequent contrast enhanced scans. Dynamic scanning during a bolus injection of contrast may demonstrate areas of intense enhancement which would correspond to the more vascular parts of the tumour. In addition, enhancement of the liver parenpchyma may facilitate detection of other small hypodense foci of tumour which might be overlooked. On delayed post-contrast scans, there is progressive enhancement over a period of minutes. This supports the diagnosis of a highly

vascular tumour. In our patient only dynamic contrast enhanced scans were obtained as there was no suspicion of the tumour being a hepatic angiosarcoma. The CT scan of the patient demonstrated an illdefined hypodense mass in the right lobe of the liver.

The computed tomographic features described are not specific to angiosarcoma. The differential diagnosis include simple hemangioma, giant cavernous hemangioma, hepatocellular carcinoma and vascular metastasis. Hemangiomas may be multiple and the patient is usually asymptomatic and liver function test are usually normal. Hemangiomas have a characteristic CT appearance, such as, appearing hypodense on the pre-contrast scan, early peripheral contrast enhancement, progressive opacification from periphery to the centre and an eventual isodense appearance on the delayed scans. Giant cavernous hemangioma have some similar features of simple hemangioma but are distinguished by the larger size of the former and characteristic non-enhancing central cleft. CT features of angiosarcoma are consistent with a vascular tumour. These features are also seen in other malignant liver neoplasms. In a recent study of patterns of contrast enhancement of liver tumours during dynamic and delayed post-contrast CT, contrast enhancement occurred in about 50% of malignant neoplasms which include liver metastasis and a small percentage of hepatocellular carcinomas. The patterns of contrast enhancement included, central or peripheral enhancement during dynamic scanning and partial or rarely complete isodense enhancement on delayed scans (4).

To obtain a definitive diagnosis in most liver tumours, percutaneous biopsy is usually necessary. Histologic specimens should be obtained from the margins of the tumour. Liver biopsy in hepatic angiosarcoma is a potentially dangerous procedure due to the vascular nature of the tumour. There have been reports of fatal or serious hemorrhage following percutaneous biopsy. In our patient, gel foam was injected during the withdrawal of the biopsy needle to aid hemostasis. Hepatic arteriography is the best method for diagnosing vascular lesions. Typically, there is a "pooling" of contrast into "vascular lakes", central areas of hypovascularity and peripheral contrast staining. The hepatic artery or branches may often be displaced by the tumour. The hepatic arteriogram also

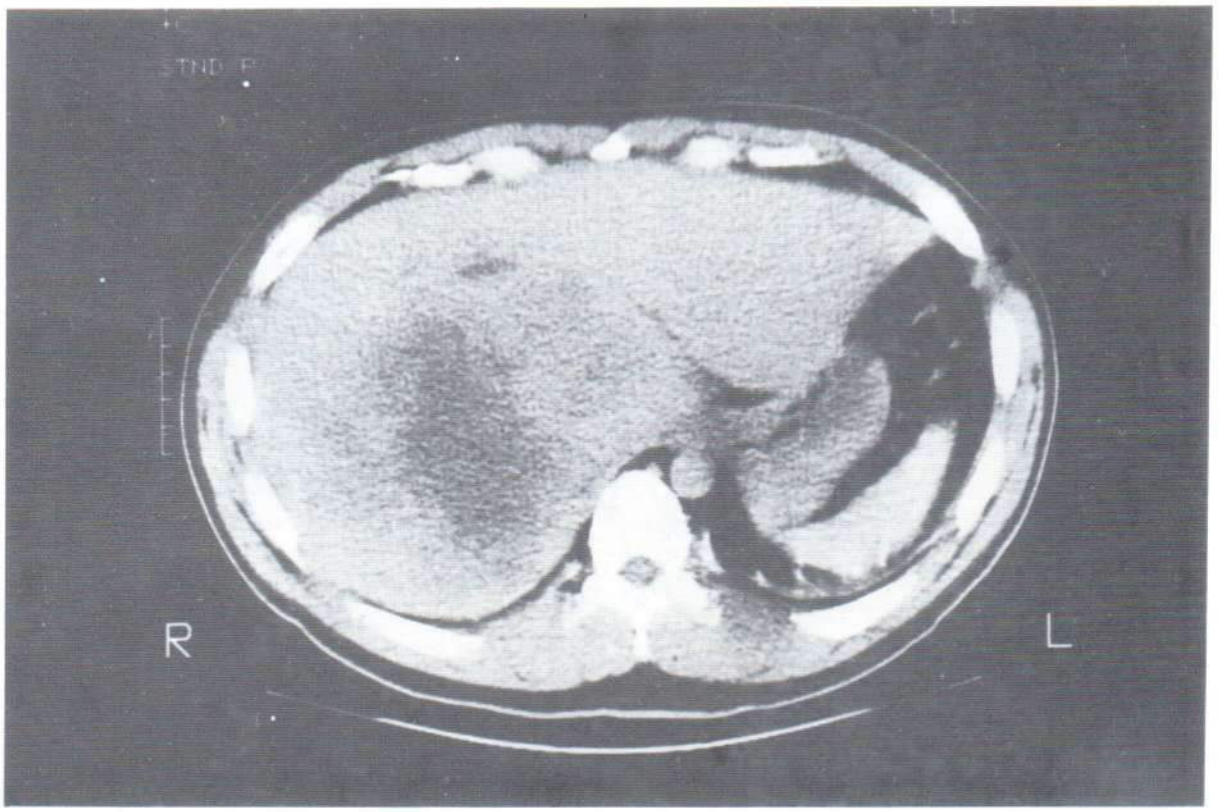

Fig. 1 Non-contrast CT scan of the liver showing a poorly defined, predominantly hypodense mass in mainly the right lobe and medial segment of the left lobe.

serves to outline the vascular supply of the tumour and whether the tumour is localised to one lobe and the remainder of the liver is not compromised. Surgery may then be an option. In our patient surgery was not considered as the tumour involved both the right and left lobes of the liver. Neoadjuvant chemotherapy via a hepatic artery catheter may in the future prove to be useful in following resection in more cases.

Brain metastasis from angiosarcoma is rarely seen because of the rarity of the primary tumour. Sites affected by metastasis from angiosarcoma in decreasing order of frequency are the cervical lymph nodes, lung and spleen. Our patient developed a focal enhancing mass in the right cerebellum. This cerebellar mass was most likely a metastasis from the primary angiosarcoma of the liver.

In summary, inhomogeneous focal intrahepatic lesions are commonly encountered in ultrasonography and CT of the liver. Angiosarcoma appears inhomogeneous and predominantly hypoechoic on ultrasonography. Computed tomographic features are that of a highly vascular tumour. On pre-contrast scans, angiosarcoma appears hypodense relative to normal liver. Contrast enhanced scans demonstrate areas of intense enhancement which corresponds to the more vascular parts of the tumour. Progressive enhancement of the tumour is seen on the delayed post-contrast scans. Although these features are helpful in the diagnosis of angiosarcoma, they are not specific to angiosarcoma. To achieve a definitive diagnosis in most cases of a liver mass, a biopsy is usually necessary, although certain precautions must be taken when there is a suspicion of angiosarcoma.

REFERENCES

1. Halvorsen, R.A., Korobkia, M., Foster, W.L., Silverman, P.M., Thompson, W.M. The variable CT appearance of hepatic abscesses. AJR 1984; 141: 941-946.
2. Neshwat, L.F., Friendland. M.L., Lesnic, B.S., Feldman, S., Glucksman, W.J., Russo, F.D. Hepatic angiosarcoma. AJM. 1992; 93: 219-222.
3. White, F.G., Adams, H., Smith, P.M. The computed tomographic appearances of angiosarcoma of the liver. Clinical Radiology 1993; 48: 321-325.

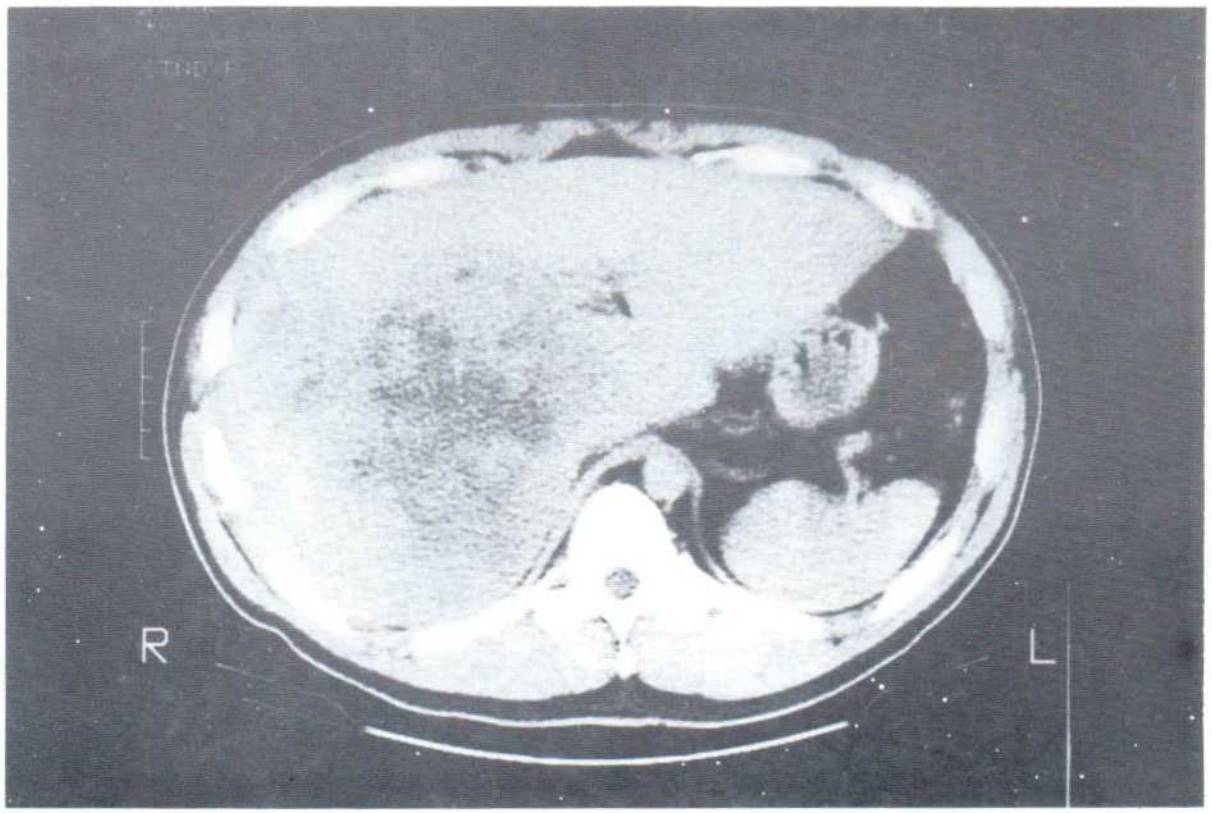

Fig. 2 Contrast enhanced CT of the liver demonstrate areas of intense enhancement, which corresponds to the vascular parts of tumour.

4. Freeny, P.C., Marks, W.M. Patterns of contrast enhancement of benign and malignant hepatic neoplasms during bolus dynamic and delayed CT. Radiology 1986; 160: 613-618.
5. Vasile, N., Larde, D., Safrani, S., Bernard, H., Mathiew, D. Hepatic angiosarcoma: A case report. Journal of Computed Tomography 1983; 35: 899-901.
6. Freeny, P.C., Marks, W.M., Pattern of contrast enhancement of benign and malignánt hepatic neoplasms during bolus dynamic and delayed CT. Radiology; 1986; 160: 613-618.
7. Werneck, K., Vassallo, P. Bick, U., Diedrich, S. Peters, P.E. The distinction between benign and malignant liver tumours on sonography: value of a hypoechoic halo. AJR 1992; 159: 1005-1009.
8. Kuratsu, J., Seto H., Kochi, M., Itoyama, Y., Uemura, S., Ushio, Y. Metastatic angiosarcoma of the brain. Surg Neurol 1991; 35: 305-309.

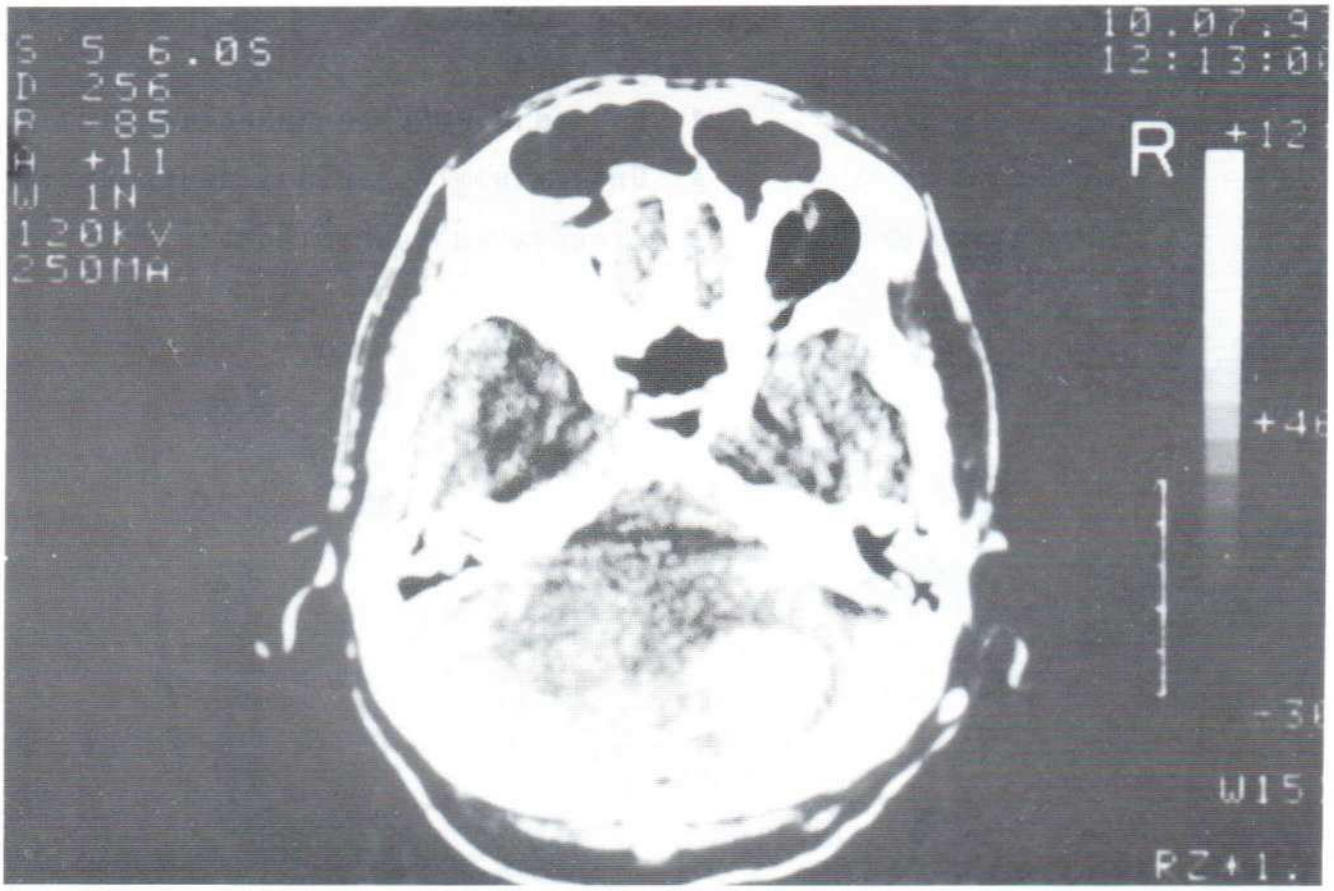

Fig. 3 Contrast enhanced CT of the brain shows a focal enhancing nodule in the right cerebellar hemisphere representing metastatic angiosarcoma.

บริษัท คงศักดิ์เอ็กซเรย์การแพทย์อุตสาหกรรม จำกัด
KONGSAK X-RAY MEDICAL INDUSTRY COMPANY LIMITED
212/1 PHAHONYOTHIN SOI 55 BANGKHEN BANGKOK 10220
TEL. 5213214, 5511794 CABLE: KELEX FAX: 5523744

KELEX
50 mA 100 KV MOBILE TYPE DIAGNOSTIC X-RAY UNIT MODEL MD 50-99

- # เหมาะสำหรับคลินิคเอกชนและโรงพยาบาลทั่วไป
- # มีช่างผู้ชำนาญให้การบริการ ตลอดอายุการใช้งาน
- # พร้อมทั้งจำหน่ายอุปกรณ์เอ็กซเรย์

KELEX
MD 100-99 X-RAY SYSTEM
FULL WAVE 100 MA 100 KV

IFOSFAMIDE INDUCED RICKETS WHICH IS REVERSIBLE FOLLOWING TREATMENT:

Dr. Chong Aun Kee M.B.B.S. (Senior Resident)[1]
Associate Professor C.R. Jayakumar M.B., D.M.R.D., M.D.[1,2]
Dr. Saw Lwin. M.B.B.S., D.M.R.D.[1]

ABSTRACT

Ifosfamide is a derivative of cyclophosphamide used in the treatment of malignant tumors both in child and adult. One of its side effect is nephrotoxicity. A 5 years old child who received ifosfamide for treatment of retroperitoneal rhabdomyosarcoma subsequently developed hypophosphatemic rickets which improved with phosphate supplement is described.

Key Words: Ifosfamide, Fanconi's syndrome, Rickets.

INTRODUCTION

Ifosfamide is an oxazophosphorine derivative of cyclophosphamide and is currently used in the treatment of childhood rhabdomyosarcoma and other malignancies. It is widely used because of its low bone marrow toxicity and its treatment of cyclophosphamide resistant tumor.

Adverse effects of ifosfamide include nausea, vomiting, alopecia, myelosuppression, central nervous system toxicity, haemorrhagic cystitis and nephrotoxicity (1). Hypophosphatemic rickets has been recognized as an additional complication of ifosfamide treatment (1,2,3,5). We report a child with reversible hypophosphatemic rickets but an irreversible Fanconi's syndrome following treatment with ifosfamide.

CASE REPORT

A 5 years old Indian boy with retroperitoneal rhabdomyosarcoma stage IV and renal failure secondary to compression of ureters by tumor bilaterally, received post operative chemotherapy for almost 12 months. The chemotherapy consisted of vincristine, adriamycin and ifosfamide in combination with other chemotherapeutic drugs. He responded well to the treatment. Seven months after completion of chemotherapy his mother noticed that his eyes were puffy in the evening. Radiographs of chest showed cupping of the anterior end of the ribs which is characteristic of rickety rosary. (Fig. 1a) The wrist changes were also typical of rickets with widened growth plate, fraying, splaying and cupping of the metaphysis to surround the uncalcified growth plate. (Fig. 1b) Laboratory investigations revealed an elevated alkaline phosphatase and lower end normal limits of calcium and phosphate. Serum creatinine and urea were elevated. The parathyroid hormone level was within the normal range. (See table 1)

Urine analysis showed aminoaciduria (mainly cysteine), mild proteinuria, glycosuria, calciuria and phosphaturia. (See table 2) Following treatment with oral phosphate supplement the serum concentration rose back to normal. Follow up radiographs also showed healing of rickets. (Fig. 2a&b).Urine examination showed a persisting disturbance of urine excretion which is suggestive of proximal tubular dysfunction.

DISCUSSION

The patient described, had rachitic changes thought to be caused by nephrotoxicity of ifosfamide.

[1] Department of Radiology, University Hospital, Kuala Lumpur.
[2] Correspondence: Assoc. Prof. C.R. Jayakumar,
Department of Radiology University Hospital, Kuala Lumpur 59100, Malaysia.

The specific features include abnormal urinary excretion of amino acids, phosphate, bicarbonate, glucose and small protein otherwise known as Fanconi's syndrome. The renal toxicity is predominantly tubular, although glomerular abnormalities may occur (1). Renal damage is usually irreversible (3) although reversible renal tubular dysfunction has been described (7).

There have been several recent report of development of Fanconi's syndrome with or without associated rickets (1,3,5). It has been shown that the total dose of ifosfamide received correlated with the severity of nephrotoxicity. It has also been suggested that the younger age may be a risk factor (8). Although it is thought that the toxic effect of ifosfamide is cumulative, Fanconi's syndrome may occur after a single dose of ifosfamide (9).

Rickets in Fanconi's syndrome is related to phosphate deficiency and in some cases to impaired conversion of 25-OH vitamin D3 to 1.25-OH vitamin D3. This in turn will cause a decrease in gastrointestinal tract absorption of calcium. A decrease in serum calcium will cause secondary hyperparathyroidism. In contrast, ifosfamide causes renal phosphate wasting with no effect on serum calcium level. An interesting observation made in this boy was the rachitic changes were reversible following treatment with oral phosphate supplement.

Therefore early detection of impaired renal function by close monitoring of serum and urine during and after ifosfamide therapy will allow earlier detection of Fanconi's syndrome and development of bone disease. The radiologist should also be attuned to the possibility of rickets when examining radiographs obtained for tumor surveillance.

REFERENCE

1. Skinner R, Pearson A.D., Price L., Coulthard M.G., Craft A.W., Nephrotoxicity after Ifosfamide. Arch. Dis. Child '1990; 65: 732-738.
2. James E.S., J.O. Haller, S. Miller, Ifosfamide : A new cause of rickets. AJR 1992; 158: 823-824.
3. Burk C.D., Restaino L., Kaplan B.S., Meadows A.T., Ifosfamide-induced rickets proximal tubular toxic reaction. J. of Pediatrics 1990, Vol. 117: 331-335.
4. L.E. Sweeney, Hypophosphatemic rickets after Ifosfamide treatment in children. Clinical Radiology 1993; 47: 345-347.
5. J.D. Schepper, G. Stevens, M. Verboven, C. Beata, J. Otten, Ifosfamide-induced Fanconi's syndrome with growth failure in 2 year old child. American Journal of Pediatrics Haematology/Oncology 1991; 13: 39-41.
6. Skinner R., Pearson A.D., Price L., Cunningham K., Craft A.W., Hypophosphatemic rickets and Ifosfamide treatment in children. BMJ 1989; 298: 1560-1561.
7. Newbury-Ecob R.A., Noble V.W., Barber P.R.H., Ifosfamide-induced Fanconi's syndrome, (letter), Lancet 1989; 1: 1328.
8. Skinner R., Pearson A.D.J., Price L., Coulthard M.G., Craft A.W., Nephrotoxicity after Ifosfamide induced. Arch of Dis. in children 1990; 65: 732-73.
9. Devalck C., Ismaili K., Ferster A., Sariban E., (letter), Acute Ifosfamide-induced proximal tubular toxic reaction. J. of Pediatric 1991; 118: 325-326.

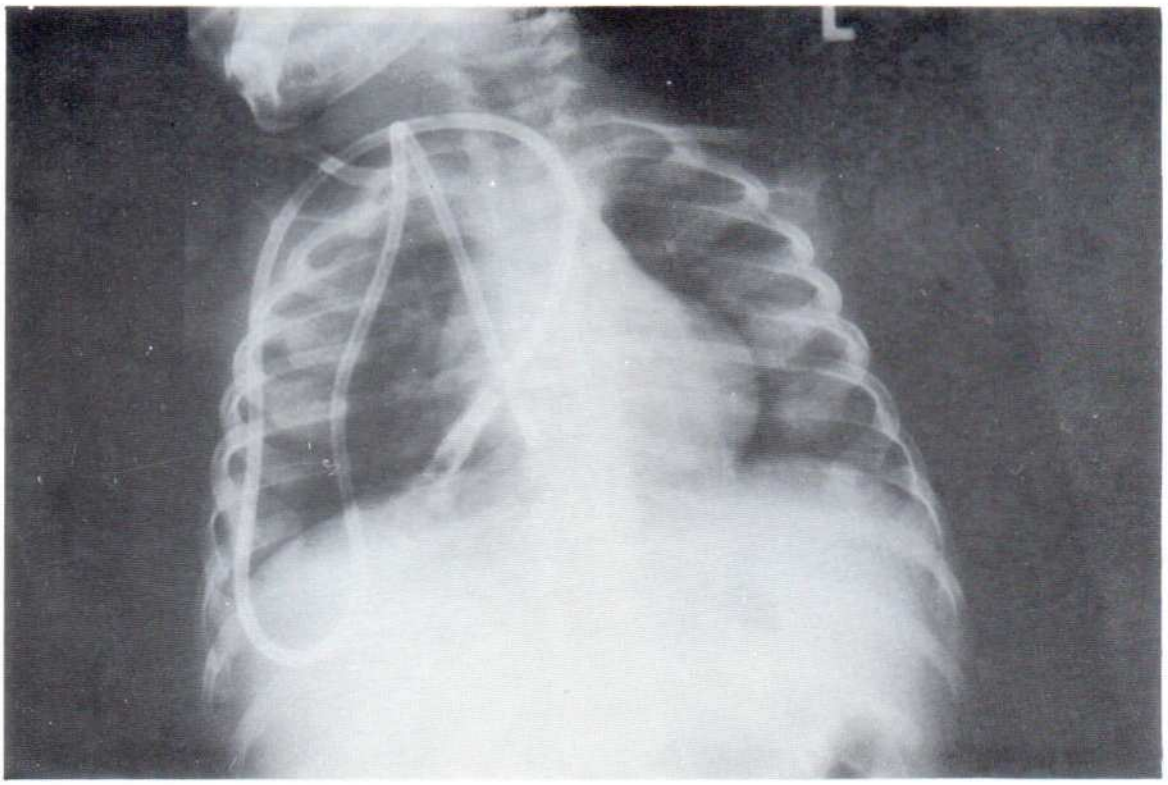

Fig. 1a Anteroposterior radiograph of chest showed cupping of the anterior end of ribs characteristic of rickety rosary.

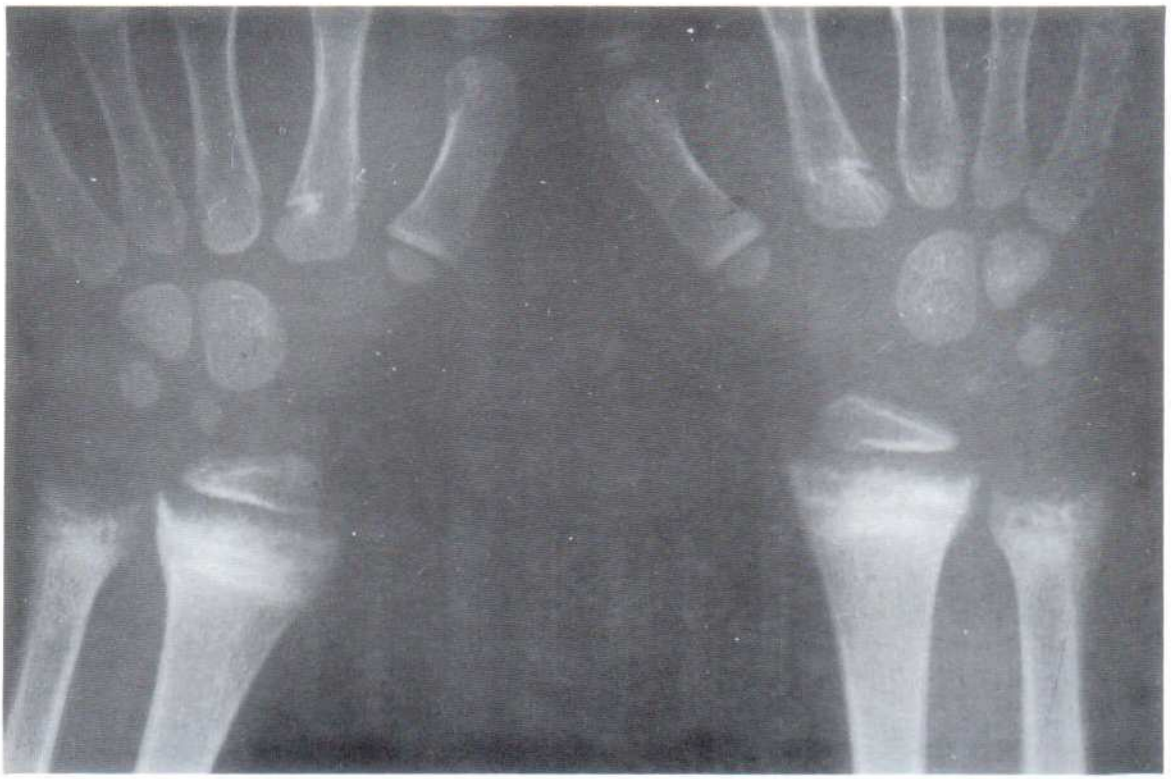

Fig. 1b Radiograph of the wrists showed widened growth plates, fraying, splaying and cupping of the metaphysis to surround the uncalcified growth plates.

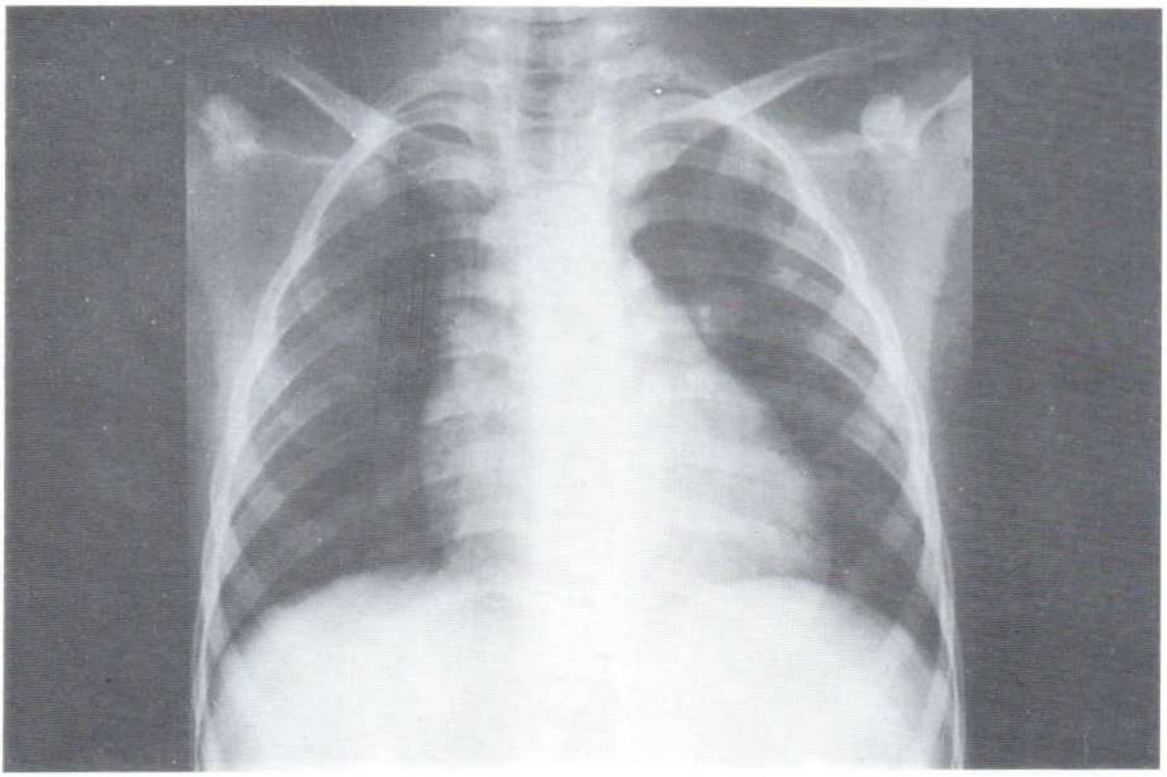

Fig. 2a Post treatment with oral phosphate radiograph of the chest, reveal healing of the rickets.

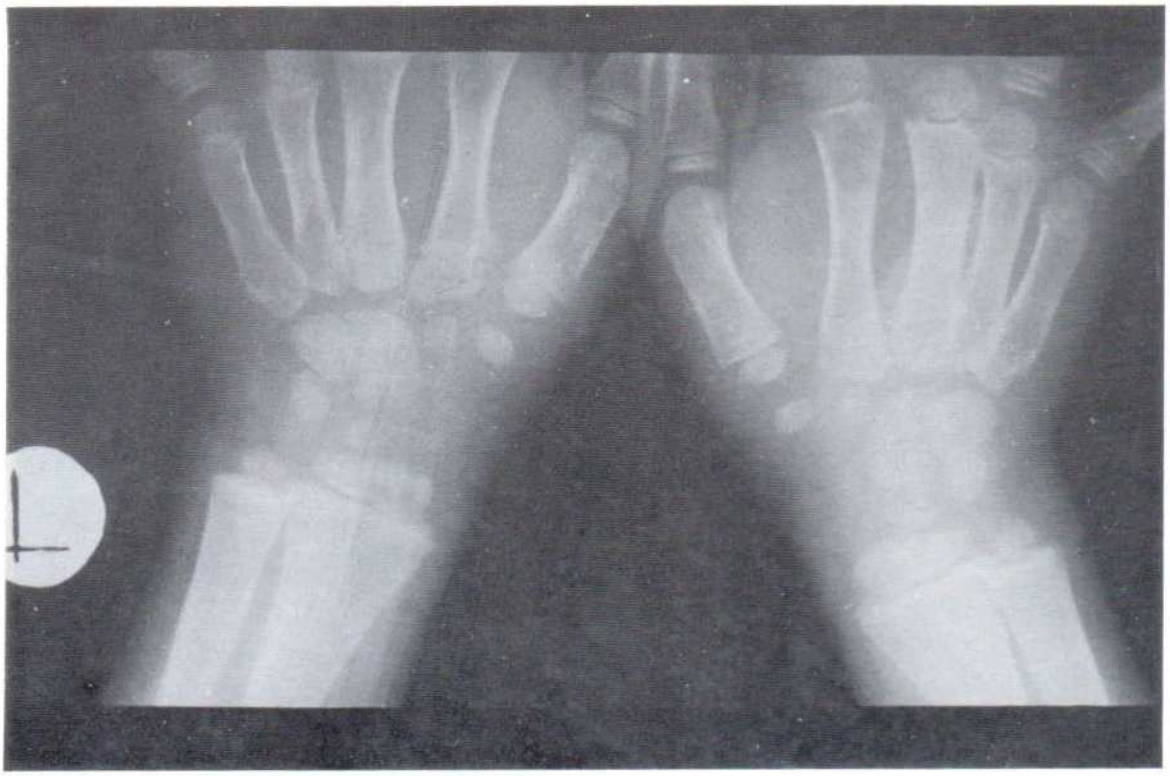

Fig. 2b Radiograph of the wrists reveal resolution of rickets after oral phosphate therapy.

Table-1 Evaluation of serum studies indicating renal tubular dysfunction in a 5 year old child.

SERUM	April 1993	August 1995	Normal range
Alkaline phosphatase	677 iu/L	371 mmol/L	0
Caicium	2.3 mmol/L	2.5 mmol/L	2.1-2.5 mmol/L
Phosphate	0.7 mmol/L	1.7 mmol/L	0.6-1.4 mmol/L
Creatinine	112 mmol/L	89 mmol/L	80-133 mmol/L
Urea	7.2 mmol/L	8.3 mmol/L	3.2-6.8 mmol/L
Potassium	2.3 mmol/L	3.2 mmol/L	3.5-5.3 mmol/L
Chioride	104 mmol/L	109 mmol/L	93-108 mmol/L
Bicarbonate	14 mmol/L	20.8 mmol/L	24-323 mmol/L
Base excess	-10	-4.1	-2- +2
Parathyroid hormone	4.9 pmol/l		1.1-6.5 pmol/L
Glomerular filtration rate	51 ml/min/1.73 metre squared		124ml/min/1.73 metre squared

Table-2 Urine analysis of a child with Fanconi's syndrome

24 Hours urine collection		Normal
Protein	0.52 gm/24 hrs	0-0.1 gm/24 hrs
Calcium	0.4 mmol/24 hrs	2.5-7.5 mmol/24 hrs
Phosphate	8.3 mmol/24 hrs	15-50 mmol/24 hrs
Creatinine	1.4 mmol/24 hrs	1.4 mmol/24 hrs

Urine analysis	1993	1995
Protein	+	Trace
Glucose	4+	2+
PH	6	9

SHIMADZU

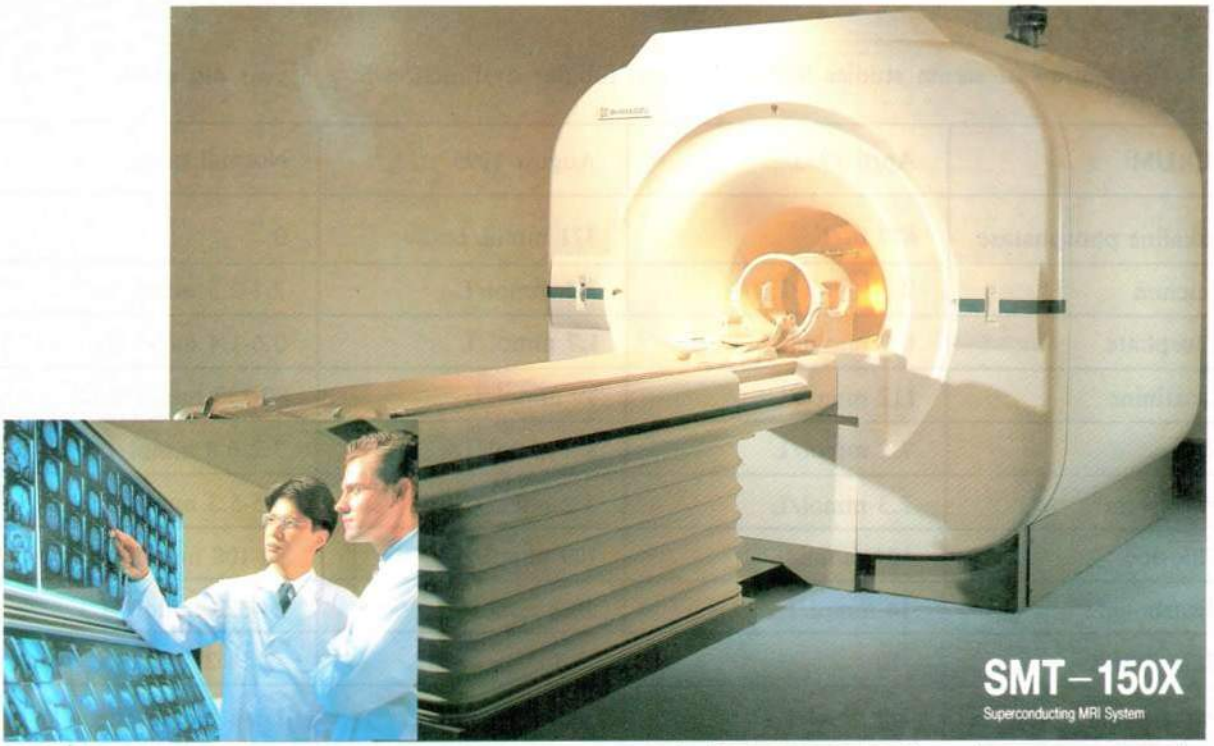

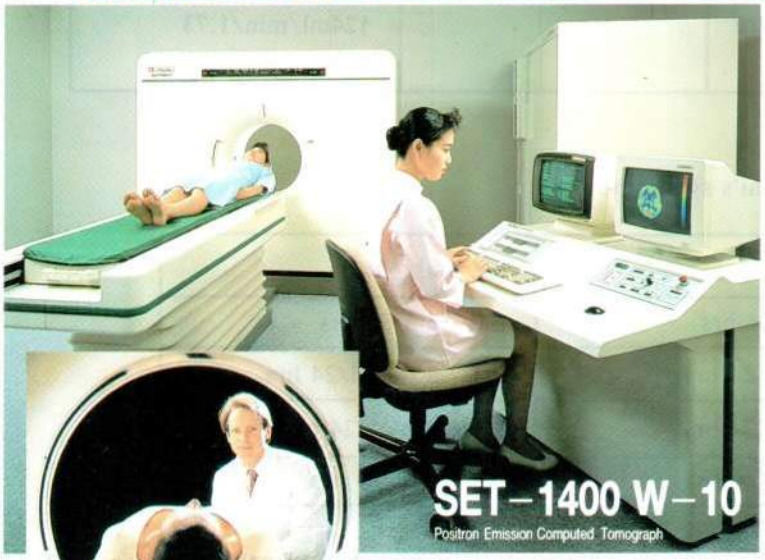

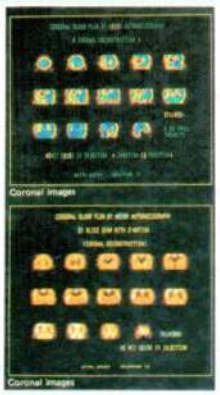

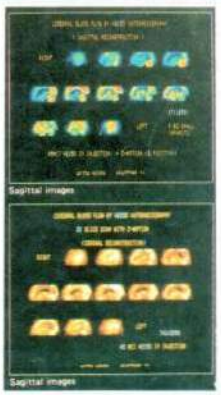

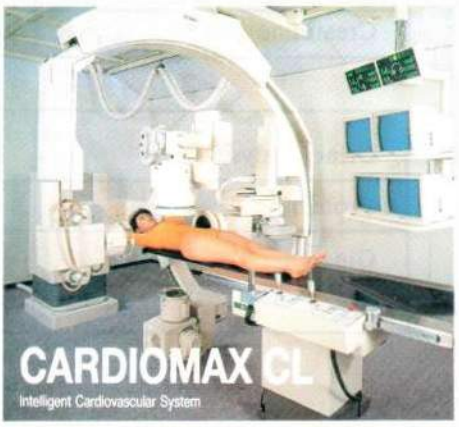

SOLE DISTRIBUTOR :

INTERNATIONAL COSMETICS CO., LTD.

757/10 Soi Pradoo 1, Sathupradit Road, Yannawa, Bangkok. 10120

Tel. 2949541, 2940294 (Ext. 264, 273) Telefax : 2949541

AMNIOTIC BAND SEQUENCE - A REVIEW OF ARTICLES WITH DEMONSTRATION OF A CASE.

Patchrin PEKANAN, Boonchuay SATHAPATAYAVONGS

ANNIOTIC BAND SEQUENCE

Its synonyms are steeter dysplasia, amniotic band disruption complex, amniotic band syndrome, ring constriction etc. (1-16).

The mode of inheritance is sporadic. Familial amniotic bands and amniotic band disruption in twins have rarely been reported.

Compression-related deformities due to amnion rupture with retained chorion integrity are most likely the cause of the anomalies; a possibility of chorionic villus biopsy as a cause of the amniotic band syndrome has been suggested.

The pathology includes triad of amniotic-denuded placenta, fetal attachment to or entanglement by amniotic remnants and fetal malformations.

The clinical and radiologic manifestations are

1. head: facial clefts, calvarial defects, hydrocephalus, anencephaly, encephalocele, microphthalmos, microcephaly, sutural synostosis, hypertelorism, etc.

2. limbs: single or multiple ring constrictions, most common distally, varying in severity from minor grooves to total amputation, digital fusion, clubfoot deformity, pseudoarthrosis etc.

3. trunk: gastroschisis, omphalocele, malformed genitalia, imperforate anus, hypoplastic lungs, chest deformity, scoliosis, meningomyelocele, ectopia cordis, strangulation of the umbilical cord, etc.

4. other reported abnormalities: association with Ehlers-Danlos syndrome, type IV, and osteogenesis imperfecta; transient oligohydramnios etc.

The differential diagnosis includes the "Michelin tire baby" syndrome; accidental or purposeful band formation around the extremities.

Plain film of both lower legs showed the ring constriction above left ankle joint in the 7-month-old boy (Fig. 1)

REFERENCES:

1. Taybi H, Lachman RS. Radiology of Syndromes, membolic disorders and skeletal dysplasias. Chicago: Year book medical publishers, Inc. 1990.
2. Askins G, et al. Congenital constriction band syndrome. J Pediatr Orthop 1988; 8: 461.
3. Bieber FR, et al. Amniotic band sequence associated with ectopia cordis in one twin. J Pediatr 1984; 105: 817.
4. Chen H, et al. Amniotic band sequence and its neurocutaneous manifestations. Am J Med Genet 1987; 28: 661.
5. Donnenfeld AE, et al. Discordant amniotic band sequence in monozygotic twins. Am J Med Genet 1985; 20: 685.
6. Fisher RM, et al. Limb defects in the amniotic band syndrome. Pediatr Radiol 1986; 5: 24.
7. Fried AM, et al. Omphalocele in limb/body wall deficiency syndrome: atypical sonographic appearance. J Clin Ultrasound 1982; 10: 400.
8. Heifetz SA. Strangulation of the umbilical cord by amniotic bands: Report of 6 cases and literature review. Pediatr Pathol 1984; 2: 285.
9. Herva R, et al. Cluster of severe amniotic adhesion malformations in Finland. Lancet 1980; 1: 818.
10. Hill LM, et al. Prenatal ultrasound diagnosis of a forearm constriction band. J Ultrasound Med 1988; 7: 293.
11. Hudgins RJ, et al. Pediatric neurosurgical implications of the amniotic band disruption complex. Case reports and review of the literature. Pediatr Neurosci 1985; 12: 232.
12. Hunter AGW, et al. Implications of malformations not due to amniotic bands in the amniotic band sequence. Am J Med Genet 1986; 24: 691.

Department of Radiology, Ramathibodi Hospital, Rama 6 Street, Bangkok 10400, Thailand.

13. Johnson CF. Constriction hands. Manifestations of possible child abuse. Case reports and a review. Clin Pediatr (Phila) 1988; 27: 439.
14. Young ID, et al. Amniotic bands in connective tissue disorders. Arch Dis Child 1985; 60: 1061.
15. Zionts LE, et al. Congenital annular bands in identical twins. J Bone Joint Surg (Am) 1984; 66: 450.
16. Zych GA, et al. Congenital band causing pseudarthrosis and impending gangrene of the let. J Bone Joint Surg (Am) 1983; 65: 410.

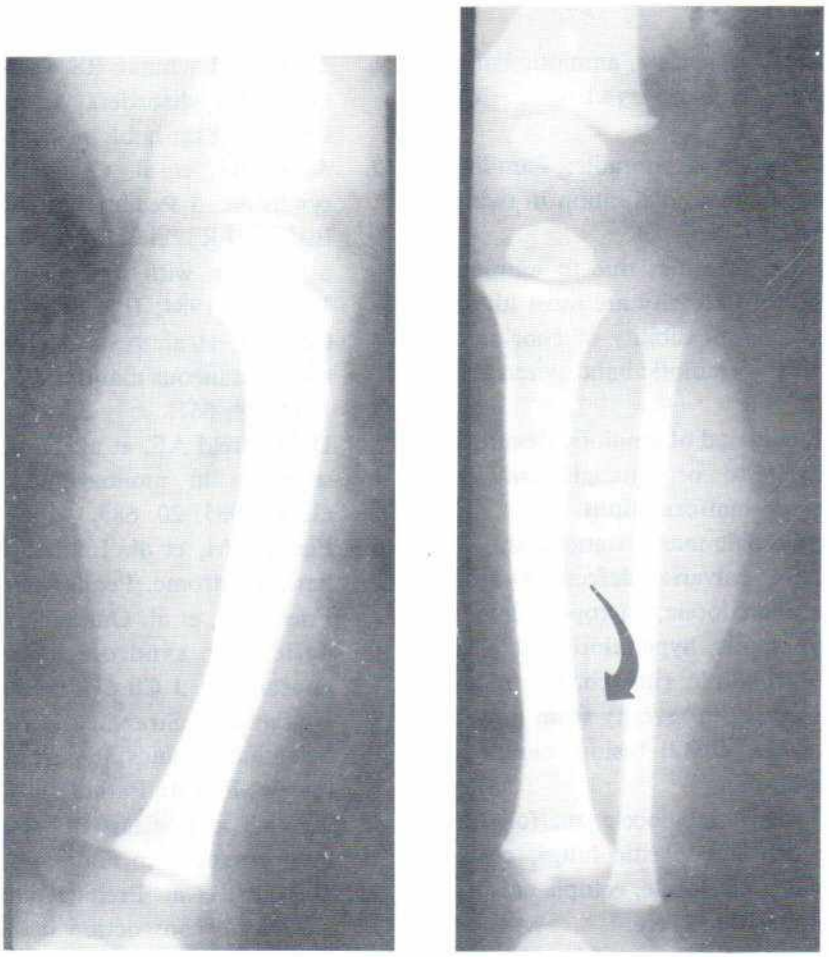

Right leg Left leg

Fig. 1 The ring contriction is noted above the left ankle joint in the 7-month-old boy.

LYMPHEDEMA (NONNE-MILROY TYPE) - A CASE DEMONSTRATION

Patchrin PEKANAN, Boonchuay SATHAPATHAYAVONGS

Lymphedema (Nonne-Milroy type) has its synonyms as Milroy disease, Nonne-Milroy-type hereditary lymphedema. It is autosomal dominant (1-10).

Clinical manifestations are (a) lymphedema, often of the lower limbs; (b) associated reported findings: congenital chylous ascites, protein-losing lymphangiectasia of the bowel, pleural effusion; (c) susceptibility of affected tissues to infection, acute nephritis.

Radiologic manifestations are (a) hypoplasia (decreased number and/or size of subcutaneous lymphatics) or absence of lymphatic channels; (b) dermal lymphatic filling in feet on visual and roentgenographic lymphangiograms; (c) weakness of the lymphatic wall resulting in extravasation; (d) absence of lymphatic valves.

The figure showed generalized thickening of soft tissue of the lower limbs of both sides with diffuse radiolucent lines due to lymphedema. The bony structures appear normal.

Lymphedema classification (1, 11-18)

1. Genetic lymphedema syndromes.
2. Primary lymphatic dysplasia : (a) association with chylothorax, chylous ascites; (b) other reported abnormalities: splenomegaly, thrombocytopenia, afibrinogenemia, hemangioma, lymphangioma, hydrops fetalis, congenital heart disease.
3. Acquired lymphedema.

TABLE I

Hereditary Lymphedema Syndromes

Type	Inheritance	Age at Onset of L	Associated Features
Milroy disease	AD*	At birth	Pleural effusion
Meige Disease	AD	Puberty	
L + intestinal lymphangiectasia	AD	Infancy	Diarrhea, growth failure
L + yellow nails	AD	Adulthood	Pleural effusion
L + distichiasis	AD	Puberty or later	Ectropion of lower lid, spinal anomalies
L + recurrent lymphangitis	AD	Childhood or puberty	
L + recurrent cholestasis (syndrome)	AR	At birth or childhood	May develop into cirrhosis of the liver
L + cerebrovascular anomaly	AD	Puberty or later	Pulmonary hypertension
L + ptosis	AD	Puberty	
L + microcephaly	AD	At birth	
Noonan syndrome	AD	Puberty	
Turner syndrome	"XO"	At birth	

"Modified after Kaarianen H: Hereditary lymphedema: A new combination of symptoms not fitting into present classifications. Clin. Genet. 26:254, 1984.

L = lymphedema; AD* = autosomal dominant; AR = autosomal recessive.

Department of Radiology, Ramathibodi Hospital, Rama 6 Street, Bangkok 10400, Thailand.

REFERENCES:

1. Taybi H, Lachman RS. Radiology of Syndromes, metabolic disorders, and skeletal dysplasias. Chicago: Year book medical publishers, Inc. 1990.
2. Buonocore E, et al. Lymphangiographic evaluation of lymphedema and lymphatic flow. AJR 1965; 95: 751.
3. Feldman MA, et al. Acute nephritis complicating Milroy's disease. Lancet 1987; 1: 336.
4. Gough MH. Primary lymphedema: Clinical and lymphangiographic studies. Br J Surg 1966; 63: 917.
5. Hurwitz PA, et al. Pleural effusion in chronic hereditary lymphedema (Nonne-Milroy-Meigh's disease): Report of two cases. Radiology 1964; 82: 246.
6. Kinmonth JB, et al. Primary lymphoedema: Clinical and lymphangiographic studies of a series of 107 patients in which the lower limbs were affected. Br J Surg 1957; 45: 1.
7. Meige H. Le trophoedeme chronique hereditaire. Nouv Lconogr (Salpetriere) 1889; 12: 453.
8. Milroy WF. An undescribed variety of hereditary edema. N Y Med J 1892; 56: 505.
9. Nonne M. Vier Faelle von Elephantiasis congenital hereditaria. Arch Pathol Anat (Belin) 1891; 125: 189.
10. Schroeder E, et al. Chronic hereditary lymphedema (Nonne-Milroy-Meige's syndromes). Acta Med Scand 1950; 137: 198.
11. Corbett CRR, et al. Congenital heart disease in patients with primary lymphedemas. Lymphology 1982; 15: 85.
12. Crowe CA, et al. A genetic association between microcephaly and lymphedema. Am J Med Genet 1986; 24: 131.
13. Kaariainen H. Hereditary lymphedema: A new combination of symptoms not fitting into present classifications. Clin Genet 1984; 26: 254.
14. Leung AKC. Dominantly inherited syndrome of microcaphaly and congenital lymphedema. Clin Genet d1985; 27: 611.
15. Lewis JM, et al. Lymphedema praecox. J Pediatr 1984; 104: 641.
16. Smeltzer DM, et al. Primary lymphatic dysplasia in children: Chylothorax, chylous ascites, and generalized lymphatic dysplasia. Eur J Pediatr 1986; 145: 286.
17. Vajro P et al. Aagenals' syndrome in an Italian child. Acta Paediatr Scan 1984; 73: 695.
18. Windebank KP, et al. Hydrops fetalis due to abnormal lymphatics. Arch Dis Child 1987; 62: 198.

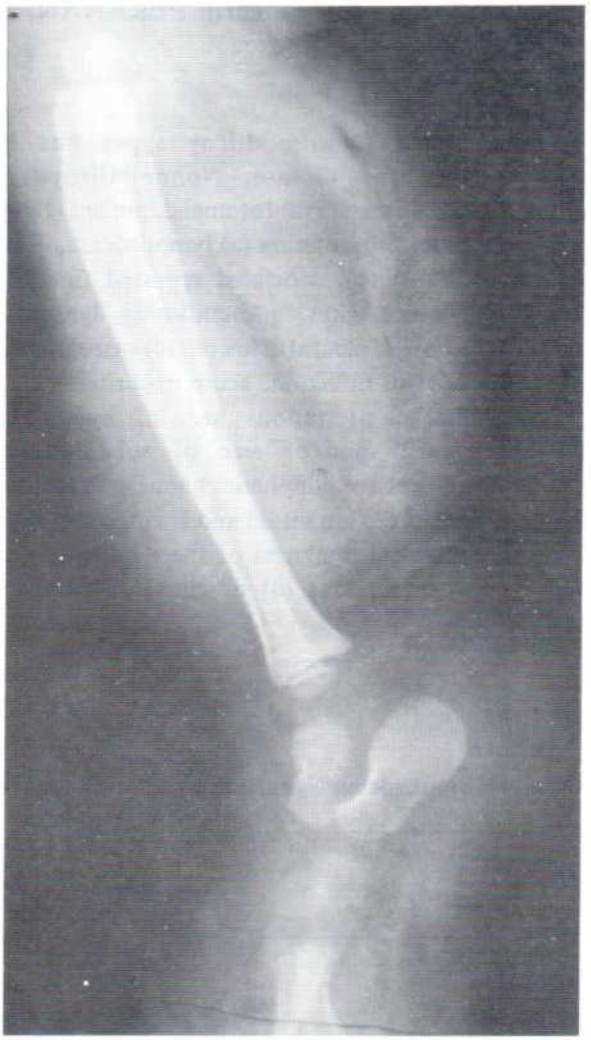

Fig. 1 Generalized thickening of the soft tissue of the lower limb with diffuse radiolucent lines due to lymphedema. The bony structures are normal.

PARASPINAL HEMORRHAGE FROM WHOOPING COUGH

A CASE DEMONSTRATION

Patchrin PEKANAN[1], Boonchuay SATHAPATAYAWONGS,[1] Siripan VONGSHABSHI.[2]

Whooping cough or pertussis is a noninvasive, highly communicable bacterial respiratory illness. It occurs at all ages but is most common and most severe in infants and young children. The etiologic agent of the syndrome is usually Bordetella pertussis. Whooping cough is estimated to cause 600,000 to 1 million deaths yearly in infants from areas where pertussis immunization is not practiced (1-5). Bordetella pertussis is a gram-negative coccobacillus. An estimated 5 to 10 percent of clinical whooping cough is caused by B. parapertussis. The animal pathogen B. bronchieseptica is responsible for a minor percentage of cases.

In nonimmune households, the attack rate is 80-90 percent. Transmission is by droplet infection. Carriers of B. pertussis are found infrequently, but persons previously immunized have been shown during outbreaks of disease to excrete the organism in the absence of clinical symptoms or in the presence of mild or atypical illness.

The incidence of whooping cough is fallen after the 1940's, when immunization of young children became standard practice. Neither immunization against pertussis nor natural disease provides lifelong protection. In the case of immunization, an attack rate greater than 50 percent has been reported when the interval after immunization exceeds 12 years. Adolescents and adults represent a large reservoir of susceptibles who can transmit the disease to unimmunized infants.

Lesions caused by B. pertussis are found principally in the bronchi and bronchioles, but changes are also seen in the nasopharynx, larynx, and trachea. Masses of bacteria and mucopurulent exudate are intertwined with the cilia of the columnar epithelium. There is necrosis of the midzonal and basilar epithelium with infiltration of polymorphonuclear leukocytes and macrophages. The most frequent findings in the lung are bronchopneumonia, interstitial pneumonitis, and numerous small areas of atelectasis. The brain can show edema and scattered petechiae at autopsy.

Whooping cough begins with symptoms indistinguishable from those of a mild viral upper respiratory infection. Sneezing is frequent, conjunctivae are injected, and a nocturnal cough appears. The temperature may be slightly elevated.

Seven to 14 days after onset, the cough becomes more frequent, then paroxysmal. In a typical paroxysm there is a series of 15 to 20 short coughs of increasing intensity, and then a deep inspiration, making the "whoop". A tenacious mucous plug is usually expelled, and vomiting frequently follows. Paroxysms may occur as often as every half hour and are accompanied by signs of increased venous pressure, including deeply engorged conjunctivae, periorbital edema, petechial hemorrhages, particularly about the forehead, and epistaxis. The chest roentgenogram sometimes reveals hilar and mediastinal nodal enlargement.

This 2 months-old boy developed thoracic paraspinal hemorrhage due to severe cough in the course of the disease-whooping cough. Figure I showed a sharp border paraspinal mass at mid and lower thoracic level. Bony structures appeared intact.

REFERENCES:

1. Wyngaarden JB, Smith LH, Bennett JC. Cecil Textbook of Medicine. Philadelphia: W.B. Saunders Company, 1992.
2. Geller RJ. The pertussis syndrome: A persistent problem. Pediatr Infect Dis J 1984; 3: 182.
3. Griffin MR, Ray WA, Mortimer EA. Risk of seizures and encephalopathy after immunization with the diphtheria-tetanus-pertussis vaccine. JAMA 1990; 263: 1641.
4. Pittman M. The concept of pertussis as a toxin-mediated disease. Pediat Infect Dis 1984; 3: 467.
5. Wardlaw AC, Parton R (eds). Pathogenesis and immunity in pertussis. New York: John Wiley and Sons, 1988.

[1] Department of Radiology, Ramathibodi Hospital, Rama 6 Street, Bangkok 10400, Thailand.

[2] Department of Radiology, Bangkok Christian Hospital, Silom Street, Bangkok, Thailand.

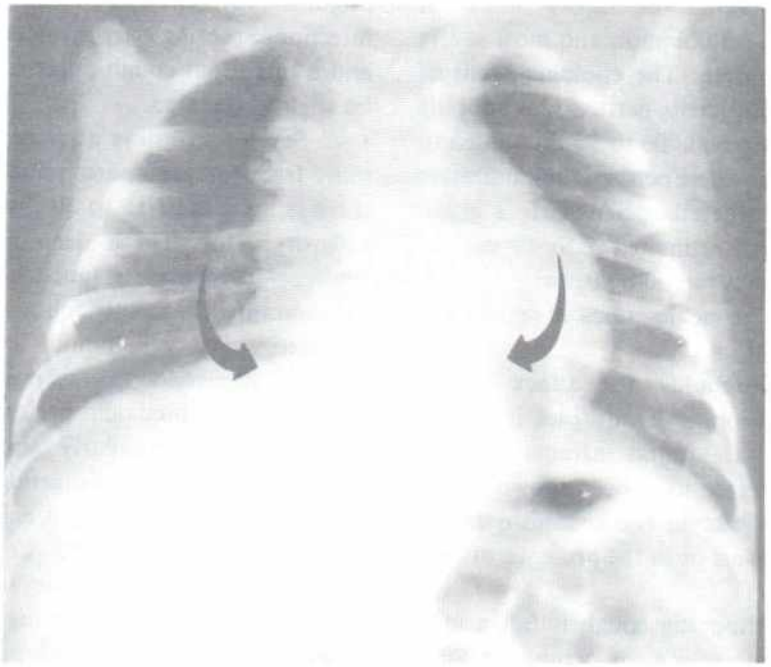

Fig. 1 Bilateral paraspinal hemorrhage in the 2 months-old boy, demonstrated by plain chest film.

MAGNETIC RESONANCE IMAGING IN SOFT TISSUES MASSES OF THE MUSCULOSKELETAL SYSTEM

Dr. M A Png, MBBS, FRCR, Senior Registrar [1,3]
Dr. T S G Chee, MBBS, FRCR, Consultant [2]

ABSTRACT

The MR images of 27 soft tissue lesions were retrospectively reviewed to assess the accuracy of MR in distinguishing benign from malignant lesions based on their morphological characteristics. Gadolinium-DTPA was also given in 16 and the pattern of enhancement was evaluated to determine whether this was helpful. Results were correlated with histological findings. 81.5% of lesions were correctly classified and the MR features were sufficiently characteristic to allow a specific diagnosis in 13 (48.0%) lesions (including cysts) and 7 (33.3%) tumours.

Key Words: MRI, soft tissue tumour, benign, malignant, enhancement.

INTRODUCTION

Magnetic resonance (MR) imaging has become the investigation of choice for the evaluation of soft tissue masses. This is due to its superior lesion definition and therefore more accurate assessment of size and extent as compared to computed tomography (CT). It has also been said that in many cases, the nature of the lesion can be reliably predicted by morphologic features noted on the MR examination. It is controversial whether MR imaging can reliably differentiate benign from malignant lesions.

Our aim was to review the MR findings in extremity soft tissue tumours to determine whether benign and malignant lesions can be reliably differentiated based on morphological characteristics and pattern of enhancement and to ascertain the reliability of tissue characterization based on MR.

MATERIALS AND METHODS

We retrospectively reviewed the MR images of 27 patients with extremity soft tissue masses diagnosed clinically who came for MR between October 1991 and September 1992. There were 14 male patients and 13 females with ages ranging from 11 years to 75 years. 4 of the masses were located in the upper extremity, 22 in the lower extremity and 1 in the buttocks. 3 were recurrent tumours but assessment was made without knowledge of the previous histology. 22 were proven to be benign on histology and 5 were malignant.

All MR scans were performed with a 1.0 Tesla Siemens Magnetom Impact scanner. Both T1-weighted and T2-weighted conventional spin-echo sequences were performed in all cases and intravenous contrast (7-10 mls of Gadolinium-DTPA) was given only when deemed necessary.

(1) Department of Diagnostic Radiology, Singapore General Hospital Pte.Ltd.
(2) Department of Diagnostic Imaging, Tan Tock Seng Hospital Pte.Ltd.
(3) Correspondence : Dr. M A Png, c/o Department of Diagnostic Radiology, Singapore General Hospital Pte.Ltd., Outram Road, Singapore 0316.

Differentiation of malignant and benign lesions was predicted based on the morphologic appearances (signal homogeneity, margin definition and involvement of neuovascular structures and bone). After Gadolinium-DTPA, lesions were assessed for the presence of enhancement and the enhancement pattern.

All cases had histological confirmation except case 4. This case had needle aspiration which yielded gelatinous liquid and a presumptive diagnosis of a bursal cyst was made.

In our study, we found that MR was able to tissue characterize 13 out of 27 (48.0%) lesions and this made it possible to suggest the final diagnoses. Of these, there were 4 lipomas, 1 well-differentiated liposarcoma, 3 bursal cysts, 1 meniscal cyst, 2 haemangiomas and 2 ganglion cysts. When cystic lesions were excluded specific diagnoses were possible in 7 out of 21 cases (33.3%).

Classification of the masses into benign and malignant categories was correctly made in 22 out of 27 cases (81.5%). However, 1 case which was classified by the pathologist as a benign granular cell tumour with malignant potential presented 4 years later with 3 soft tissue masses in the ipsilateral thigh and calf plus inguinal lymphadenopathy. Histology of the tumour in the thigh showed groups of cells with abundant cytoplasm and occasional mitoses consistent with a granular cell tumour. The histology was similar to that of the previous tumour. However, based on the evidence of tumour recurrence and the size of the tumour, the pathologist concluded that the tumour behaviour was malignant.

Intravenous contrast was given in 16 cases. We found that the presence of enhancement alone did not help in differentiating benign from malignant lesions. We feel it is necessary to assess the pattern of enhancement together with the morphologic appearance. Enhancement was present in 10 out of 11 (90.9%) benign lesions and 4 out of 5 (80.0%) malignant lesions. Of the 10 benign lesions which showed enhancement, 3 showed minimal enhancement, 2 showed peripheral enhancement (1 bursal cyst and 1 case of chronic synovitis), 2 homogeneous enhancement (1 false aneurysm and 1 neurilemmoma) and 3 showed patchy enhancement (1 hamartoma, 1 granular cell tumour and 1 aggressive fibromatosis).

1 malignant lesion showed no enhancement. This was a recurrent malignant fibrous histiocytoma. In the 4 malignant lesions which enhanced, all showed a patchy pattern.

DISCUSSION

There have been a number of previous reports concerning the value of MR in the evaluation of soft tissue tumours. The ability to characterize lesions and to differentiate benign and malignant lesions has been assessed. It remains controversial whether MR imaging can differentiate benign from malignant masses reliably.

Kransdorf et al[1] retrospectively studied 112 soft tissue masses by MR and conclude that MR was sufficiently characteristic to allow a specific diagnosis in 27 (24%) of cases but was incapable of reliably distinguishing between benign and malignant soft tissue tumours. However, I note that this group of authors studied MR characteristics (margin definition, signal intensity, inhomogeneity, surrounding soft tissue oedema and involvement of neurovascular structures and bone) independently rather than in concert when attempting to differentiate benign from malignant lesions and it would therefore be more accurate to conclude from their study that no one criteria was reliable in differentiating benign from malignant lesions.

On the other hand, Berquist et al,[2] using the same criteria with the addition of lesion size, studied 95 lesions and found that the specificity and accuracy of diagnosis averaged 90% for both benign and malignant lesions and the negative predictive value for malignancy averaged 94%. They confirmed that benign lesions tended to be well-marginated, have homogenous signal intensity and do not encase neurovascular structures or invade bone. Malignant lesions generally have irregular margins and inhomogeneous signal and more often encase neurovascular structures and involve bone. In their series, they noted that the benign lesions that were often classified incorrectly were desmoid tumours (also called aggressive fibromatosis) and necrotic benign neoplasms (e.g. neurofibromas). The malignant lesion most commonly misdiagnosed as benign was synovial sarcoma.

Our results support previous authors findings that MR can often successfully characterize soft tissue masses allowing a specific diagnosis. With the availability of fat suppression techniques, this will be even more reliably achieved. The lesions we were able to characterize successfully were benign cysts, haemangiomas and benign and malignant lipomatous lesions. Benign cysts showed low to intermediate signal on T1-weighted sequences and high signal intensity on T2-weighted sequences. They show either no enhancement or a thin rim of peripheral enhancement in the wall of the lesion. Soft tissue haemangiomas may be hyperintense on

RESULTS

Case No.	Actual Histology	Tissue Characterisation	Correct Classification into Benign and Malignant	Specific Diagnosis	I/V Gd-DTPA	Enhancement Pattern
1	Intramuscular lipoma	Yes	Yes	Yes	No	—
2	Metastatic adenocarcinoma	No	Yes	No	Yes	Marked, Patchy
3	Bursal cyst	No	Yes	No	No	—
4	Bursal cyst	Yes	Yes	Yes	No	—
5	Ganglion	Yes	Yes	No	No	—
6	Hamartoma	No	No	No	Yes	Marked, Patchy
7	Bursal cyst	Yes	Yes	Yes	Yes	Yes, peripheral
8	Granular cell tumour	No	No	No	Yes	Yes, slightly patchy
9	Chronic synovitis	No	Yes	No	Yes	Yes, peripheral
10	Well-differentiated liposarcoma	Yes	Yes	Yes	Yes	Yes, patchy
11	Intramuscular lipoma	Yes	Yes	Yes	No	—
12	False aneurysm	No	No	No	Yes	Yes, homogeneous
13	Haematoma	No	Yes	No	No	—
14	Meniscal cyst	Yes	Yes	Yes	Yes	No
15	Intramuscular rupture of adductor longus	No	Yes	No	Yes	Yes, minimal
16	Neurilemmoma	No	Yes	Yes	Yes	Yes, homogeneous
17	Haemangioma	Yes	Yes	Yes	No	—
18	Capillary haemangioma	Yes	Yes	Yes	Yes	Yes, minimal
19	Benign fibrous proliferation	No	Yes	No	Yes	Yes, minimal
20	Ganglion	Yes	Yes	Yes	No	—
21	Lipoma	Yes	Yes	Yes	No	—
22	Low grade fibrosarcoma	No	Yes	No	Yes	Yes, patchy
23	Ganglion	Yes	Yes	Yes	No	—
24	Intramuscular lipoma	Yes	Yes	Yes	No	—
25	Recurrent aggressive fibromatosis	No	No	No	Yes	Marked, patchy
26	Recurrent malignant fibrous histiocytoma	No	Yes	No	Yes	No
27	Recurrent low grade myxoid liposarcoma	No	Yes	No	Yes	Yes, patchy

T1-weighted sequences due to the presence of fat. They showed high signal on T2-weighted sequences. They can be definitively diagnosed by the presence of flow voids due to vascular channels. Lipomatous lesions showed high signal intensity on both T1-weighted and T2-weighted spin echo sequences similar to the subcutaneous fat. However, it is worthwhile noting that the absence of fat signal on the MR examination did not exclude a liposarcoma as evidenced by case 27, a recurrent myxoid liposarcoma. This has been noted by previous authors.[1,3,4] Although we had no cases of pigmented villonodular synovitis, it is said to have fairly typical MR features. It shows a heterogeneous pattern of varied signal intensities on T1-weighted and T2-weighted images which is dependent on the relative proportion of lipid, haemosiderin, fluid, cellular elements and fibrous stroma. A low signal intensity rim may be produced by a fibrous capsule or peripheral haemosiderin.[5]

In our study we could not reliably distinguish between malignant and benign lesions based on MR characteristics and the contrast enhancement pattern. We note that it is worthwhile to take into account the plain radiographic findings when interpreting the MR. Take for example case 6 : the presence of phleboliths and organized periosteal reaction on the plain radiograph would point to a benign lesion. It is well known that MR is not sensitive for detecting calcification and does not show periosteal changes well. In some cases such as this, CT may provide additional information with regard to periosteal changes and calcifications that may not be shown on MR.

Herrlin et al[6] has suggested that T1-weighted Gadolinium sequences may be of value in differentiating benign from malignant lesions. However, in their series there were relatively few benign tumours. Our series on the other hand has few malignant lesions. We found that the presence of enhancement alone was not a useful criterion as many benign lesions showed enhancement. However, we found that patchy enhancement was a useful finding as this was present in 4 out of 5 the malignant lesions but only 3 out of 11 benign lesions. Peripheral and homogeneous enhancement was only seen with benign lesions in our study. However, our sample group was small so it is not possible to generalize. Indeed, it has been reported that neurogenic tumours (benign or malignant) have a varied appearance on post-contrast T1-weighted sequences. Their enhancement pattern may be homogeneous, inhomogeneous or peripheral depending on the degree of cystic degeneration.[7] In view of the additional cost of contrast administration, it would be important to do further studies to determine whether routine administration of contrast in patients with soft tissue tumours is justified.

More recent literature suggests that phosphorus-31 (^{31}P) MR spectroscopy may improve the diagnostic specificity of MR imaging in differentiating benign from malignant soft tissue tumours. Negendank et al[8] and Zlatkin et al[9] have found that malignant lesions can be distinguished from benign lesions on the basis of significantly higher mean peak ratios of phosphomonoester to ß-nucleoside triphosphate and phosphodiester to nucleoside triphosphate (NTP), a significantly lower mean peak ratio of phosphocreatine to NTP and a higher mean pH.

SUMMARY

In our small study, we have found that although MR can suggest whether a soft tissue lesion is benign or malignant, it is not reliable. Lesions in which a specific diagnosis can be made include benign cystic lesions, lipomatous lesions and haemangiomas.

Contrast enhancement may be a helpful adjunct to T1 and T2-weighted imaging but is again not reliable in differentiating benign from malignant lesions.

ACKNOWLEDGMENTS

The authors would like to thank Mr. A Rahmad for his photographic assistance.

REFERENCES

1. Kransdorf MJ, Jelinek JS, Moser RP Jr, Utz JA, Brower AC, Hudson TM et al. Soft-tissue masses: Diagnosis using MR imaging. AJR 1989; 153: 541-7.
2. Berquist TH, Ehman RL, King BF, Hodgman CG, Ilstrup DM. Value of MR imaging in differentiating benign from malignant soft-tissue masses. AJR 1990; 155: 125-5.
3. Petasnick JP, Turner DA, Charters JR, Gitelis S, Zacharias. Soft-tissue masses of the Locomotor System : Comparison of MR Imaging with CT. Radiology 1986; 160: 125-33.
4. Armstrong SJ, Wakeley CJ, Goddard PR, Watt I. Review of the Use of MRI in Soft Tissue Lesions. Clin Rad 1992; 46: 311-7.
5. Mink JH, Deutsch AL, editors. MRI of the Musculoskeletal System, A Teaching File. 1st ed. New York: Raven Press, 1990.

6. Herrlin K, Ling LB, Pettersson H, Willen H, Rydholm A. Gadolinium-DTPA enhancement of soft tissue tumours in MRI. Acta Radiol 1990; 31 (3): 233-6.
7. Berquist TH, editor. MRI of the Musculoskeletal System. 2nd ed. New York: Raven Press, 1990.
8. Negendank WG, Crowley MG, Ryan JR, Keller NA, Evelhoch JL. Bone and soft-tissue lesions: Diagnosis with combined H-1 and P-31 MR spectroscopy. Radiology 1989; 173: 181-8.
9. Zlatkin MB, Lenkinski RE, Shinkwin M, Schmidt RG, Daly JM, Holland GA et al. Combined MR imaging and spectroscopy of bone and soft tissue tumors. J Comput Assist Tomogr 1990; 14: 1-10.

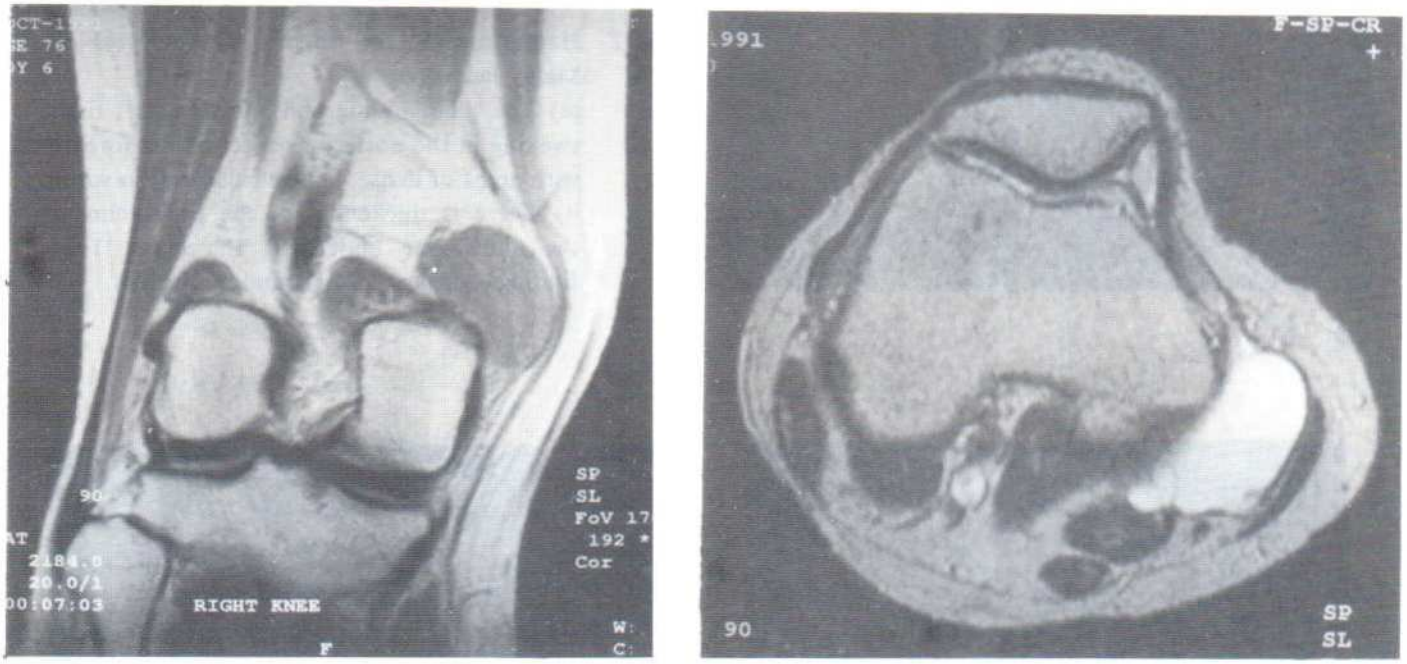

Fig. 1 Gastrocnemius-semimembranosus bursal cyst in a 86 year old Chinese lady. MR shows a well-defined mass of low signal intensity on the (a) intermediate-weighted coronal image and homogeneous high signal intensity on the (b) T2-weighted transaxial image, suggesting it is cystic. It is located deep to the semimembranosus and sartorius muscles and lateral to the medial head of the gastrocnemius muscle and has fine septations within it.

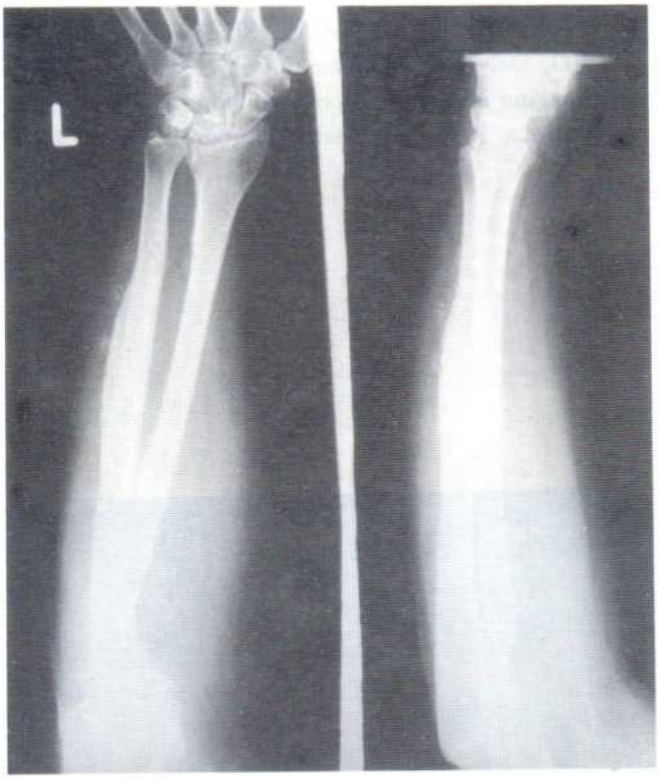

Fig. 2a

Fig. 2 Hamartoma in the forearm of a 49 year old Malay lady.
(a) The plain radiograph shows a soft tissue swelling in the posterior aspect of the forearm with areas of dense, coarse calcification within it. There is thickening of the periosteum of the ulna bone underlying the mass. These findings suggest a long-standing process.

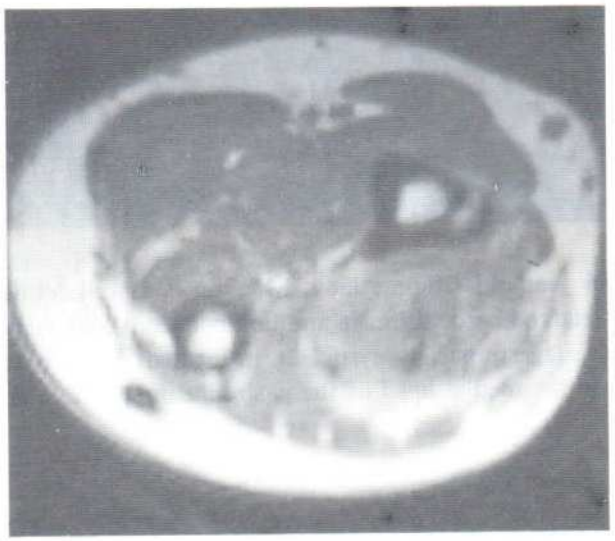

Fig. 2b

(b) Axial T1-weighted spin echo image shows a mass in the posterior compartment which has poorly-defined margins.

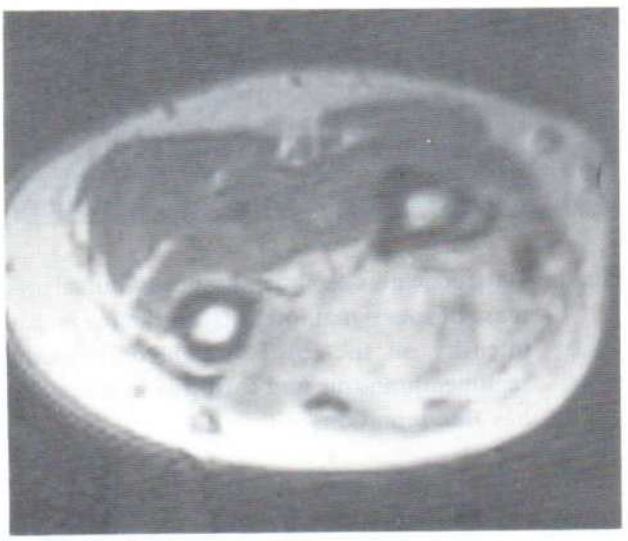

Fig 2c

(c) Post-Gadolinium axial T1-weighted scan shows avid but patchy uptake of contrast. This was thought to be a malignant soft tissue tumour.

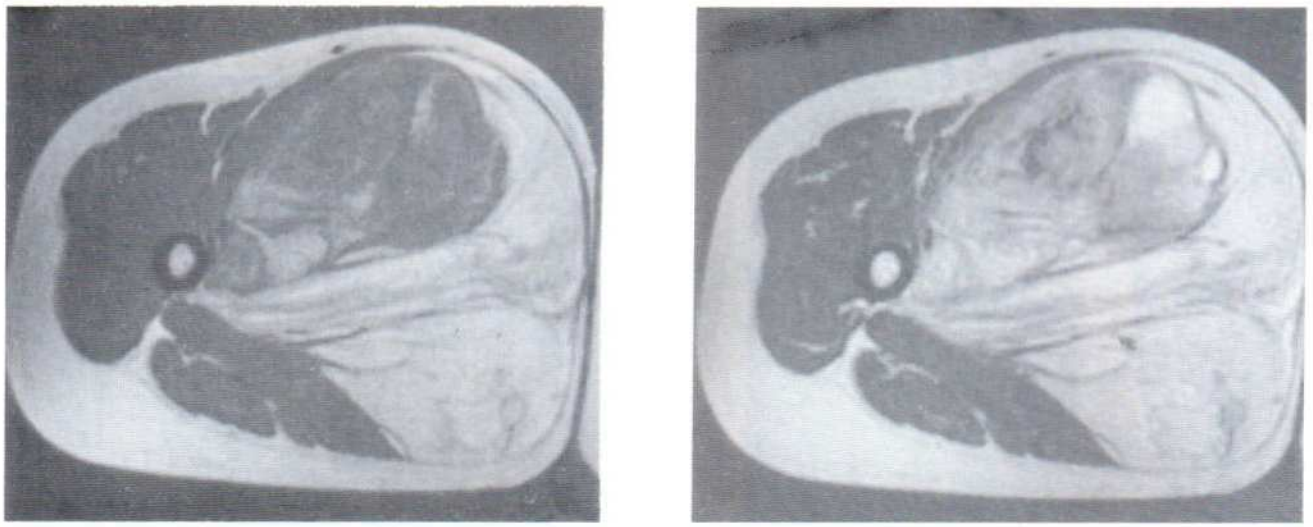

Fig. 3 Liposarcoma in the thigh of a 45 year old Chinese female. MR shows a large mass involving the adductor compartment which has heterogeneous signal characteristics. There are large areas of high signal on the (a) axial T1-weighted sequence (SE 750/15) and intermediate to high signal on (b) T2-weighted (SE 2024/60) sequences similar to the signal seen in the subcutaneous fat. In addition, there is an area which is of low signal on T1-weighted sequences and high signal on T2-weighted sequences. The findings were highly suggestive of a liposarcoma.

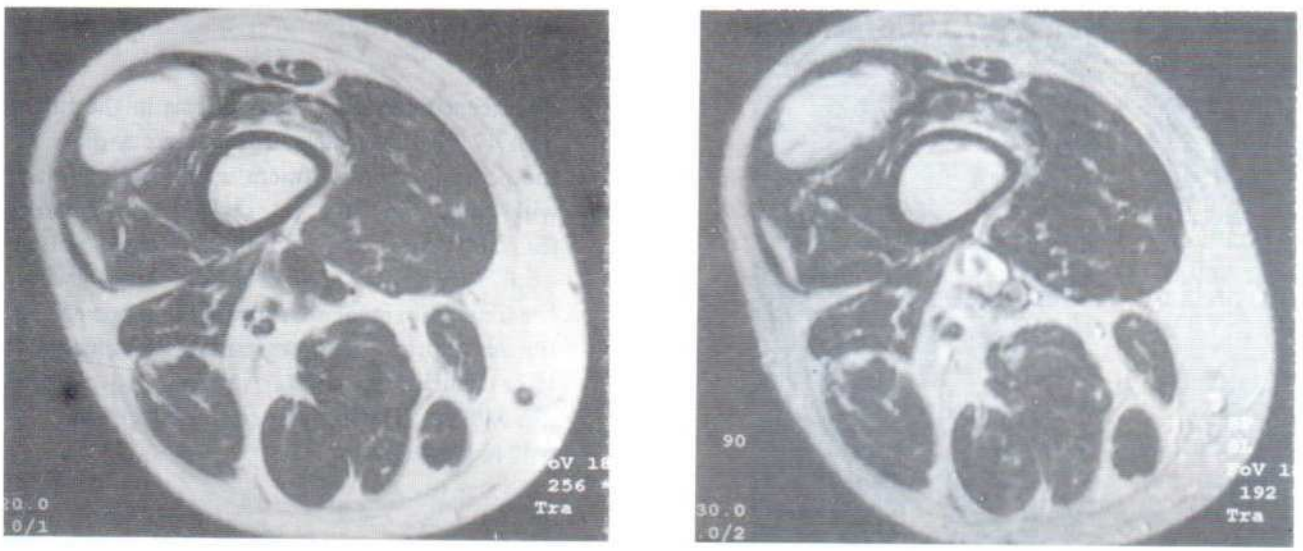

Fig. 4 Intramuscular lipoma in the thigh in a 45 year old Chinese lady (a) Axial T1-weighted and (b) axial T2-weighted MR images shows a well-defined mass in the vastus lateralis. It displays high signal on both the T1-weighted and T2-weighted spin-echo sequences with signal characteristics similar to that of the subcutaneous fat. There are fine septae within it. The features are suggestive of a lipomatous lesion, most likely an intramuscular lipoma.

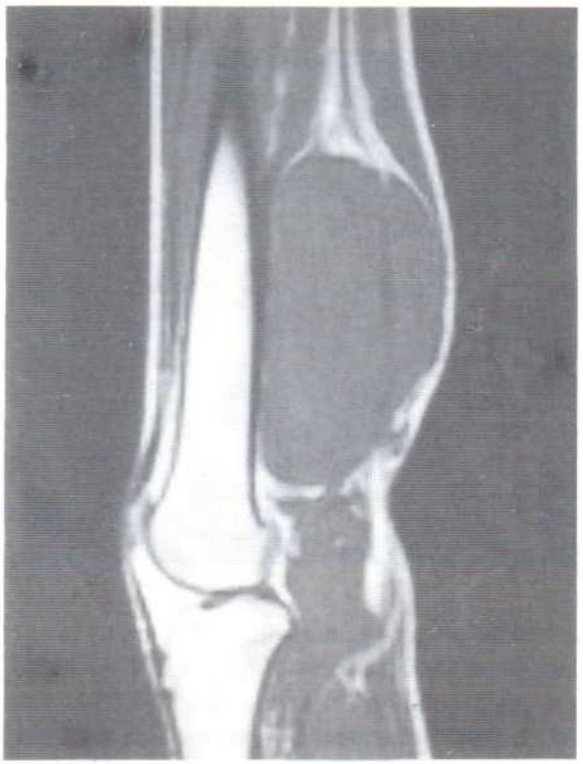

Fig. 5a

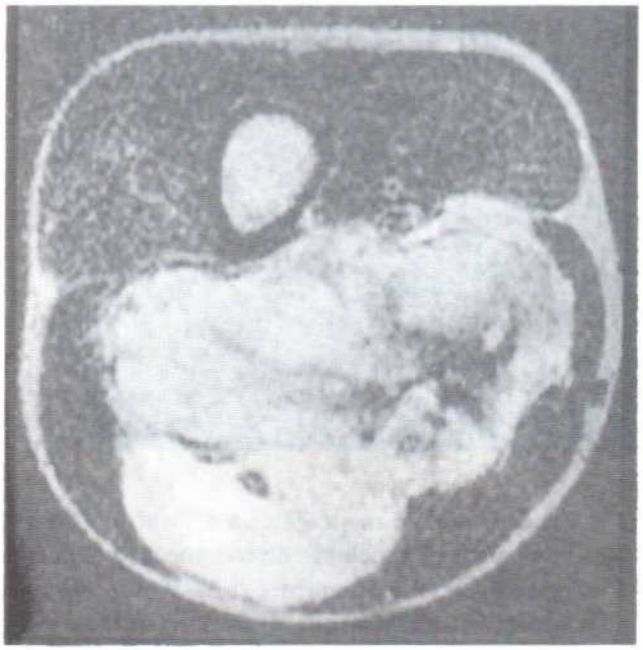

Fig. 5b

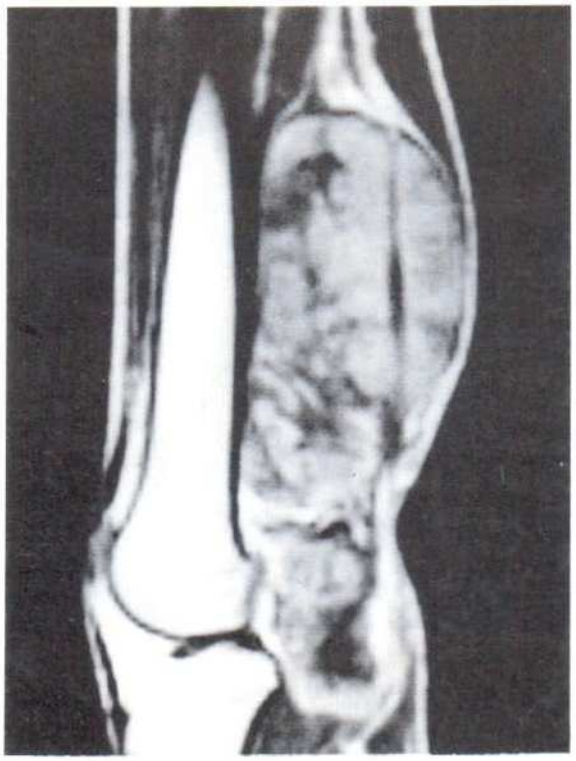

Fig. 5c

Fig. 5 Recureent aggressive fibromatosis in the thigh in a 17 year old male. MR shows a mass in the posterior compartment which is isointense with muscle on the (a) sagittal T1-weighted (SE 580/15) image and hyperintense on (b) axial T2-weighted (SE 2900/80) image except for some low signal areas probably representing fibrous septae. It shows patchy enhancement after contrast on the (c) sagittal T1-weighted (SE 580/15). The findings suggested a malignant soft tissue tumour.

THE PREOPERATIVE DIAGNOSIS OF PRIMARY ALDOSTERONISM BY THIN-SECTION COMPUTED TOMOGRAPHY

Malai MUTTARAK, M.D., Saowalak DEEWIJIT, M.D.,

ABSTRACT

Primary aldosteronism or Conn's syndrome is characterized by hypertension and hypokalemia resulting from elevated aldosterone. Up to 80% of cases are due to adrenocortical adenoma and the remaining 20% of cases are due to bilateral adrenal hyperplasia. Fewer than 1% of cases are due to carcinoma. The radiologic distinction between adenoma and hyperplasia is important because the treatment for adenoma is adrenalectomy, whereas medical therapy is indicated in hyperplasia. Several techniques have been used to make this distinction including: adrenal venous sampling, adrenal venography, scintigraphy, CT and MR imaging. Adrenal venous sampling and venography are invasive procedures even when done by the most experienced angiographer. Scintigraphy and MR imaging are not widely available. Many studies have advocated computed tomography in the investigation of patients with primary aldosteronism. We present 5 cases of primary aldosteronism due to functioning adrenocortical adenomas correctly diagnosed by thin-slice CT. All adenomas were less than 2 cm. with homogeneous low density.
We propose that CT should be the investigation of choice for patients with clinically suspected primary aldosteronism.

INTRODUCTION

Primary aldosteronism, or Conn's syndrome, is characterized by hypertension, hypokalemia and metabolic alkalosis resulting from the hypersecretion of the adrenal mineralocorticoid aldosterone. It is an unusual cause of hypertension but curable by surgery, as most cases (70-80%) result from single adrenocortical adenoma. The remaining cases result from bilateral adrenocortical hyperplasia and, rarely, adrenocortical carcinoma. Several techniques have been used in the evaluation of primary aldosteronism to distinguish adenoma from hyperplasia so that surgery is performed only in case of an adenoma.[1-7]

We present the value of thin-section CT in the evaluation of 5 patients with primary aldosteronism.

MATERIALS AND METHODS

Five patients with a diagnosis of primary aldosteronism were evaluated by CT examination during the past 4 years. There were 4 women and 1 man, 28-41 years old (mean 35 years). CT scans were obtained on a Hitachi W500 (3 patients) and General Electric 3000 i (2 patients) scanner. Plain and contrast scans with contiguous 5 mm-thick sections were performed in all cases. In one patient, additional contiguous 2 mm-thick sections wer made. Adrenalectomy was performed in all patients.

RESULTS

CT accurately localized the tumors in all cases. Adenoma appeared as a nodule of homogeneous low

Department of Radiology, Faculty of Medicine, Chiang Mai University, Chiang Mai 50200 THAILAND.

density (Fig. 1,2) with no additional diagnostic information after contrast enhancement. Tumor size ranged from 8-12 mm. Four masses were detected in the left adrenal gland and one in the right adrenal gland. Adenoma was confirmed on pathologic examination in all patients.

DISCUSSION

Accurate preoperative localization of an adrenocortical adenoma is essential for optimal surgical management in patient with primary aldosteronism. Most aldosteronomas are smaller than 2 cm. Previously reported CT sensitivity before, thin-section, high-resolution CT image were available ranged from 58-75%.[1-2] As the spatial resolution of CT scanners has increased, the sensitivity of CT in showing small aldosteronomas has improved.[8-10] Our results show that 5 mm-section CT is highly sensitive in detecting aldosteronoma as the lesions in all 5 patients were smaller than 1.5 cm. In our series there were no false positives. However, we have only 5 cases which is too small to have much statistical power.

Several other techniques, including adrenal vein hormone sampling, ^{131}I-6B-iodomethyl-19-norcholesterol (NP-59) scintigraphy and MR have been used to distinguish an aldosteronoma from hyperplasia. In 1983, Geisinger et al[2] reported that selective adrenal venous sampling for aldosterone level is the most sensitive for detecting aldosteronomas. However, this method is invasive, difficult to perform even by the most experienced angiographer. We have no experience in using this technique.

Ikeda et al[6] reported 100% sensitivity of NP-59 scintigraphy in detection of an aldosteronoma. In fact, NP-59 scintigraphy is not specific for aldosteronama. It is sensitive to detect hyperfuntioning adrenal cortical tumors, particularly in patients with Cushing syndrome.[7] NP-59 scintigraphy is useful in evaluating adrenal masses occuring in the oncologic patient, to distinguish adenoma from metastasis. However, NP-59 is an investigational drug and is not commercially available.

MR signal intensity or relaxation time characteristics are not useful in characterizing adrenal cortical hyperfunctioning lesions.[5,11] Its inability to detect small nodules is also a major limitation. Ikeda et al[6] found MR had lower specificity and accuracy for adenoma identification than either CT or NP-50 scintigraphy.

CT is now widely available, noninvasive, and can be performed on an outpatient basis. With recent improvement in CT technology, detection of small adenomas is now a reliable procedure. Although the number of patients in this study is too small to have statistical significance we suggest that CT should be the investigation of choice for patients with a clinically suspected primary aldosteronism.

ACKNOWLEDGEMENT

We are grateful to Dr. Ezekiel Freed (Northridge Medical Center, LA, USA) for his kindly reviewing the manuscript.

REFERENCES:

1. Dunnick NR, Doppman JL, Gill JR, et al. Localization of functional adrenal tumors by computed tomography and venous sampling. Radiology 1982; 142: 429-33.
2. Geisinger Ma, Zelch MG, Bravo EL, et al. Primary hyperaldosteronism: Comparison of CT, adrenal venography, and venous sampling. AJR 1983; 141: 299-302.
3. Huebner KM, Treugut H. Adrenal cortex dysfunction: CT findings. Radiology 1984; 150: 195-9.
4. Conn JW. Primary aldosteronism, a new clinical syndrome. J Lab Clin Med 1955; 45: 3: 17.
5. Glazer GM, Francis IR, Ouint LE. Imaging of the adrenal glands. Invest Radiol 1988; 23: 3-11.
6. Ikada DM, Fzancis IR, glazr GM, et al. The detection of adrenal tumors and hyperplasia in patients with primary aldosteronism: Comparison of scintigraphy, CT and MR imaging. AJR 1989; 153: 301-6.
7. Dunnick NR. Adrenal imaging: Current status. AJR 1990; 154: 927-36.
8. Francis IR, Gross MD, Shapiro B, et al. Integrated imaging of adrenal disease. Radiology 1992; 184: 1-13.
9. Doppman JL, Gill JR, Mill DL, et al. Distinction between hyperaldosteronism due to bilateral hyperplasia and unilateral aldosteronoma: Reliability of CT. Radiology 1992; 184: 677-82.
10. Dunnick NR, Leight GS, Roubidoux MA, et al. CT in the diagnosis of primary aldosteronism: Sensitivity in 29 patients. AJR 1993; 160: 321-4.
11. Remer EM, Weinfeld RM, Glazer Gm, et al. Hyperfunctioning and nonhyperfunctioning benign adrenal cortical lesions: Characterization and comparison with MR imaging. Radiology 1989; 171: 681-5.

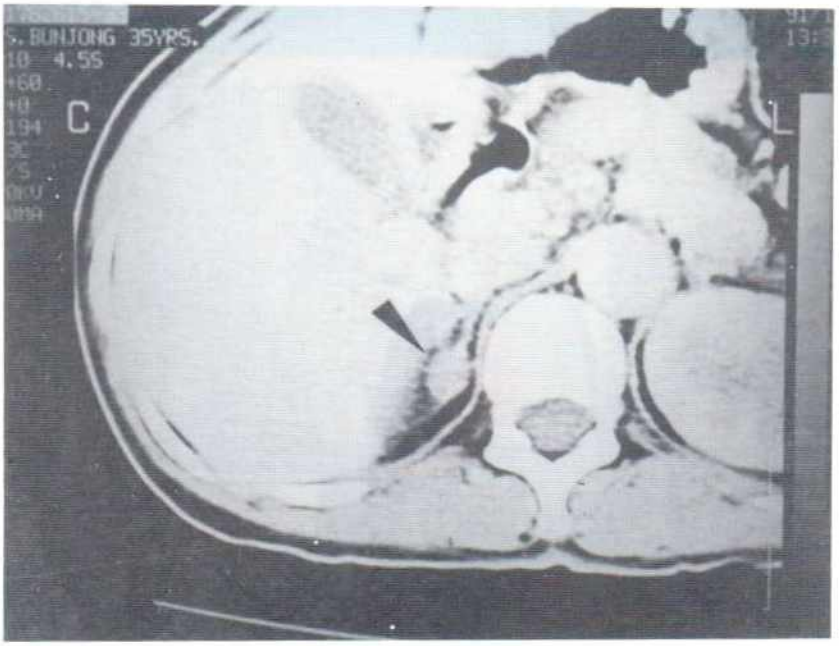

Fig. 1 A 35-year-old woman with hypertension and hypokalemia. Contrast enhancement, 5 mm-thick CT section shows homogeneous low-attenuation right adrenal nodule (arrow head).

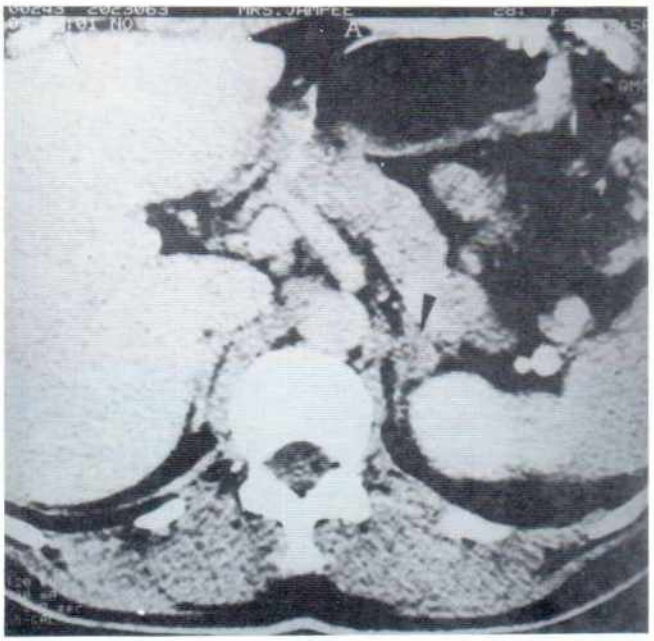

Fig 2. 2 mm-thick sections shows low-attenuation left adrenal nodule (arrow head) in a 28-year-old woman with hypertension and hypokalemia.

Philips Medical Systems

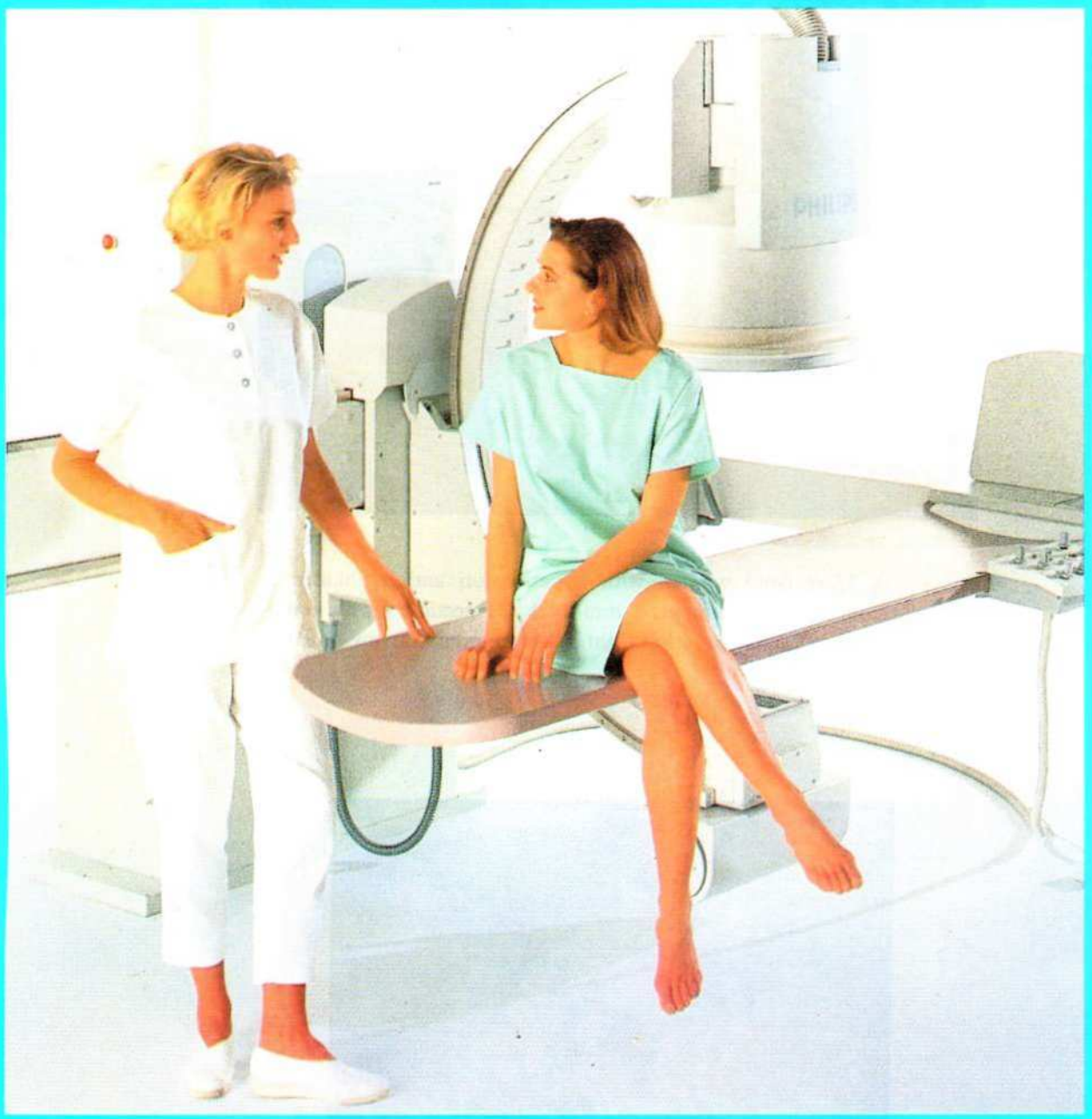

ร่วมสร้างสรรค์สิ่งที่ดีกว่า

Let's make things better

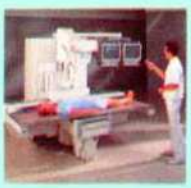

Multi DIAGNOST 3

The Multi DIAGNOST 3 is one of a new generation of remote-controlled systems, complementing the DIAGNOST 93 and DIAGNOST 96. All three systems have an attractive family look. With quality built-in, all were designed to be reliable, easy-to-use, efficient and provide digital image quality second to none.

Philips Medical Systems
Philips Electronics (Thailand) Ltd.
209/2 Sanpavut- Bangna Road Prakanong Bangkok 10260
Tel (662) 745-4090 Fax (662) 398-0792

PHILIPS

PHILIPS

AGGRESSIVE FIBROMATOSIS OF THE EXTREMITIES

Patchrin PEKANAN[1], Sopon KUMPOLPUNTH[1],
Boonchuay SATHAPATAYAVONGS[1],
Pimjai SIRIWONGPAITRAT[1], Sirikan WONGSRISOONTORN[1]

ABSTRACT

Three cases of aggressive fibromatosis of the lower extremities were presented. The patients were female, age ranged from 13 to 27 years old. Ultrasonography showed a mass with infiltrative border and inhomogeneous low echoic pattern. Non contrast CT scan showed isodensity to the muscle. MRI study showed mixed signal on both T1WI and T2WI and strong Gd-DTPA enhancement. Angiography revealed faint tumor stain.

INTRODUCTION

Desmoids or aggressive fibromatosis biologically lie in the interface between exuberant fibroproliferations and low-grade fibrosarcomas. On the one hand, they present frequently as large, infiltrative masses that may recur incomplete excision but, on the other hand, may be small masses composed of well-differentiated fibroblasts that do not metastasize. They may occur at any age but are frequent in the second to fourth decades. Desmoids are divided into extra-abdominal, abdominal and intra-abdominal, but all have essentially similar gross and microscopic features. Extra-abdominal desmoids occur in men and women with equal frequency and arise principally in the musculature of the shoulder, chest wall, back and thigh (1,2). In addition to their possibly being disfiguring or disabling, desmoids are occasionally painful. Although curable by adequate excision, they stubbornly recur in the local site when incompletely removed. The rare reports of metastais of a desmoid must be interpreted as misidentification of a low-grade fibrosarcoma.

CASE REPORTS

CASE 1

A 13-year-old female patient, had a lemon-sized mass at right popliteal fossa. There was no tenderness at the mass. The mass was firm and fixed to the surrounding tissue. She was operated for this problem two years ago. Ultrasonography showed an inhomogeneous low echoic nodule, with infiltrative border at the muscle plane (Fig. 1). At operation, the infiltrative soft tissue mass, size 5 cm, rubbery in consistency, was noted at around popliteal vessels and nerve. The operation was unsuccessful due to vascular injury. Histology revealed aggressive fibromatosis.

CASE 2

A 27-year-old woman, had a recurrent mass at right popliteal fossa for 5 months. She was operated for aggressive fibromatosis at the same area 8 months ago. At physical examination, a 11 cm-diameter mass was seen at right popliteal fossa. The mass was hard and irregular border. Non i.v. enhanced CT scan of the mass showed an isodensity mass, at right popliteal

[1] Department of Radiology, Ramathibodi Hospital, Rama 6 Street, Bangkok 10400, Thailand.

area, involving the subcutaneous fat plane and muscular plane. The density of the mass was 30 H.U. There was no bony involvement (Fig. 2). At angiography, the two lobulated massesd were noted with vascular staining. Small neovasculature was observed (Fig. 2).

CASE 3

A 20-year old woman, had a palpable mass at posterior aspect of the left thigh for 2 years, without tenderness. Plain films at the mass showed no calcification. At angiography, the mass had the tumor stain and small faint neovasculature was observed. There was no bony involvement. At MRI study, the mass had well defined border and mixed signal pattern. On TIWI, two signal pattern was observed, dark grey, grey and faintly bright areas were noted. On T2WI, similar mixed signal pattern was noted, except that the dark grey area turned grey and faintly bright area turned brighter signal-area. Some residual dark grey area was noted. The lesion was totally in the muscle plane (Fig. 3). Gd-DTPA enhancement showed strongly enhanced pattern (fig. 4). Biopsy revealed aggressive fibromatosis.

DISCUSSION

Morphologically, the lesions of aggressive fibromatosis occur as unicentric grey-white, firm, poorly demarcated masses varying from 1 to 15 cm in greatest diameter. They are rubbery and tough and infiltrate surrounding structures. Histologically, they are composed of plump fibroblasts having minimal variation in cell and nuclear size interspersed within a densely collagenous background. Mitoses are infrequent. Regenerative muscle cells when trapped within these lesions may take on the appearance of multinucleated giant cells.

Aggressive fibromatosis at the angle of mandible was demonstrated by ultrasonography by Lewis (3) to be a hypoechoic mass with bone destruction.

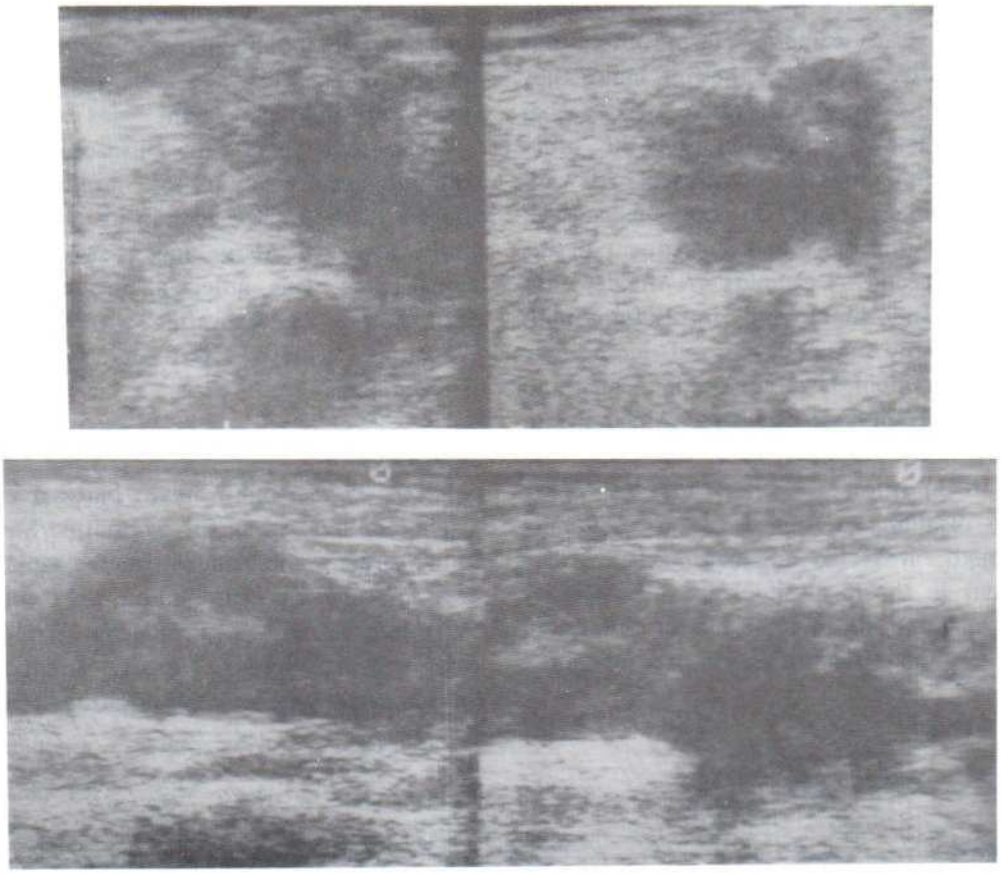

Fig. 1. Case 1. L-and X-section ultrasonography of the mass of fibromatosis showed mixed iso and low echoic lobulated border mass in the muscle plane.

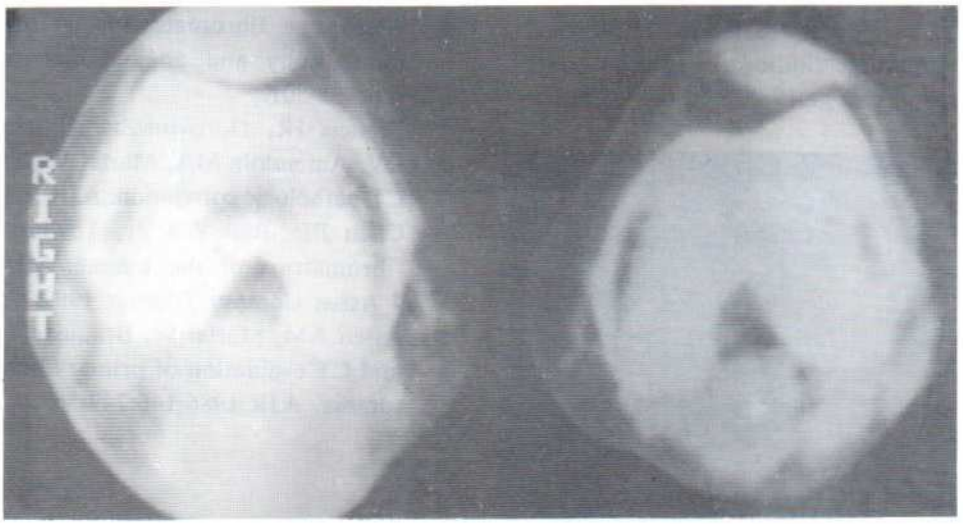

Fig. 2A. Case 2. Non contrast CT scan of the right popliteal area showed a soft tissue mass in the subcutaneous fat plane and muscle plane with the CT density of 30 H.U. which is equal to the muscle of the normal side.

Leibman (4) reported sonographic features of this condition in the breast in two patients. It showed an irregularly shaped hypoechoic mass with lack of posterior attenuation in one case and a hypoechoic mass with internal echoes in the center with decreased through-transmission laterally in another case. The lesion was seen as a hypoechoic nodule of uniform consistency localized superficial to the medial slip of the plantar fascia by Reed (5).

The CT appearance of fibromatoses in childhood was reported by Campbell (6), and in all three cases, the lesions were hypodense on post contrast scans. Hudson (7) reported the CT and angiographic appearance of fibromatoses in 13 cases. They concluded that the tumors were usually better demonstrated after contrast infusion and that no relationship could be established between the vascularity of the tumors and their histologic features. Francis (8) reported four patients with fibromatoses by CT scan. Three of the patients had the lesions which were hyperdense relative to the skeletal muscle on non contrast scans and one patient had the lesion which was hypodense. The lesion post contrast enhancement showed a variable appearance; ranged from minimal contrast enhancement, mixed hyperdense and hypodense areas and uniformed hyperdense lesions. Chen (9) reported MR demonstration of aggressive fibromatosis of the tongue. It showed the mass to be mildly hypointense on T1-weighted image and minimally hyperintense on T2-weighted image. Aisen (10) reported two cases of this condition by MRI study, the lesions were low signal intensity on both images sequence.

In conclusion, the imaging by ultrasonography, angiography, CT scan and MRI study of this condition is not specific and biopsy is needed for the definitive diagnosis.

REFERENCES

1. Cotran RS, Kumar V, Robbins SL. Robbins; Pathologic basis of disease. Philadelphia: W.B. Saunders Company, 1994.
2. Markhede G. Extra-abdominal desmoid tumors. Acta Orthop Scand 1986;57:1.
3. Lewise GJS, Leithiser RE Jr, Glasier CM. Ultrasonography of pediatric neck masses. Ultrasound Quarterly 1989;7:315-355.
4. Leibman AJ, Kossoff MB. Sonographic features of fibromatosis of the breast. J Ultrasound Med 1991;10:43-45.
5. Reed M, Gooding GAW, Kerley SM, Himebaugh-Reed MS, Griswold VJ. Sonography of plantar fibromatosis. J Clin Ultrasound 1991;19:578-582.

6. Campbell AN, Chan HSL, Daneman A, Martin DJ. Aggressive fibromatosis in childhood: computed tomographic findings in three patients. J Assist Comput Tomogr 1983;7:109-113.
7. Hudson TM, Vandergriend RA, Springfield DS. Aggressive fibromatosis:evaluation by computed tomography and angiography. Radiology 1984; 150:495-501.
8. Francis IR, Dorovini-Zis K, Glazer GM, Lloys RV, Amendola MA, Martel W. The fibromatoses: CT-pathologic correlation. AJR 1986;147:1063-1066.
9. Chen PE, Ball WA Jr, Towbin RB. Aggressive fibromatosis of the tongue: MR demonstration. J Assist Comput Tomogr 1989;13:343-345.
10. Aisen AM, Martel W, Braunstein EM, et al. MRI and CT evaluation of primary bone and soft tissue tumors. AJR 1986;146:749-56.

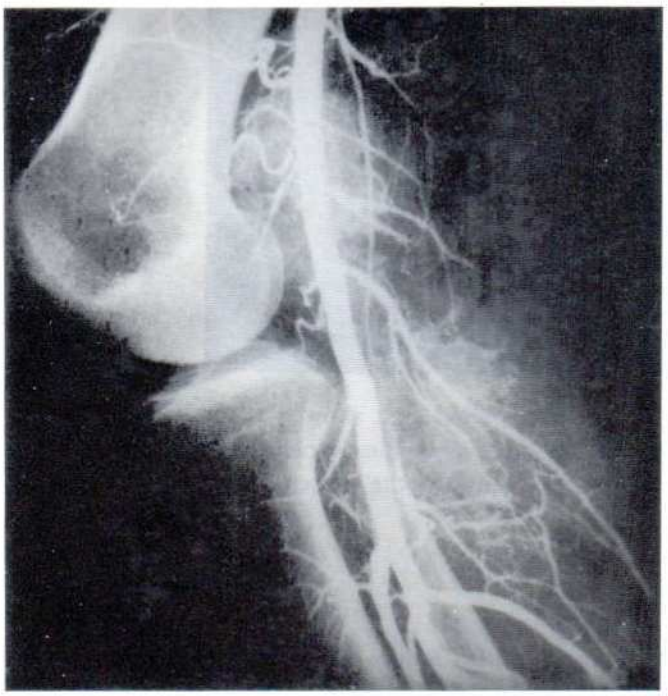

Fig. 2B. Case 2. Right femoral angiography showed two lobulated masses at right popliteal fossa with faint neovasculature and tumor stain.

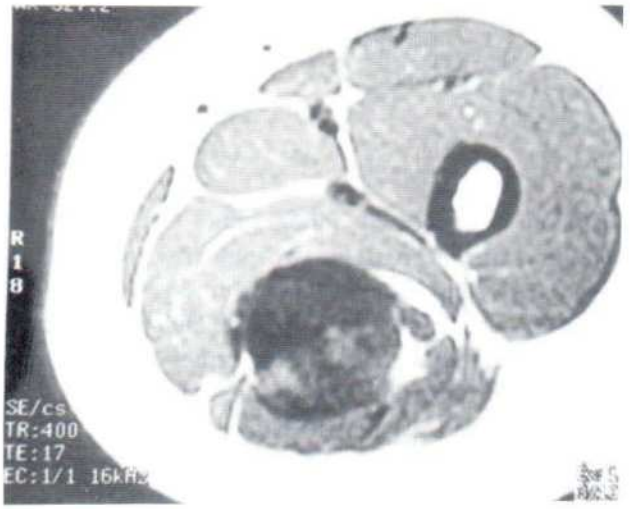

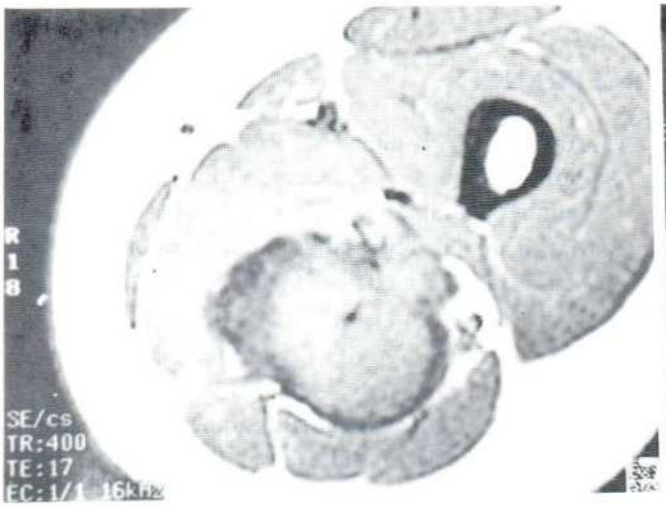

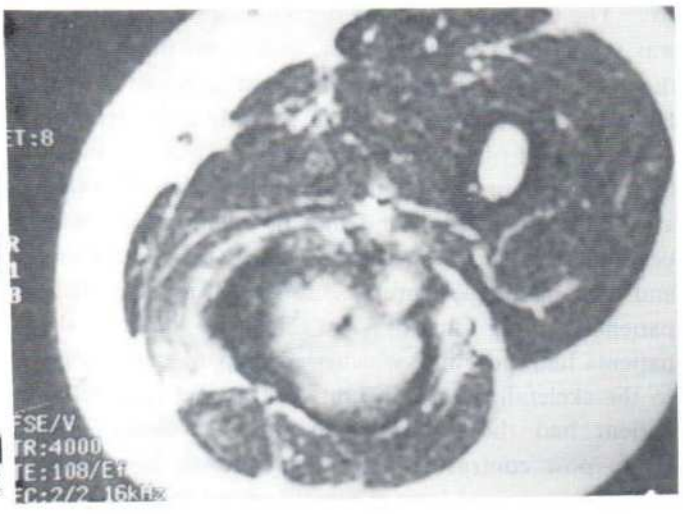

Fig. 3A Case 3. MRI study of the mass at posterior aspect of left thigh showed mixed signal lobulated mass at the semimembranosus muscle. The signal included dark grey, light gray, faintly bright on T1WI and dark grey, light grey, faintly bright and very bright on T2WI.

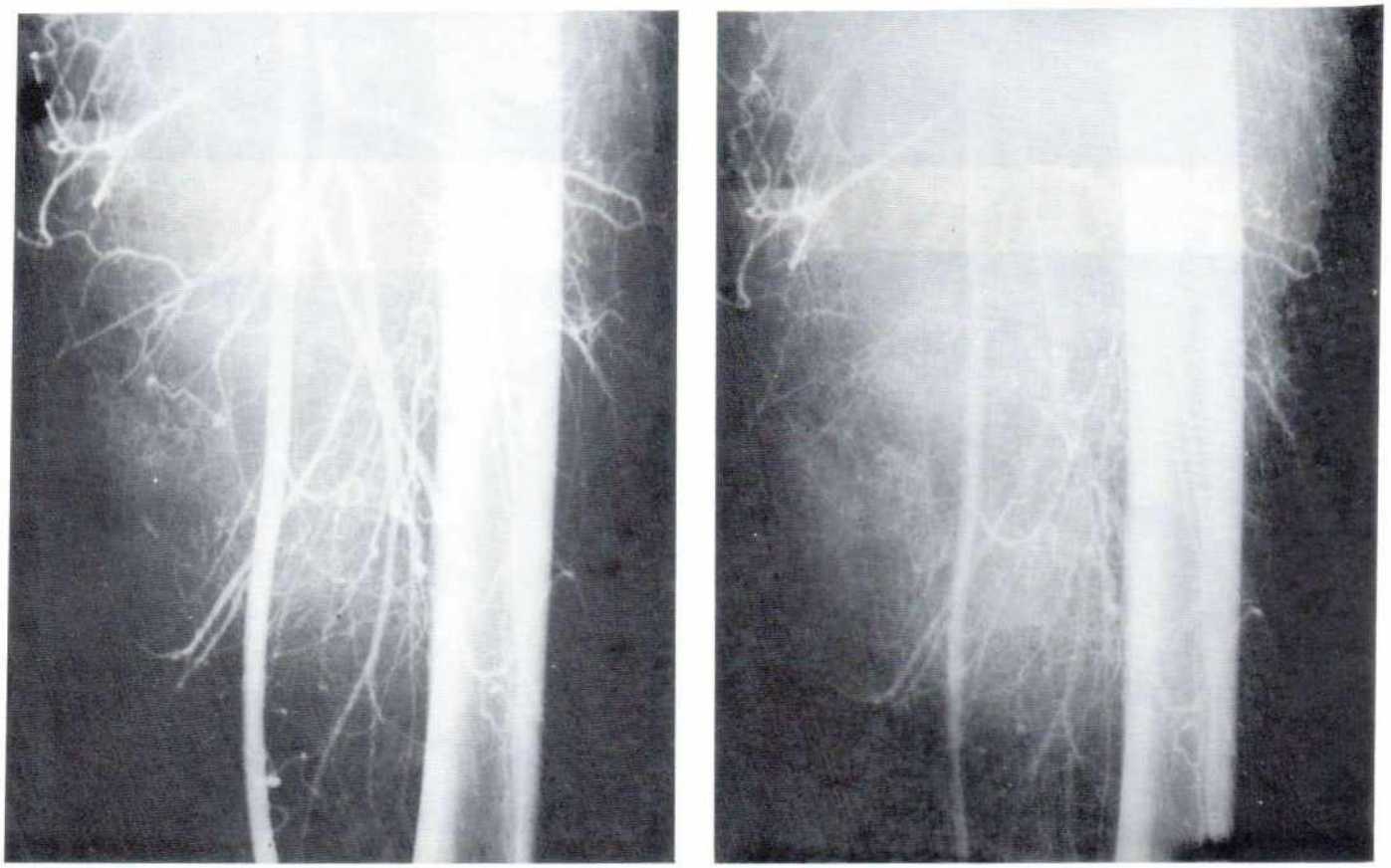

Fig. 3B Case 3. Left femoral angiography showed ill defined border lesion with fainter tumor stain than the tumors in case 2.

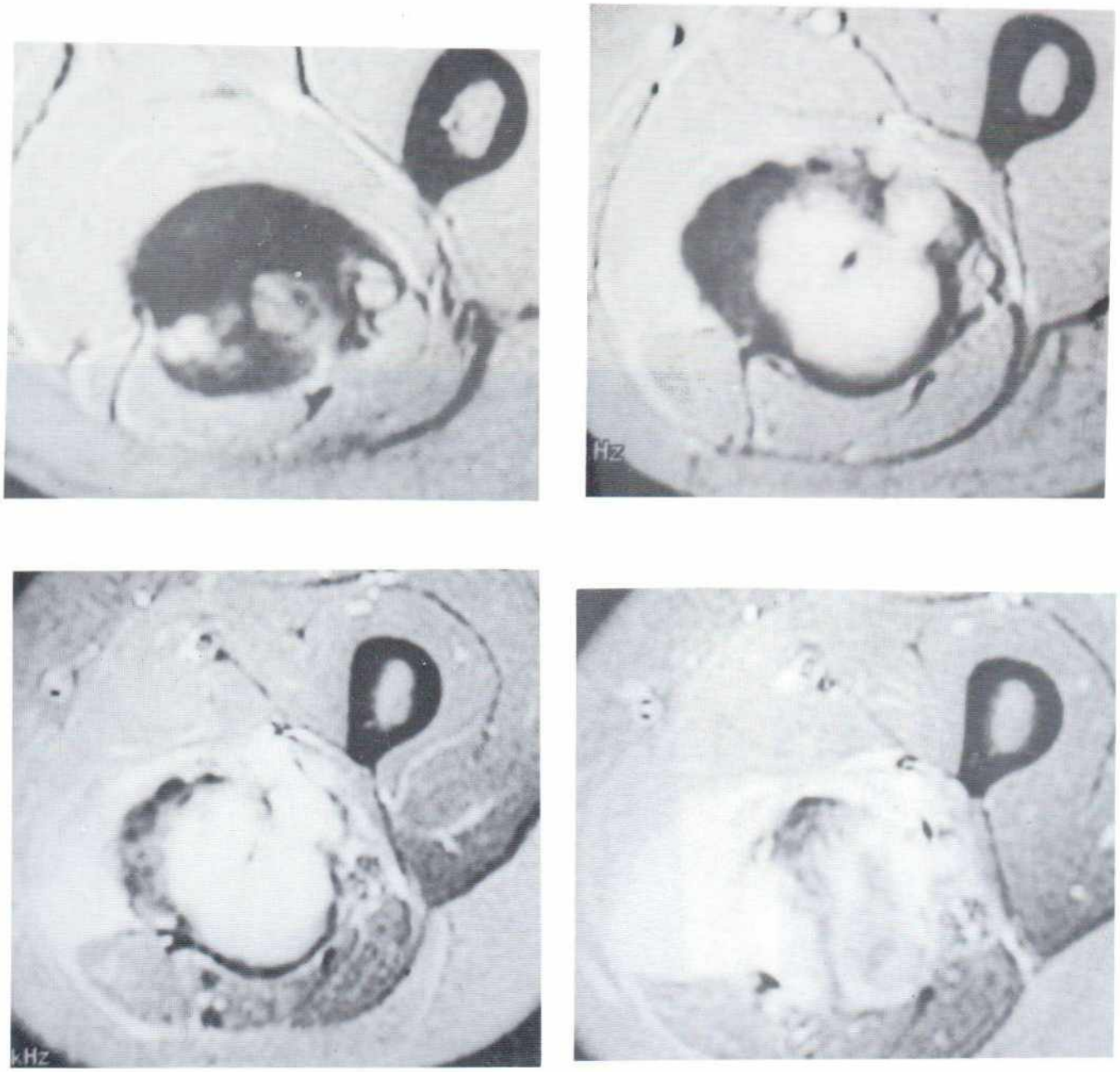

Fig. 4A.Case 3. T1WI axial view post Magnevist showed strongly enhanced pattern in many areas in the mass and the surrounding tissue.

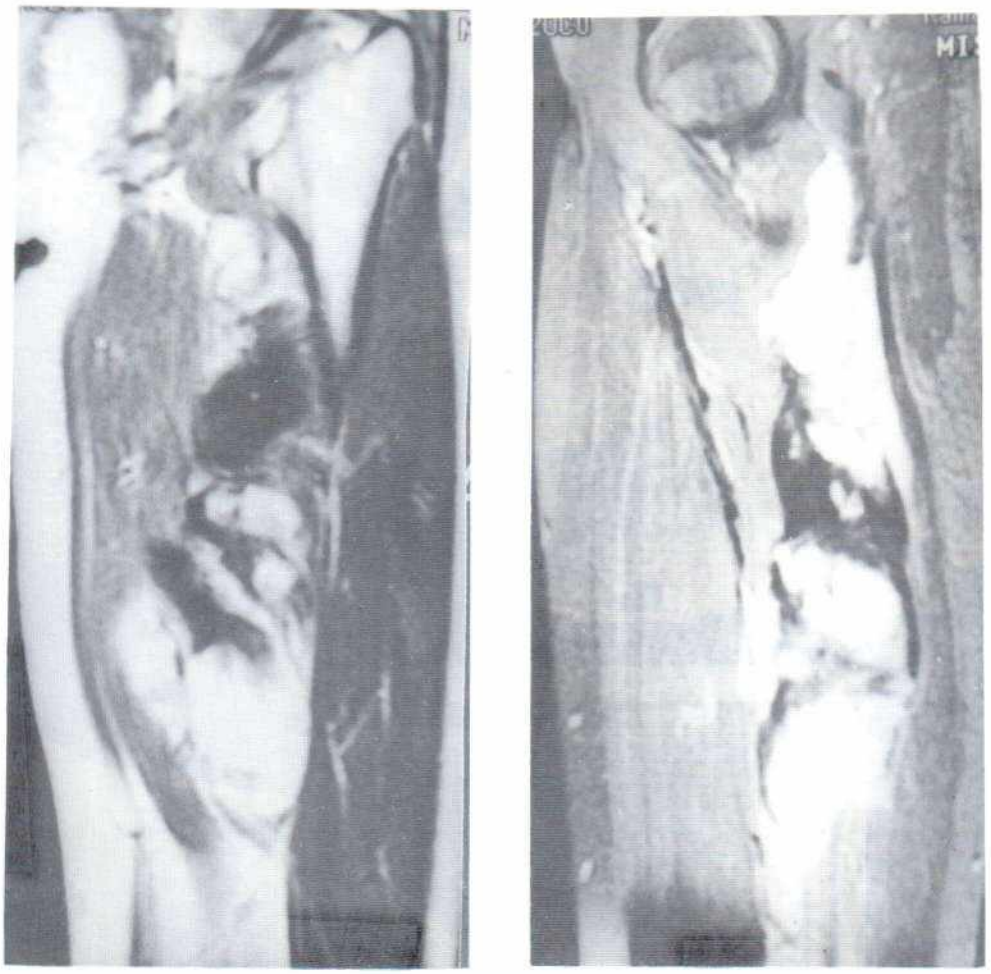

Fig. 4B. Case 3. Post contrast enhancement MRI of the lesion in coronal and sagittal view.

SKELETAL MUSCLE METASTASES FROM CA LUNG

Sopon KUMPONPUNTH[1], Patchrin PEKANAN[1], Sirintara PONGPECH[1]

ABSTRACT

Metastatic nodule to the thigh muscle from carcinoma of the lung in a 57 year-old foreign male patient was presented. The nodule was seen faintly on T1WI axial MRI scan. The nodule was seen better by coronal view T1WI and axial view T2WI. Skeletal muscles are still considered rare sites for metastases.

INTRODUCTION

Previously, it was thought that the skeletal muscle was remarkable free of metastatic disease (1,2). It had been said that almost all secondary tumors of striated muscle represent invasion from contiguous structures (1,3). However, Schultz (3) reported 12 patients with proven skeletal muscle metastases by CT scan.

CASE REPORT

A 57 year-old male European patient came with the palpable mass at the thigh. He had a bronchogenic carcinoma under treatment. MRI study of the mass showed a solid mass in the Vastus lateralis muscle, size 4 cm in diameter. The mass was hardly seen on axial T1WI and isosignal bright to the marrow of the femur on T2WI (TR 3000, TE 80); small brighter area 5 mm diameter was shown in the mass. There was no surrounding edema (Fig. 1). T1WI-coronal image shadowed more obvious lesion than the axial one (Fig. 2). Streaks of low signal was seen radiating from the center (Fig. 3). Metastatic process from Ca lung was noted.

[1] Department of Radiology, Ramathibodi Hospital, Rama 6 Street, Bangkok 10400, THAILAND.

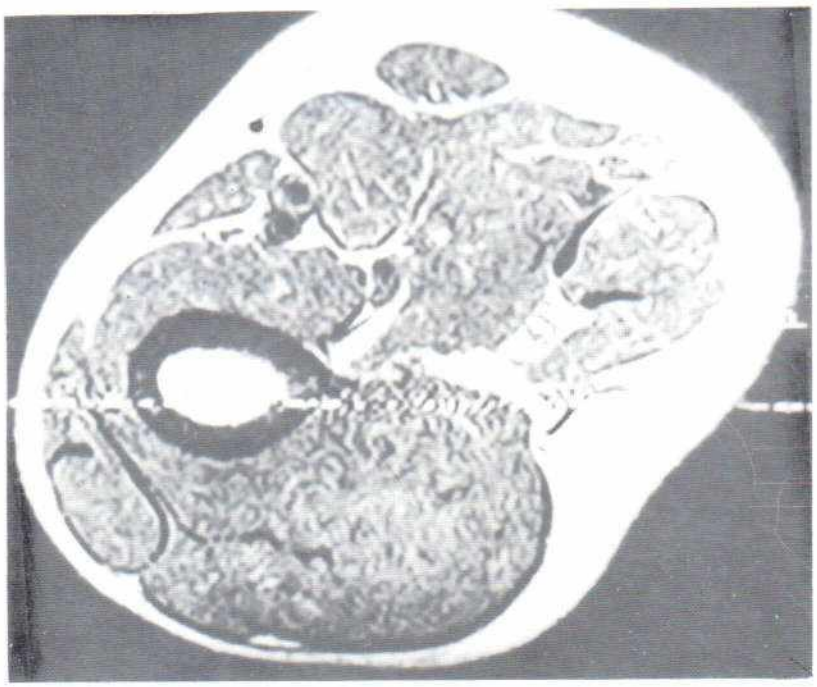

Fig. 1a. Axial T1WI (TR 500, TE 25) of the nodule in the Vastus lateralis showed very faint outline of the lesion.

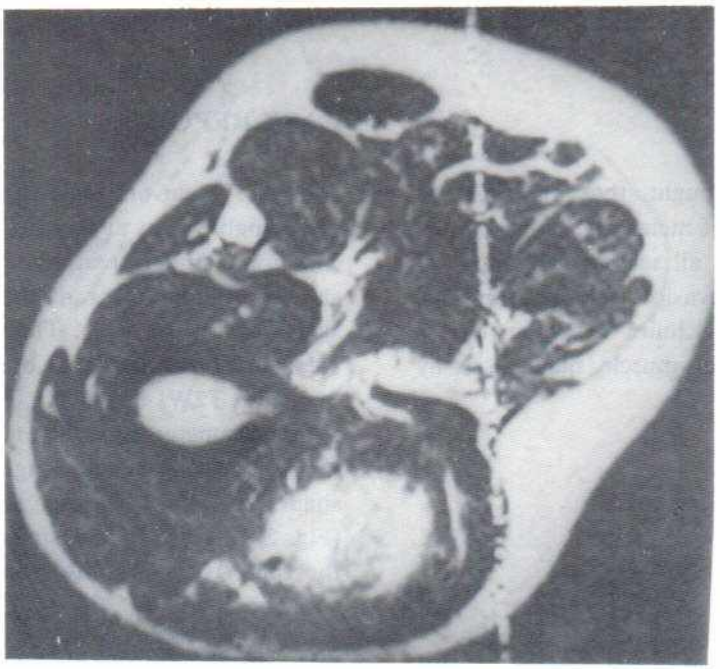

Fig. 1b T2WI-axial MRI study (TR 300, TE 80) of the nodule shows homogeneously bright nodule with a small brighter area at the anterior portion, represent necrosis.

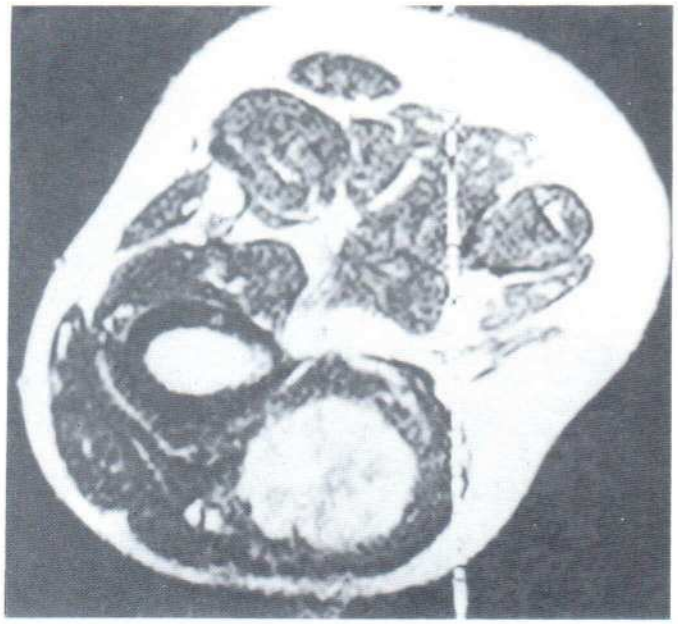

Fig. 2 Streaks of low signal radiated from the center to the periphery of the nodule was shown on the axial view, T2WI.

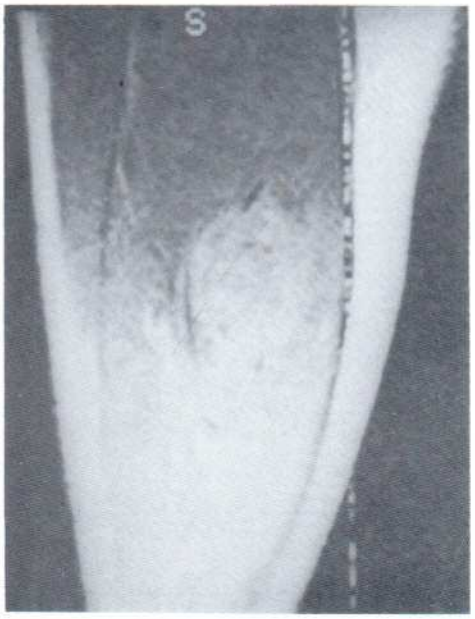

Fig. 3 Coronal view T1WI of the nodule showed faint hypersignal nodule embedded in the muscle of the Vastus lateralis. Better visualization of the nodule than the axial plane was observed.

DISCUSSION

Metastatic disease of the skeletal muscle has been documented on rare occasions from melanoma, thyroid, or pulmonary carcinoma (1,3). Bone forming metastatic muscle disease has been seen from gastric adenocarcinoma, breast, ovary, thyroid, colon, bladder, skin and prostate gland (4).

Locations of masses reported (3) included iliopsoas muscles, gluteal muscle group, calf muscles, thigh muscles, anterior chest wall and quadratus lumborum muscle. Primary carcinoma sites reported by Schultz were endometrium, breast, esophagus, ovary, prostate, kidney, and lymph nodes.

CT findings reported by Schultz were enlargement of the muscle with a well defined or ill defined areas of decreased attenuation, which represented necrosis. The use of contrast enhancement was helpful in many instances to clarify the extent of the tumor (3).

MRI demonstrates the outline and the content of the tumor better. The tumor is usually low on T1WI and bright on T2WI and can be seen better than the CT scan. The surrounding edema is also well visualized by T2WI-sequence.

REFERENCES

1. Delaney W. Non-myogenic tumors involving skeletal muscle. An Clin Lab Sci 1975;5:236-41.
2. Seely S. Possible reasons for high resistance of muscle to cancer. Med Hypotheses 1980;6:133-7.
3. Schultz SR, Bree RL, Schwab RE, Raiss G. CT detection of skeletal muscle metastases. J Comput Tomogr 1986;10:81-83.
4. Obley D, Slasky B, Peel R, Rosenbaum L, Nicholas J, Ellis L. Bone-forming gastric metastases in muscle-computed tomographic demonstration. J Comput Tomogr 1983;7:129-34.

ACOUSTIC IMAGING
A Dornier Company

Presents...

HIGH PERFORMANCE, COST EFFECTIVE ULTRASOUND FOR:

- ABDOMINAL
- OBSTETRICS
- GYNECOLOGY
- VASCULAR
- PROSTATE
- MUSCULOSKELETAL
- SMALL PARTS
- MAMMOGRAPHY
- PEDIATRICS

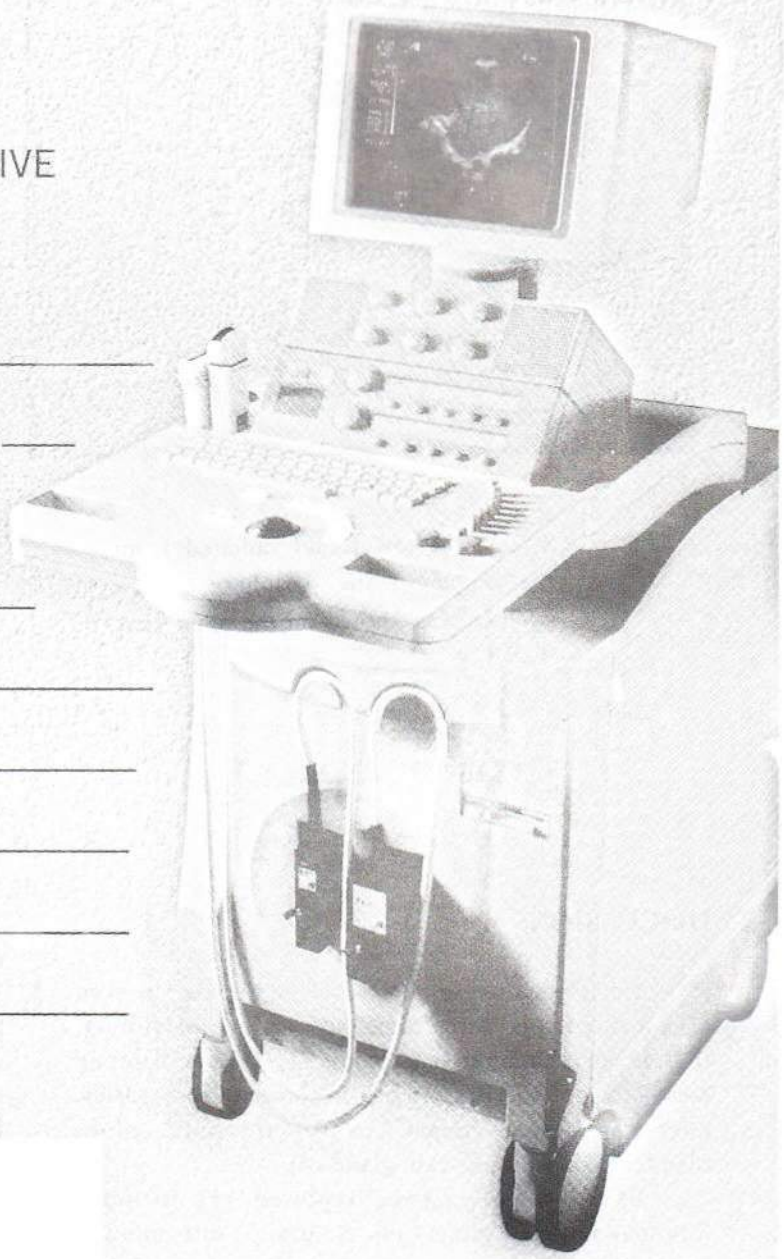

MEDICAL MEDIA PRODUCT CO., LTD.
บริษัท เมดิคอล มีเดีย โปรดักส์ จำกัด
633/14 ถนนสาธุประดิษฐ์ เขตยานนาวา กรุงเทพฯ 10120
โทร. (662) 2943364-8 โทรสาร : (662) 2943373

Performa™

High resolution ultrasound imaging scanner

NASAL AND PERINASAL FIBRO-OSSEOUS LESIONS

Patchrin PEKANAN[1], Sopon KUMPOLPUNTH[1],
Jiamjit TAPANEEYAKORN[1], Alisara SAPTHOESATAYA[2]

ABSTRACT

Three cases of nasal and perinasal fibro-osseous lesions were described. Two cases of ossifying fibroma appeared in a 12 year old boy and a 23-year old female patient. One case of cementifying fibroma was seen in a 60-year old female patient. The imaging appearance of the first case of ossifying fibroma and of the cementifying fibroma was similar. It appeared as a well defined border ossified mass with expansion of the structures that contain it without destruction of the surrounding structures. The second case of ossifying fibroma showed a huge invasive mass, however, maintaining the expanded behavior and containing ossified or calcified area. The images studied included plain films and CT scan.

INTRODUCTION

Fibro-osseous lesions of the craniofacial bones are a challenging group of pathologic conditions that are difficult to classify and treat (1,2). A common denominator to all is the replacement of the bone with a benign fibrous tissue containing various amounts of mineralized (calcified) structures (1,2). Margo et al (3) have offered the following classifications of the various fibro-osseous lesions: fibrous dysplasia, ossifying fibroma, psammomatoid (juvenile) ossifying fibroma (active juvenile ossifying fibroma), cementifying fibroma, cemento-ossifying-fibroma, osteoma and osteoblastoma.

We reported two cases of nasal and perinasal ossifying fibroma and one case of cementifying fibroma, demonstrated by plain film and CT scan.

CASE REPORTS

CASE 1

A 12-year-old boy, had a mass in his left nasal cavity for one year and has left exophthalmos. Plain film showed an expansion of the left nasal cavity, and left ethmoid sinus. Haziness of the left nasal cavity, left frontal, left ethmoid and left maxillary sinuses was noted. Axial and coronal enhanced CT scan of the facial bones showed a well defined border mass with dense calcification in left nasal cavity extending to left maxillary sinus, left anterior and posterior ethmoid sinus and medial aspect of left orbital cavity. The size of the mass is $4 \times 6 \times 6$ cm. Retention of fluid in left maxillary sinus was due to obstruction of the ostium by mass (Fig. 1). Left exophthalmos was due to extrinsic compression by this mass. Biopsy of the lesion revealed ossifying fibroma.

[1] Department of Radiology, Ramathibodi, Hospital, Rama 6 Street, Bangkok 10400, Thailand.
[2] Department of Radiology, Vajiraphayabal, BKK.

CASE 2

A 23-year-old female patient had the problem of progressive exophthalmos for 5 years, chronic upper respiratory tract infection and epitaxis for similar duration. The eye pain was very severe 4 days prior to the admission and the patient has pus discharge from both nasal cavities. Plain films showed a large ground-glass like density mass in both nasal cavities, both ethmoid sinuses, both maxillary sinuses, extending to base of the skull, to the anterior and middle cranial fossa. The sella turcica and sphenoid sinuses, the clivus was destroyed. The involved structures were expanded. Internal and rim calcification was shown. A coronal and axial CT scan of the brain, base of the skull and the facial parts showed a large calcified expanding lesion in both nasal cavities, both maxillary, ethmoid, sphenoid and frontal sinuses, both orbital cavities, anterior cranial fossae, clivus sella and suprasellar area. A more or less soap-bubble appearance of the mass was observed (Fig. 2). Surrounding brain edema was not seen due to the lesion. Biopsy showed ossifying fibroma. The size of the mass was about 10 cm in diameter.

CASE 3

A 60-year-old female patient had a mass adjacent to the medial left eye-brow for one year. She had been operated due to intra-nasal mass twice between 7-10 years of age. Plain film showed a ground-glass expanding lesion in left nasal cavity, medial part of left maxillary, left ethmoid and left frontal sinus and left orbital cavity. Axial plain and i.v. enhanced CT scan of the facial part showed a well defined border mass with ossification in the mass. The mass was in left nasal cavity, medial left maxillary sinus, left ethmoid sinus, medial left orbital cavity. There was no destruction of the bony structures (Fig. 3). The size of the mass is $4 \times 5 \times 6.5$ cm. Biopsy showed cementifying fibroma.

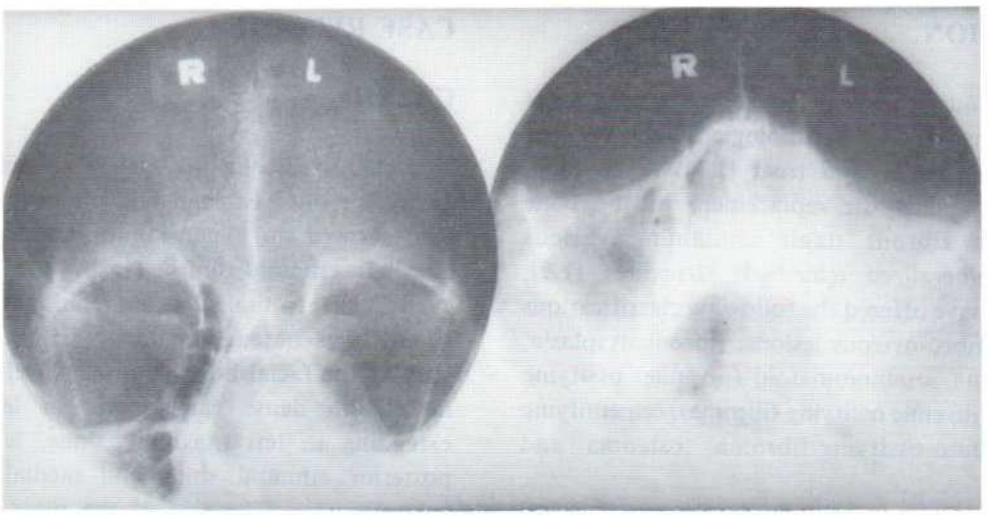

Fig. 1A Case 1. Plain film of the paranasal sinuses showed an expansion of the left nasal cavity and left ethmoid sinus with haziness. Left maxillary sinus was not expanded but cloudy. Disappearance of the medial left orbital wall was noted.

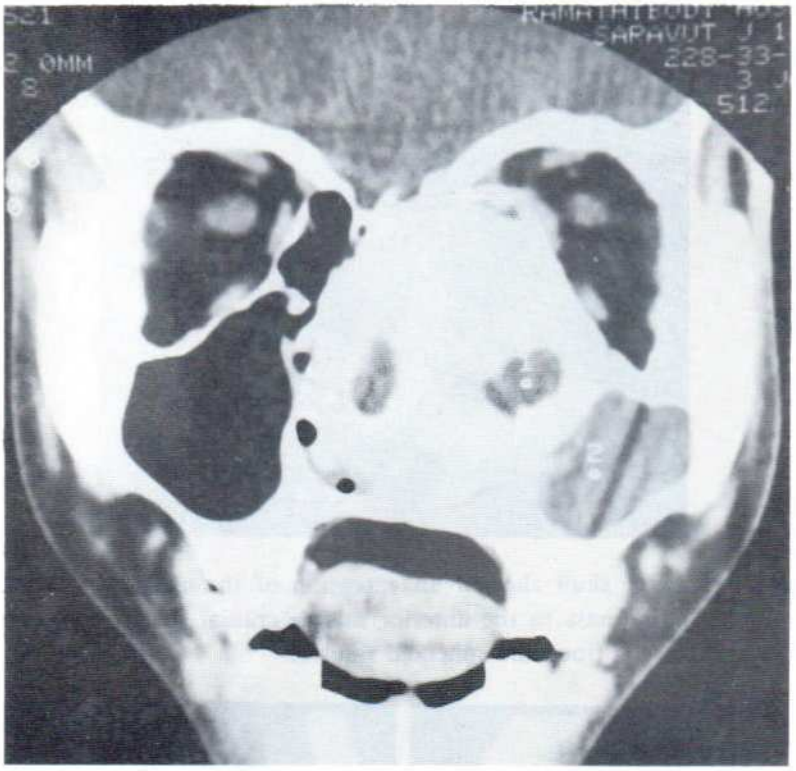

Fig. 1B. Case 1. Coronal CT scan of the face showed a well defined border mass, size 4.5×5×5 cm, in the left nasal cavity, extending to left ethmoid sinus, left maxillary sinus and left orbital cavity. The mass was densely calcified or ossified. Retention of fluid in left ethmoid and left maxillary sinus was observed. There was no destructive behavior of the mass

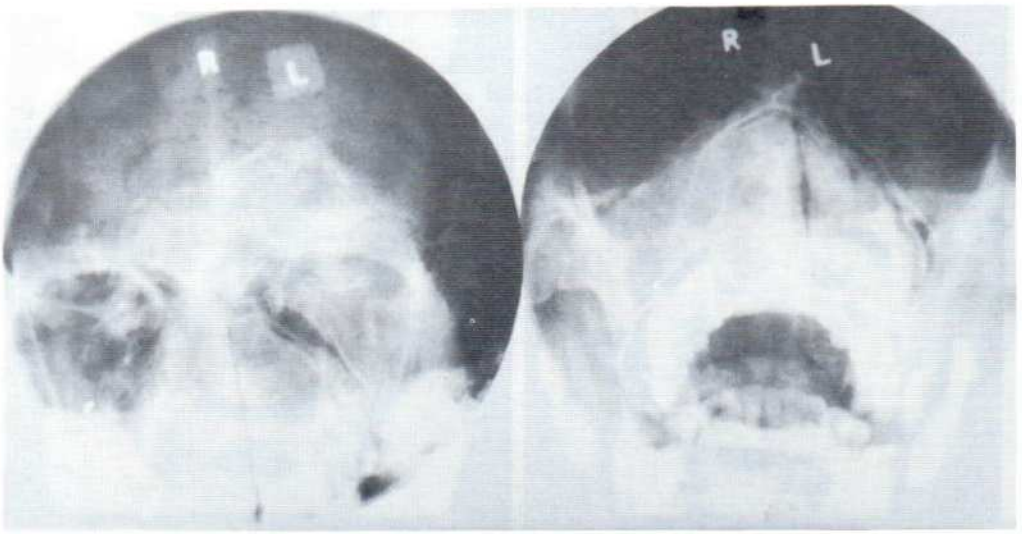

Fig. 2A Case 2. Plain film of the face in AP and Water's views showed a densely and both frontal sinuses. There was an expansion of both nasal calcified or ossified mass in the region of both ethmoid sinuses, cavities and ethmoid sinuses.

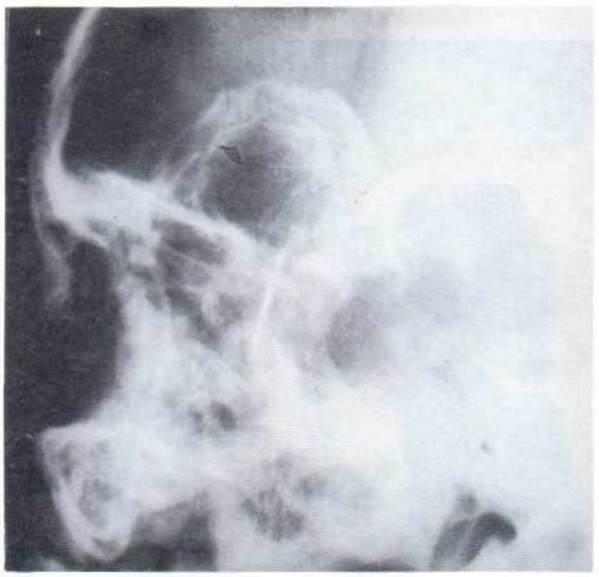

Fig. 2B. Case 2. Lateral skull showed an extension of the calcified or ossified protion of the mass to the anterior middle cranial fossa with destruction of the sella floor and sphenoid sinuses.

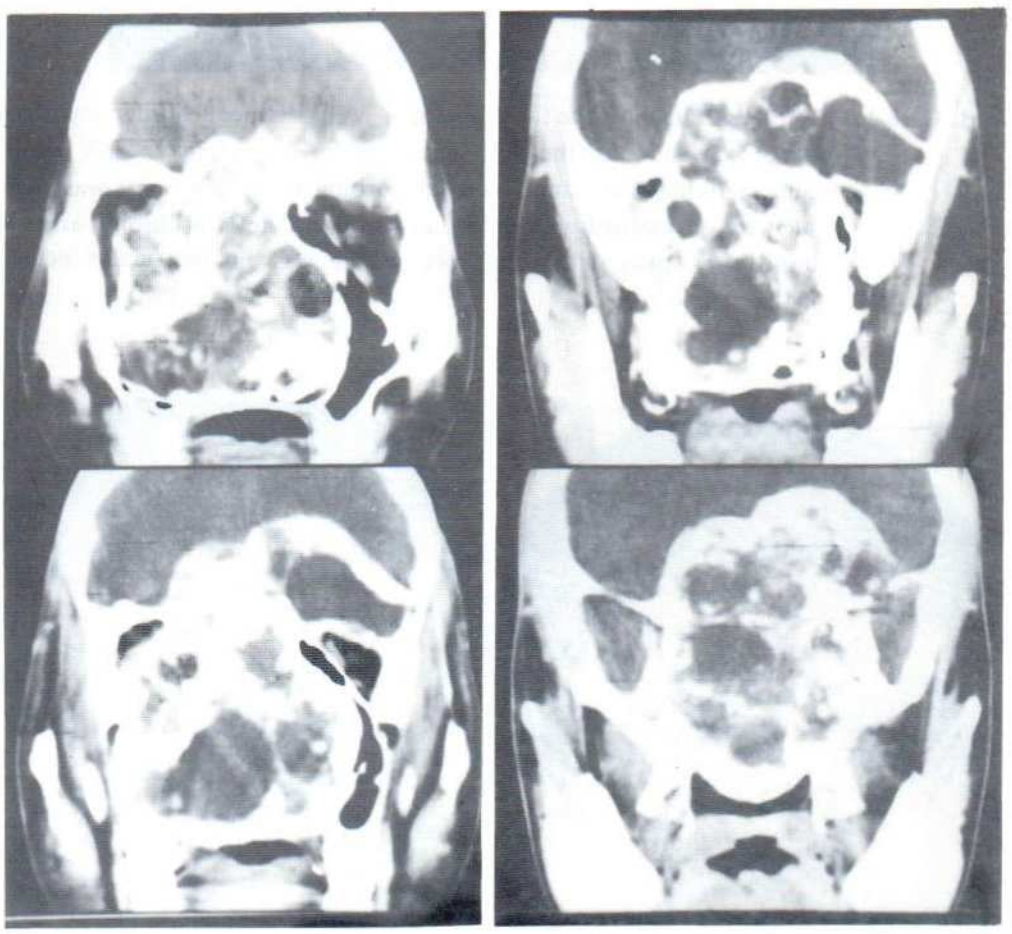

Fig. 2C Case 2. I.V. enhanced coronal CT scan of the brain and face portion showed a large calcified or ossified mass in the nasal cavities, both maxillary sinuses, both orbital cavities, sphenoid sinuses, pituitary fossa, suprasellar cistern, anterior and middle cranial fossae. The mass was less dense than the mass of the case 1. There was as aggressive behavior, judging from the destruction of the involved bones.

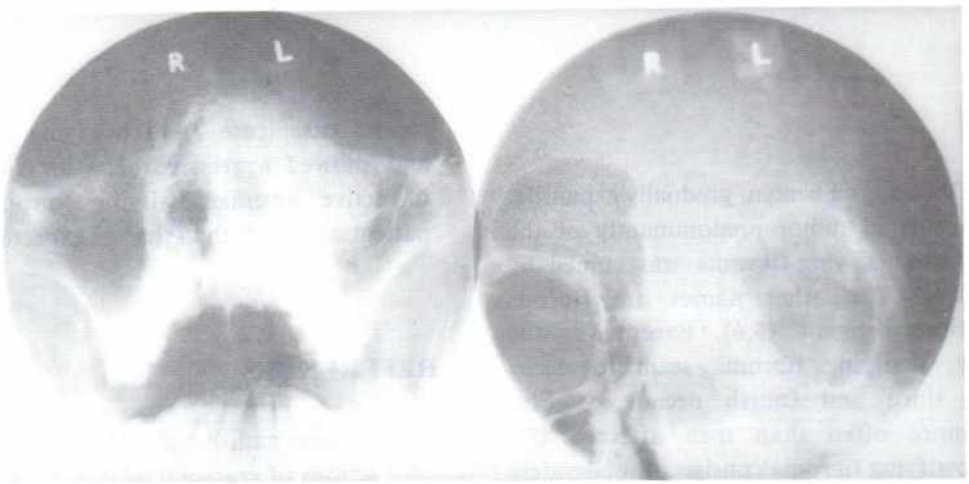

Fig. 3A Case 3. Plain film of the paranasal sinuses showed an expanding lesion in the left nasal cavity, left ethmoid sinus with haziness of left nasal cavity, left maxillary sinus, left ethmoid sinus, medial left orbital cavity and left frontal sinus. The margin of the lesion was well defined.

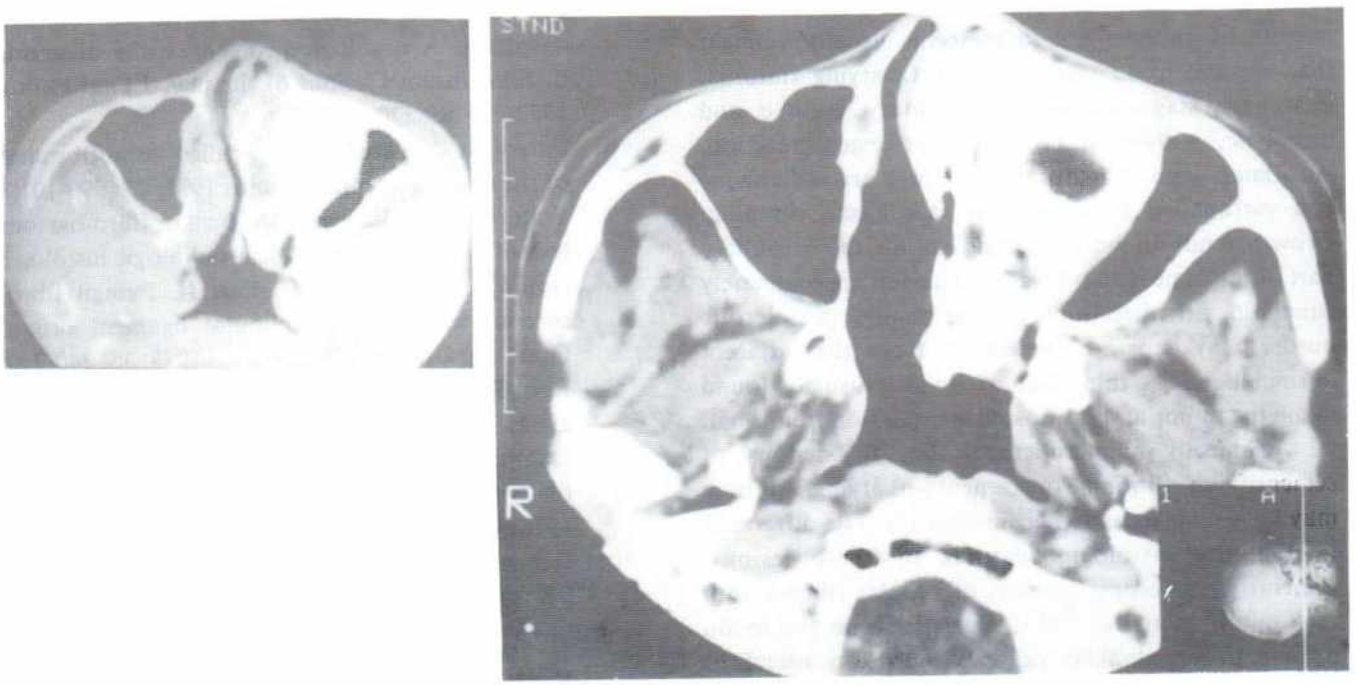

Fig. 3B Case 3. Axial CT scan of the mass showed a densely calcified or ossified mass in the left nasal cavity, left maxillary-frontal sinus, and medial left orbital cavity. Lack of destructive behavior was obvious, which was similar to the lesion of Case 1.

DISCUSSION

Ossifying fibroma is a benign, gradually expansile, and fairly encapsulated tumor predominantly of the jawbones. The term ossifying fibroma was coined by Montgomery (1,4). The other names are fibrous osteoma and fibro osteoma (5,6). Except for the juvenile variety, ossifying fibroma seem to occur mostly in the third and fourth decade of life, with women more often than men affected (7). Histologically, ossifying fibroma consists of moderately cellular, delicately interlacing collagen fibers and usually well vascularized stroma containing various amounts of calcified materials. Calcification may appear as irregular bony structures (woven or lamellar) and spicules. Lamellar bone formation and osteoblastic rimming found in ossifying fibroma are believed by some pathologists to be differentiating features of fibrous dysplasia (1,8). A variant of ossifying fibroma, active juvenile ossifying fibroma, has been described in children. This tumor is a rapidly enlarging as well as destructive process, occurring predominantly in the maxilla of children and adolescents usually younger than the age of 15 years (3,9-12). Ossifying fibroma, in its early stage, appears to be solitary, cystlike, and osteolytic, without a prominent periosteal reaction. At a later stage of maturation, lesions are radiopaque and surrounded by a uniform radiolucent rimming. Growth tends to be concentric within the medullary part of the bone with outward expansion approximately equal in all directions. Occasionally, a sclerotic border may separate the lesion from the adjacent normal bone. A thin shell of bone is usually found along the tumor and extraosseous expansion is unusual.

Clinically and raiographically, the lesions of cementifying fibroma or cemento-ossifying fibroma may be similar to ossifying fibroma (1). The difference lies in the histologic features of these lesions; cementifying fibroma consists of cellular fibrous with rare mitotic activity. Calcified elements in the lesion appear to be globular cementum (or an island of calcified materials surrounded by cementoid and cementoblasts). The difficulties in separating ossifying fibroma from cementifying fibroma has resulted in the term cemento-ossifying fibroma to encompass these identical tumors (1).

Our first case of ossifying fibroma and the case of cementifying fibroma had similar images. The second case (case 2) of ossifying fibroma was large and showed aggressive behavior similar to the case of active juvenile ossifying fibroma, however, the patient was older than the age expected in the literature.

REFERENCES

1. Mohammadi-Araghi H, Haery C. Fibro-osseous lesions of craniofacial bones: the role of imaging. Radiologic Clinics of North America 1993; 31: 121-134.
2. Pecaro BC. Fibro-osseous lesions of the head and neck. Otolaryngol Clin North Am 1986; 19: 489-495.
3. Margo CE, Ragsdale BD. Perman KL. Psammomatoid (juvenile) ossifying fibroma of the orbit. Ophthalmology 1985; 92: 150-159.
4. Montgomery AH. Ossifying fibroma of jaw. Arch Surg 1927; 15: 30-44.
5. Eversole LR. Sabes WR, Rovin S. Fibrous dysplasia: A nosologic problem in the diagnosis of fibro-osseous lesions of the jaw. J Oral Pathol 1972; 1: 189-220.
6. Furedi A. A study of so-called osteofibromas of the maxilla. Dental Cosmos 1935; 77: 990-1010.
7. Waldron CA, Giansanti JS. Benign fibro-osseous lesions of the jaws: A clinical-radiologic histologic review of sixty-five case. Part II. Benign fibro-osseous lesions of periodontal ligament origin. Oral Surg Oral Med Oral Pathol 1973; 35: 340-350.
8. Reed RJ. Fibrous dysplasia of bone. Arch Pathol 1963; 75: 480-495.
9. Damjanov I, Maenza RM, Snyder CG III. Juvenile ossifying fibroma: An ultrastructural study. Cancer 1978; 42: 2668-2674.
10. Georgiade N, Masters F, Horton C. Ossifying fibroma (fibrous dysplasia) of the facial bones in children and adolescents. J Pediatr 1955; 46: 36-43.
11. Schilds JA, Nelson LB, Brown JF. Clinical computed tomographic and histopathological characteristics of juvenile ossifying fibroma with orbital involvement. Am J Ophthal 1983; 96: 650-653.
12. Test D, Schow C, Cohen D, Juvenile ossifying fibroma. J Oral Surg. 1976; 34: 907.

CYSTIC DUCT LEAKAGE AFTER LAPAROSCOPIC CHOLECYSTECTOMY: DEMONSTRATED BY SPIRAL CT CHOLANGIOGRAPHY

Chirote SUCHATO[1], Patchrin PEKANAN[1,2]
Sopon KUMPOLPUNTH[2], Wasan DANGKHAO[1].

ABSTRACT

Bile leakage from the cystic duct stump, was demonstrated by spiral CT cholangiography. The patient was 55 years old and was underwent laparoscopic cholecystectomy. Spiral CT cholangiography is a simple and quick imaging study to detect such leakage.

INTRODUCTION

Laparoscopic cholecystectomy is now widely accepted as the procedure of choice for removal of the gallbladder. It offers the shorter hospital stays, less postoperative pain and lowered hospital costs (1). Injury to bile ducts and cystic duct stump leak had been demonstrated by radionuclide imaging (1-4), endoscopic retrograde cholangiography (ERC) and transhepatic cholangiography (THC) (4,5). This is the first case report of cystic stump leak, illustrated by spiral CT cholangiography.

CASE REPORT

A 55-year old male patient was underwent a laparoscopic cholecystectomy for chronic calculous cholecystitis. Ascites was detected in the postoperative period. Spiral CT cholangiography was performed to identify the site of bile leakage. The spiral CT scanner was Elscint CT twin. The contrast medium used was endocistobil 50%, 20 cc. in 100 cc. of normal saline. The mixed fluid was i.v. dripped in 30 minutes. Scanning was performed immediately afterwards. It showed distended cystic duct stump. Leakage of the contrast medium was shown from the stump to subhepatic region (Fig. la, b, c). Surgery revealed leakage of the bile from the cystic duct stump. There was an evidence of necrotic area near the stump. Large amount of bile fluid was noted at the left subhepatic and right subdiaphragmatic spaces. The metallic clamp was intact. The cystic duct was ligated close to the common bile duct.

DISCUSSION

Cystic duct leaks after laparoscopic cholecystectomy (LC) may develop for one of the three reasons: (1) misplaced or lost clips as in our case; (2) tear in the remnant proximal to the surgical clips; or (3) failure of short, necrotic ductal remnant to close because of acute inflammation (6).

Three-dimensional spiral CT cholangiography enables noninvasive volumetric imaging of the biliary tract (7). The normal-sized biliary tract was adequately depicted during three-dimensional spiral CT cholangiography (8). The use of iodinated cholangiographic agents is not indicated in the patient with known allergy, hepatic or renal failure, gamma-globulinopathies or elevated bilirubin levels (9). A relation has been shown between serum bilirubin concentration and nonvisualization of bile ducts on IV cholangiograms

[1] Urupong Medical Center, 1131/351-4 Thoeddamri Street, Bangkok 10300, Thailand.
[2] Department of Radiology, Ramathibodi Hospital, Rama 6 Street, Bangkok 10400, Thailand.

(10). IV cholangiography has not been recommended in patients who have a serum bilirubin concentration greater than 51 umol/1 (3mg/dl) (9). In the case of bile leakage as in this case, there is no problem of obstruction. In the absence of hemolysis or hepatic damage, there will be no obstacle to the study. Slow infusion cholangiography is a safe technique (11).

In conclusion, it shows that the three-dimensional spiral CT cholangiography is a feasible method for imaging the bile leak after laparoscopic cholecystectomy.

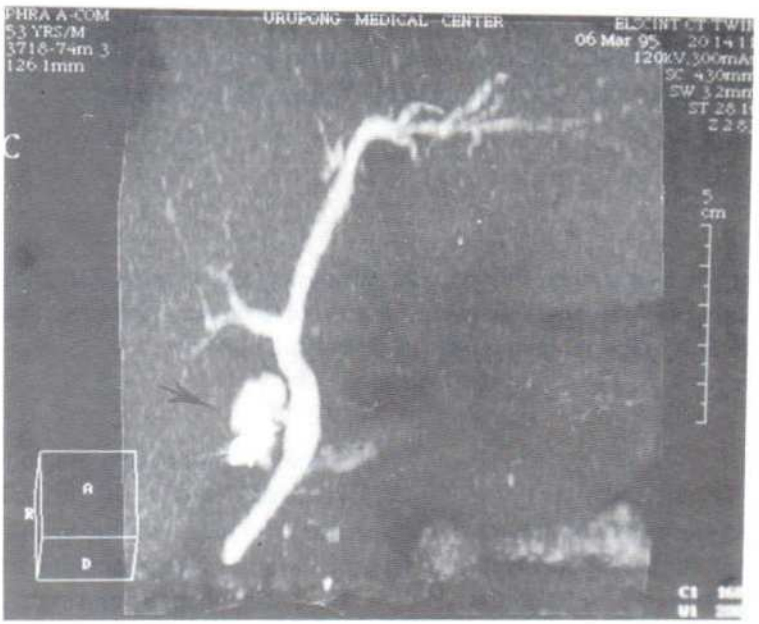

Fig. 1a. Maximum intensity projection (MIP) image of the bile duct showed a leak from the cystic duct stump.

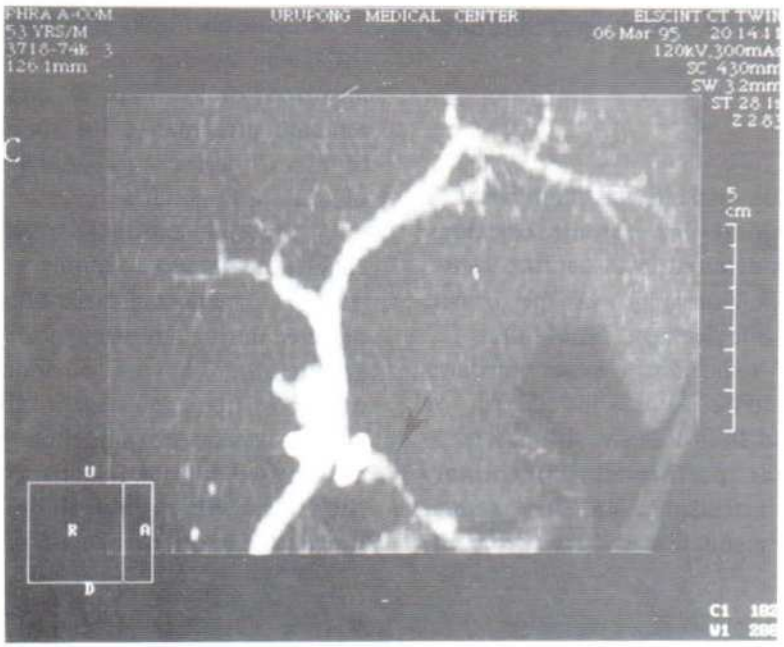

Fig. 1b. Rotating MIP image of the bile duct showed a leakage tract to subhepatic region

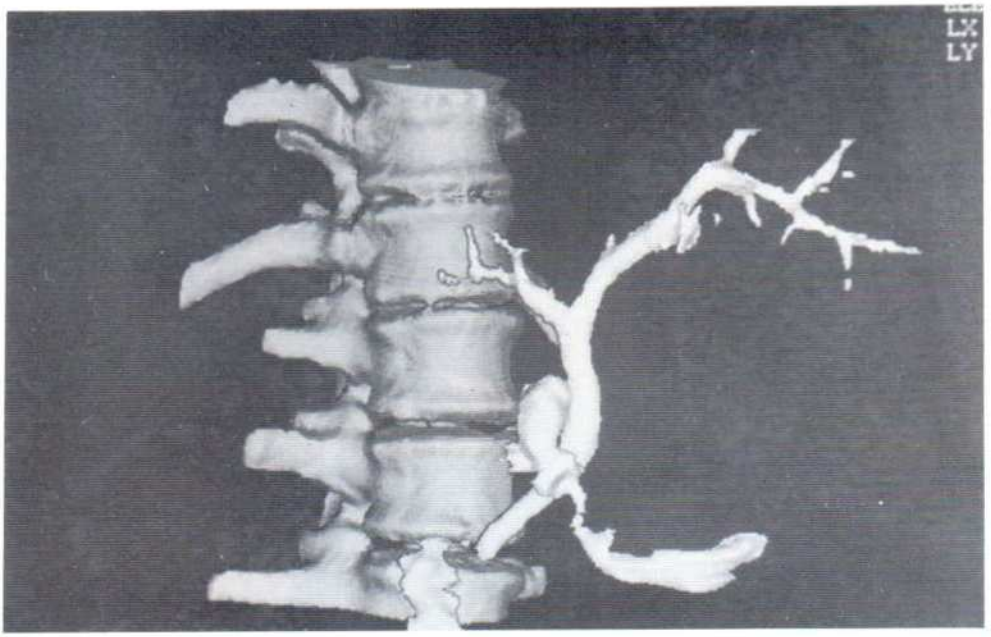

Fig. 1c. Oblique view 3D recontruction of the bile duct showed a leak from the cystic duct stump and a tract of contrast medium from the leakage site to the subhepatic region

REFERENCES

1. Politoske EJ. Bile duct leakage after laparoscopic cholecystectomy diagnosed by radioisotopic scanning. Clinical nuclear medicine 1993; 18: 318-320.
2. Estrada WN, Zanzi I, Ward R, Negrin JA, Margouleff D. Scintigraphic evaluation of postoperative complications of laparoscopic cholecystectomy. J Nucl Med 1991; 31: 1910-1911.
3. Pasmans HLM., et al. Scintigraphic diagnosis of bile leakage after laparoscopic cholecystectomy. A prospective study. Clinical nuclear medicine 1992; 17: 697-700.
4. Trerotola SO, et al. Biliary tract complications following laparoscopic cholecystectomy: Imaging and intervention. Radiology 1992; 184: 195-200.
5. Ward EM, et el. Imaging of complications of Laparoscopic cholecystectomy. Abdom Imaging 1993; 18: 150-155.
6. Brandabur JJ, Kozarek RA. Endoscopic repair of bile leaks after laparoscopic cholecystectomy. Seminars in Ultrasound, CT,and MRI 1993; 14: 375-380.
7. Klein HM, Wein B, Truong S, Pfingsten FP, Guenther RW. Computed tomographic cholangiography using sprial scanning and 3D image processing, Br J Radiol 1993;66:762-767.
8. Van Beers BE, Lacrosse M, Trigaux JP, de Canniere L, De Ronde T, Pringot J. Noninvasive imaging of the biliary tree before or after laparoscopic cholecystectomy: Use of three dimensional spiral CT cholangiography. AJR 1994; 162: 1331-1335.
9. Scott IR, Gibney RG, Becker CD, Fache JS, Burshenne HJ. The use of intravenous cholangiography in teaching hospitals:a survey. Gastrointest Radio 1989; 14: 148-150.
10. Berk RN,Loeb PM. Biliary contrast materials. In: Berk RN, Ferrucci JT, Leopold GR eds. Radiology of the gallbladder and bile ducts: diagnosis and intervention. Philadelphia: Saunders, 1983: 55-82.
11. Joyce WP, Keane R, Burke GJ, et al. Identification of bile duct stones in patients undergoing laparoscopic cholecystectomy. Br J Surg 1991; 78: 1174-1176.

Introducing 3M DryView™ Laser Imaging Systems

An important breakthrough for cost-conscious, quality-driven health care facilities

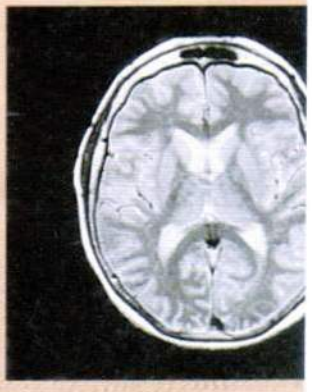

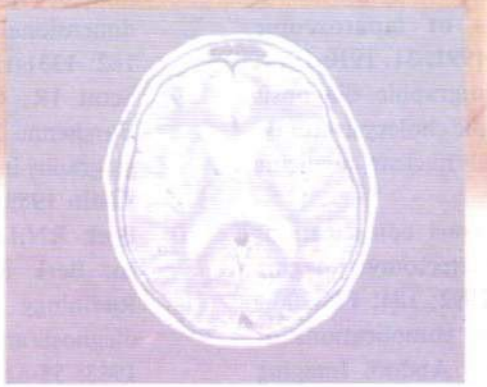

3M Health Care

OVARIAN VEIN THROMBOSIS-SPIRAL CT DETECTION

Patchrin PEKANAN[1,2], Sopon KUMPOLPUNTH[1], Udorn INTUWATANAKUL[3].

ABSTRACT

Right and left ovarian vein thrombosis was shown by coronal reformation of the spiral CT scan in a patient with colonic carcinoma, liver metastases and secondary septicemia. Clot was seen in the entire length of the right ovarian vein.

INTRODUCTION

Right ovarian vein drains into the inferior vana cava and the left ovarian vein drains into the left renal vein. Ovarian vein thrombosis is usually associated with inflammatory processes in the pelvic cavity (10), post pelvic surgery and malignancy (2). Ovarian vein thrombosis detected by CT scan has been reported by many authors (1-6), this is the first report of this condition demonstrated by spiral CT scan.

CASE REPORT

A 68-year-old female patient was referred for spiral CT scan to clarify the cause of post operative fever. The patient was operated for ascending cholangitis; the gallbladder was removed and T-tube insertion was done. Spiral CT scan was performed with i.v. contrast enhancement. The slice thickness was 5 mm. Oblique reconstruction in coronal plane to show ovarian veins was shown in Fig.1. Clots was seen as an unenhanced tubular structure in the entire length of the right ovarian vein. The sharply defined enhancing wall of right ovarian vein was demonstrated. Other findings in this patient were carcinoma of the hepatic flexure and liver metastases.

DISCUSSION

Puerperal ovarian vein thrombosis is a rare but potentially fatal condition, requiring broad-spectrum antibiotic and anticoagulation therapy and ligation of the involved vein if failed medical treatment (2). The ovarian vein thrombosis associated with malignancy and chemotherapy can be asymptomatic and the role of the medical and surgical treatment is not yet clear (1). The thrombosed vein was seen on axial CT scan as enlarged vein, containing low density central lumen and a sharply defined enhancing wall (7). The ovarian vein is lateral to the uterus and ureter, anterior to the psoas muscle, anteromedial to the kidney and anterolateral to the inferior vena cava (for the right side) (2).

In our case, the thrombus was more extensive in the right ovarian vein. Right ovarian vein was more commonly involved than the left side, almost five times as often (8). The reasons for this was believed

[1] Department of Radiology, Ramathibodi Hospital, Rama 6 Street, Bangkok 10400, Thailand.
[2] Urupong Medical Center, Thoeddamri Street, Bangkok.
[3] Department of Surgery, Ratburana Hospital, Bangkok.

to be due to the longer right ovarian vein with multiple incompetent valves, compression by the enlarged dextrotorsion of the uterus and significant retrograde drainage of the left ovarian and uterine veins into the right system (8). Right ovarian vein thrombosis associated with malignancy also predominated the left side (1). Spiral CT scan can certainly demonstrate the ovarian vein thrombosis better than the non-spiral technique, due to lack of respiratory motion, making better resolution for reconstruction in other planes.

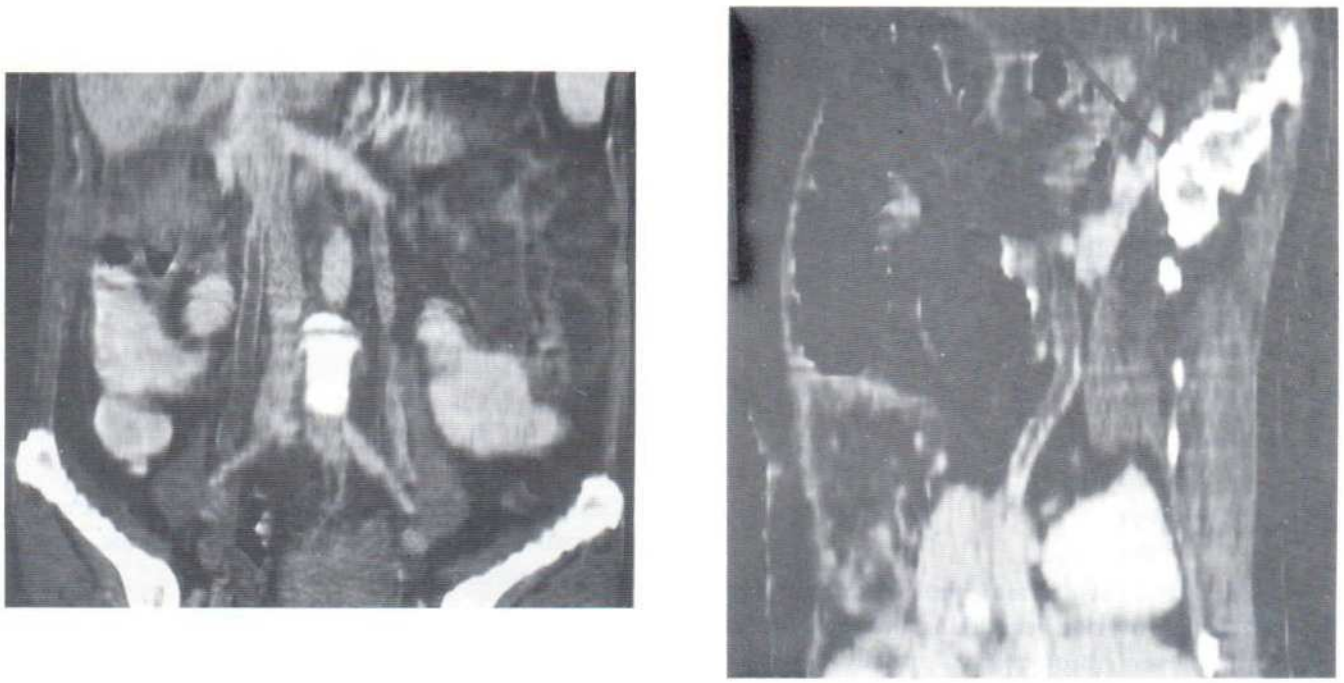

Fig. 1 Thrombus in the entire length of right ovarian vein was seen as the unenhanced low density tubular structure surrounding by the thin enhanced wall of the vein. The collapsed left ovarian vein was also shown.

ACKNOWLEDGMENT

We would like to thank DR.Suchato C. M.D. and Urupong Medical Center for providing us the spiral CT machine for the study.

REFERENCES:

1. Jacoby WT, Cohan RH, Baker ME, Leder RA, Nadel SN, Dunnick NR. Ovarian vein thrombosis in oncology patients: CT detection and clinical significance. AJR 1990;155:291-94.
2. Savader SJ, Otero PR, Savader BL. Puerperal ovarian vein thrombosis: evaluation with CT, US and MR imaging. Radiology 1988;167:637-39.
3. Rozier JC, Brown EH, Beme FA. Diagnosis of puerperal ovarian vein thrombophlebitis by computed tomography. Am J Obstet Gynecol 1988;159:737-40
4. Warhit JM, Fagelman D, Goldman MA, Weiss LM, Sachs L. Ovarian vein thrombophlebitis: diagnosis by ultrasound and CT. JCU 1984; 12:301-03.
5. Brown CE, Lowe TW, Cunningham FG, Weinreb JC. Puerperal pelvic thrombophlebitis:impact on diagnosis and treatment using x-ray computed tomography and magnetic resonance imaging. Obstet Gynecol 1986;68:789-94.
6. Khurana BK, Rao J, Friedman SA, Cho KC. Computed tomographic features of puerperal ovarian vein thrombosis. Am J Obstet Gynecol 1988;159:905-08.
7. Zerhouni EA, Barth KH, Siegelman SS. Demonstration of venous thrombosis by computed tomography. AJR 1980;134:753-58.
8. Munsick RA, Gillanders LA. A review of the syndrome of pueperal ovarian vein thrombophlebitis. Obstet Gynecol Surg 1981;36:57-66.

NEUROIMAGING OF THE CNS INVASION OF GNATHOSTOMA SPINIGERUM AND ANGIOSTRONGYLUS CANTONENSIS IN A NORTHERN THAI PATIENT

Patchrin PEKANAN[1], Sirintara PONGPECH[1],
Siriporn HIRUNPAT[2], Suthipong JONGJIRASIRI[1], Sopon KUMPOLPUNTH[1].

ABSTRACT

A case of mixed parasitic infestation of the CNS was demonstrated by CT scan, MRI scan and angiography. The patient was 51-yrs-old female farmer presented with neurological deficits. Gnathostomiasis and Angiostrongyliasis was responsible for the symptoms. Multiple hematomas are seen in the spinal cord, central canal and in the brain. Dissection of the vertebral artery was also noted. Most of the changes represented the manifestation of Gnathostomiasis.

INTRODUCTION

Gnathostoma spinigerum is a tissue nematode with an exceptionally tremendous penetrating power. It can migrate through any anatomical structure of the human body, except bone. G. spinigerum third stage larvae have been recovered from various organs such as the urinary bladder, uterus, intestine, lungs, ears, eyes, spinal cord and brain (1). Common neurological syndromes, i.e. subarachnoid hemorrhage, meningitis, encephalitis, transverse myelitis, ascending myelitis or radiculomyeloencephalitis can be caused by invasion of the parasite into the central nervous system (1). The mortality rate of CNS gnathostomiasis was approximaterly 20 percent and one of the major causes of death was direct parasite invasion into vital centers in the brain stem.

Various snails, slugs, prawns and crabs are intermediate hosts of the Angiostrongylus cantonensis. Humans are usually infected by eating infected intermediate hosts, that have not been properly cooked. In Thailand Pila snails are the main source of infections, the snails are often served in Thailand as a delicacy together with alcohol (2,3). In humans the parasite does not complete its life cycle and dies, for example, within the brain. Here it provokes a marked inflammatory response, the main clinical manifestation being eosinophilic meningitis (2,4)

We presented a case of mixed CNS infection of the two parasites, demonstrated by CT, MRI and angiographic imaging.

[1] Department of Radiology, Ramathibodi Hospital, Rama 6 Street, Bangkok 10400, Thailand.
[2] Department of Radiology, Prince of Songkla University Hospital Haadyai, Songkla, Thailand.

CASE REPORT

A fifty-one years old female from Pijit Province, came in with weakness of the lower extremities for one week. The weakness began firstly from the right side and then progressively towards the left side. She was drowsy. There was bilateral cranial nerve VI palsy and stiffneck. The sphincter tone was loose. The motor power of the lower extremities were grade O, while the upper extremities showed grade 4-5. The CSF was sent to DR. Stitaya Sirisingh Laboratory, Department of Microbiology, Faculty of Sciences, Mahidol University. It was positive for Gnathostomiasis and Angiostrongyliasis with O.D. 1.71 and 0.59 respectively (positive cut-off point = OD. + 0.20). The serum was also positive for the two mentioned parasites with OD. 1.8 and 0.46 respectively.

CT scan of the brain showed subarachnoid hemorrhage (Fig. 1). MRI of the brain showed multiple small intracerebral hematomas at pons, left posteroinferior part of the cerebellum and right cerebellar hemisphere. Large hemorrhagic infarct was noted at left parieto-temporo-occipital area (Fig. 2). The left vertebral artery was not visualized by MRA (Fig. 3).

MRI of the whole spine showed subdural hematoma at posterior aspect of C6 to T10. A hemorrhagic tract was seen along the right paramedian posterior aspect of C5 and C5-6, left paramedian area of C4 and C3. Associated cord edema was seen from CT to C6.

Angiography of the left vertebral artery showed dissection of this artery (Fig. 3).

Mild degree of hydrocephalus was present and CSF shunt was installed. The patient had hospital acquired infection. She was discharged and referred to the hospital in Pijit Province. She was quadriplegia and unable to communicate, at the discharge-time.

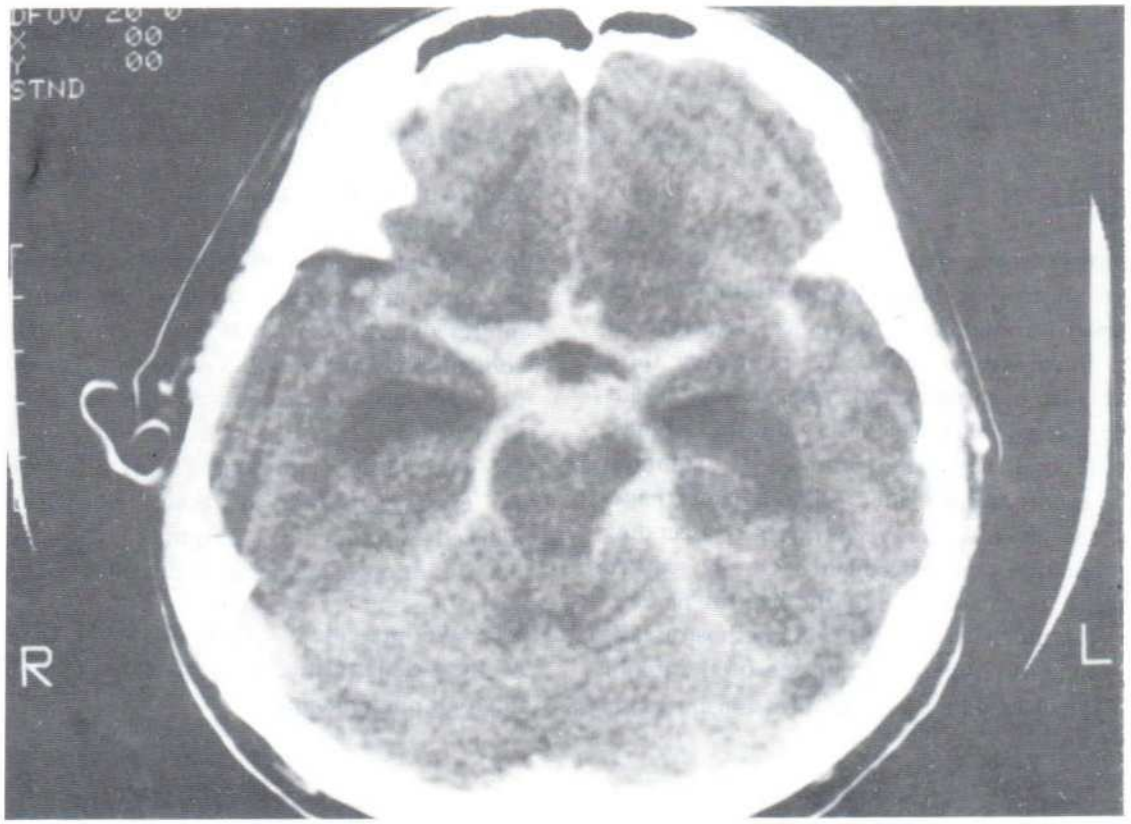

Fig. 1 Non i.v. enhanced CT scan of the brain at the cut level of the suprasellar cistern showed subarachnoid hemorrhage.

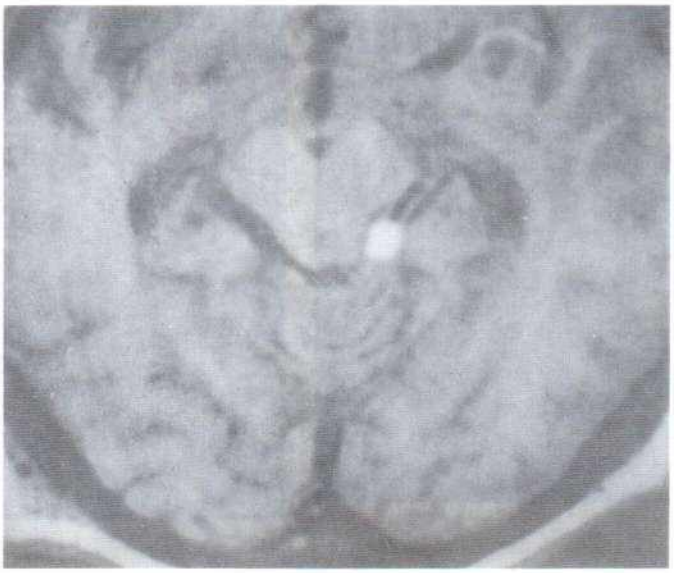

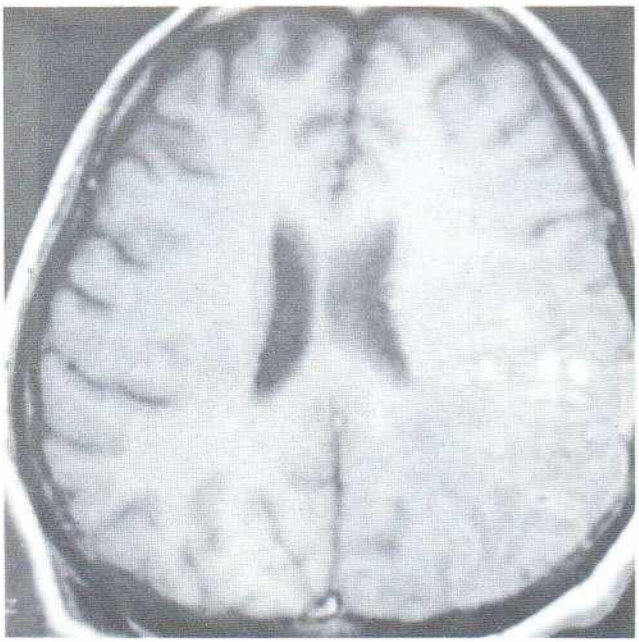

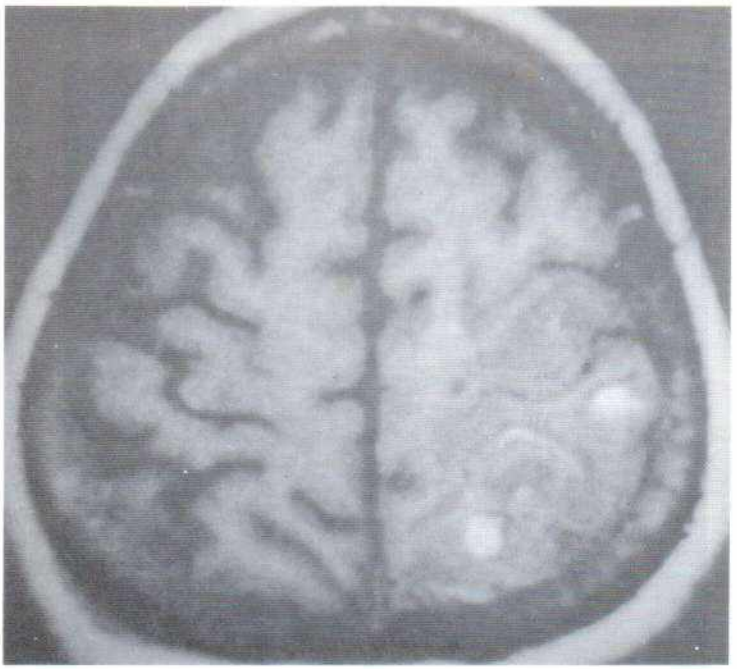

Fig. 2A T1WI-axial view MRI of the brain shows multiple small subacute hemorrhagic areas at left quadrigeminal cistern, and left parietal lobe.

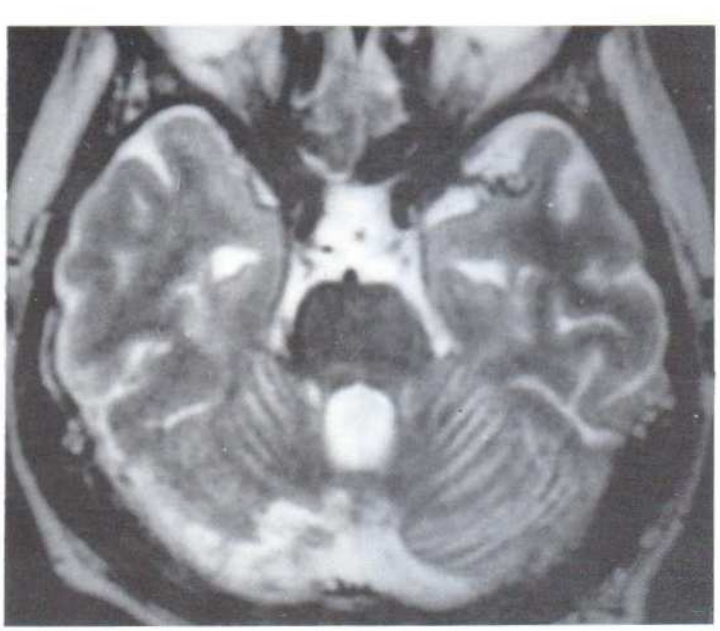

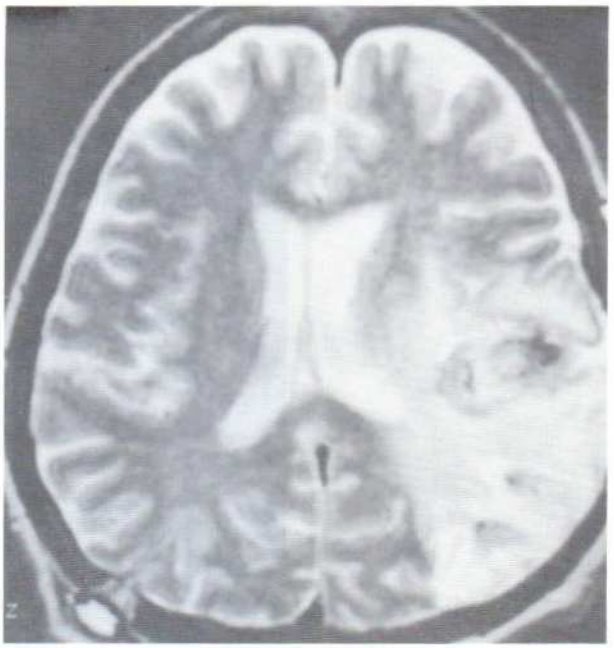

Fig. 2B T2WI-axial view MRI of the brain showed ischemic areas at postero-inferior aspect of both cerebellum and left parietal lobe, left basal ganglia with hemorrhagic component.

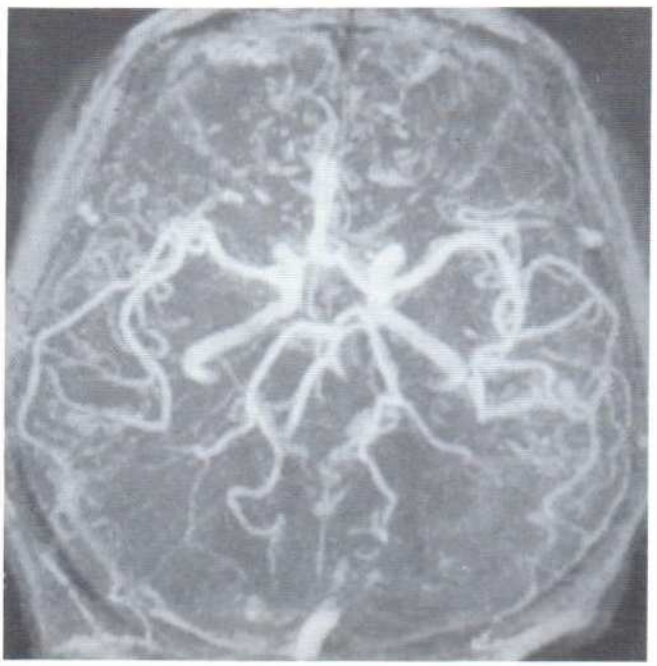

Fig. 3 MRA of the intracranial vessels showed non-visualized left vertebral artery.

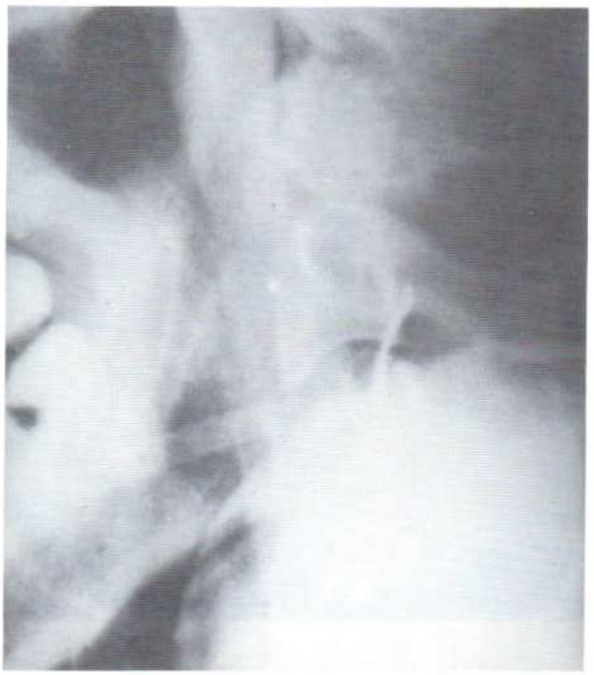

Fig. 4 Dissection of left verebral artery was seen at left vertebral angiographic injection.

DISCUSSION

The first evidence of nervous system invasion by Gnathostoma spinigerum was demonstrated by Chitanondh and Rosen in 1967 (1,5). They found a gnathostome larva embedded in the thoracocervical segment of the spinal cord of a 37-year-old Thai housewife who died of fatal esoinophilic encephalomyelitis. Adult male and female gnathostomes live in the stomach wall of definitive hosts such as the cat, dog, tiger and leopard. A G. spinigerum egg is extruded into the stomach, excreted and hatches in fresh water into the first stage larva. Three larval stages and two intermediate hosts are needed in order to complete the whole life cycle. Man is apparently an accidental host acquiring the parasite by consuming raw or inadequately cooked food which harbours G. spinigerum third stage larvae (1).

To gain access into the central nervous system, they have to go through bone openings or foramina for nerve roots, nerves, and/or blood vessels or perhaps go directly into the arterial supply system of the brain and the spinal cord. Multiple hemorrhagic tracts are the most important pathognomonic findings. These tracts may be widely distributed in the whole axis of the central nervous system or heavily concentrated in a certain segment of the nervous system such as the spinal cord in case of extensive damage, hematoma have been found in the cerebrum, cerebellum, nerve roots, and cauda equina (1,6). Massive intracerebral hematoma can be the primary cause of death (7). Secondary subarachnoid hemorrhage can either be mild, or severe with intraventricular clots (7). Microscopic examination of recent parasitic tracts reveals only hemorrhage, with none or very few cellular responses. In older lesions, microcavitation, tissue necrosis, swollen axis cylinders with phagocytosis and perivascular infiltration are seen. Cellular infiltrates may be predominantly eosinophils or other mononuclear cells, such as plasma cells, lymphocyts, and macrophages. The brain, if involved, is edematous and congested, with cellular infiltration extended to the covering meninges (1).

Paraplegia is more common than quadriplegia or triplegia. Monoplegia is also noted. The variation of weakness and sensory deficits are shown. Urinary retention is always the rule in case of radiculomyelitis of radiculomyeloencephalitis. Multiple cranial nerve palsies are noted in the encephalic form. All the cranial nerves from the second to the twelfth have been involved. Cranial nerve palsies commonly begin after paralysis of the extremities.

Five patients suffering form angiostrongyliasis were reported by Schmutzhard (2). All five presented with the signs and symptoms of meningitis, and one patient presented with bilateral abducens nerve palsy and papilledema of the left eye. No death occurred in this group.

Many helminths have been reported to be able to invade the CNS and cause a wide variety of neurological signs and symptoms. These are, besides Gnathostoma spinigerum and Angiostrongylus cantonensis, Strongyloides stercoralis (8). Trichinella spiralis (9), Toxocara canis (10), Lagochilascaris minor (11), Baylisascaris procyonis (12), Anisakis spp (13), Paragonimus westermanni (14), P. mexicanus, Schistosoma haematobium, S. japonicum, S, mansoni (15), Echinococcus granulosus (16), E multilocularis, Cysticercus cellulosae (17), Spirometra mansonoides (18).

Our presented case was the mixed infection of Gnathostoma spinigerum and Angiostrongylus cantonensis. The clinical pictures was dominated by the firstly mentioned nematode, which produced hemorrhagic incidence. The 6th nerve palsy could be seen in both parasitic infestation.

It is seldom to see the images as shown by us in this condition.

REFERENCES

1. Boongird P, Vejjajiva A. Gnathostomiasis. Travel Medicine International 1994;12:214-219.
2. Schmutzhard E, Boongird P, Vejjajiva A. Eosinophilic meningitis and radiculomyelitis in Thailand, caused by CNS invasion of Gnathostoma spinigerum and Angiostrongylus cantonensis. Journal of Neurology, Neurosurgery, and Psychiatry 1988;51:80-87.
3. Punyagupta S, Bunnag T, Juttijudata P, Rosen L. Eosinophilic meningitis in Thailand. Epidemiologic studies of 484 typical cases and the etiologic role of Angiostrongylus cantonensis. Am J Trop Med Hyg 1970;19:950-58.
4. Punyagupta S, Juttijudata P, Bunnag T. Eosinophilic meningitis in Thailand. Clinical studies of 484 typical cases probable caused by Angiostrongylus cantonensis. Am J Trop Med Hyg 1975;24:924-31.
5. Chitanondh H, Rosen L. Fatal eosinophilic encephalomyelitis caused by nematode

Gnathostome spinigerum. Am J Trop Med Hyg 1967;16:638-45.
6. Bunnag T, Comer DS, Punyagupta S. Eosinophilic myeloencephalitis caused by Ganathostoma spinigerum. Neuropathology of nine cases. J Neurol Sci 1970;10:419-34.
7. Punyagupta S, Jittijudata P, Bunnag T, Comer Ds. Two fatal cases of eosinophilic myeloencephalitis: a newly recognized disease caused by Gnathostoma spinigerum. Trans Roy Sco Trop Med Hyg 1968;62:801-9;
8. Scowden EB, Schaffner W, Stone WJ, Overwhelming strongyloidiasis: an unappreciated opportunistic infection. Medicine 1978;57:527-44.
9. Most H, Abeles MM. Trichiniasis involving the nervous system. Arch Neurol Psychiatr 1937; 37:589-616.
10. Woodruff AW. Toxocariasis. Br. Med J 1970; 2:589-616.
11. Rosenberg S, Lopes MBS, Masuda Z, Campos R, Vieria Bressan MCR. Fatal encephalopathy due to Lagochilascaris minor infection. Am J Trop Med Hyg 1986;35:575-8.
12. Fox AS, Boyer KM. Fatal eosinophilic meningoencephalitis and visceral larva migrans caused by the racoon ascarid. Baylisuscaris procyonis. N Engl J Med 1985;312:1619-23.
13. Khalil LF. Larval nematodes in the herring (clupea Harengus) from British coastal waters and adjacent territories. J Marine Biol Assoc UK 1969;49:641-59.
14. Oh SJ Cerebral paragonimiasis. Trans Am Neurol Assoc 1967;92:275-7.
15. Scrimgeour EM, Gajdusek DC. Involvement of the central nervous system in Schistosoma mansoni and S. haematobium infection. Brain 1985;108:1023-38.
16. McCorkell SJ, Lewall DB. Computed tomography of intracerebral echinococcal cysts in children. J Comp Assist Tomogr 1985;9:514-8.
17. McGormic GF, Zee CS, Heiden J. Cysticercosis cerebri, review of 127 cases. Arch Neurol 1982;39:534-9.
18. Fan KJ, Pezeshkpour GH. Cerebral sparganosis. Neurology 1986;36:1249-51.

EFFICACY AND SAFETY OF PERCUTANEOUS TRANSTHORACIC NEEDLE ASPIRATION BIOPSY UNDER SOME LIMITATIONS: A PROSPECTIVE STUDY IN 109 PATIENTS

Komgrit TANISARO[1], Wilaiwan WEERAYACHAIYO[2],
Supranee NIRAPATHAPONGPORN[3], Patchrin PEKANAN[3], Sopon KUMPOLPUNTH[3].

ABSTRACT

Percutaneous transthoracic needle biopsy was performed in 109 patients during April 1992 - April 1995. Diagnostic yield was slightly lower than the foreign reports due to different types of the needles used and the lack of immediate cytology reports. The incidence of hemoptysis was similar to other reports but the occurrence of the pneumothorax was less due to less repetition of the needle puncture. Considering socioeconomic and lack of medical-personnel-power in this country, this procedure as practised by us is quite practical.

INTRODUCTION

Percutaneous transthoracic needle biopsy (PTNB) has long been accepted as the reliable, and low complicated procedure for establishing the diagnosis of the intrathoracic mass. Few articles concerning PTNB were published from Thailand. They were different from those reported in other countries which were the retrospective ones (2,3,4).

The purpose of this study was to compare the diagnostic yield and rate of complications, compared with the foreign reports. Limitation of our procedures was the type of the needles used, the re-use of the needles and the lack of prompt interpretation of the obtained tissue or fluid.

PATIENTS AND METHODS

A prospective study of PTNB in the patients with the intrathoracic masses was performed during 1992-1995. The patients were in and out patients of Ramathibodi Hospital and Prince of Songkla University Hospital. The following data were obtained and recorded in the prepared sheet-forms:

1. Age, sex, in or out patient.
2. Important clinical data such as the indication for the biopsy, the chronic illness, pulmonary disease, smoking, previous treatment, previous bronchoscopy, any disease that increases the risk for biopsy.
3. Data concerning the nodule or mass from the diagnostic images, the lungs-background.
4. Technical aspects of PTNB, the types of the needle, the site and the number of passing the needle, the imaging used.
5. Clinical symptoms or signs during, immediately after and 4 hours after the biopsy.
6. The time and the severity that the pneumothorax occurred, duration of retained tube drain (ICD).
7. The appearance of the tissue or fluid obtained, the result of cytology, histology, staining and culture.

The planning, the chosen instruments and the PTNB was performed by the same radiologist in every case. The technique used was the standard one (5). All of the informations were recorded by the computer for statistic analysis.

[1] Department of Radiology, Prince of Songkla University Hospital, Haadyai, Songkla, Thailand.
[2] Department of Medicine, Prince of Songkla University Hospital.
[3] Department of Radiology, Ramathibodi Hospital, Bangkok.

RESULTS

There were 109 patients, 79 of them were male and 30 were female. Age ranged was 18-86 years old, the average age was 59 years old. Forty-nine cases were outpatients and 60 cases were in-patients. The indications for PTNB were 1) to diagnose the primary bronchogenic carcinoma in 62 cases (56.9 percents) 2) to diagnose the type of metastatic nodules in 17 cases (15.5 percents) 3) to differentiate between cancer and tuberculosis in 16 cases (14.7 percents) 4) to establish the infectious nodules in 14 cases (12.9 percents). Bronchoscopy was performed in twenty patients but pathological results were not informative.

Twenty patients (19.3 percents) had pulmonary emphysema or hyperaerated lung and 13 cases (12 percents) had risk factors for pneumothorax e.g. previous PTNB at the same site and history of heavy smoking.

Ninety patients (90 percents) had nodules in the lungs, 11 patients (10 percents) had nodules at other sites i.e. pleura and mediastinum. Right upper lobe nodules were seen in 38 cases, left upper lobe nodules were seen in 25 cases, right lower lobe nodules in 11 cases, left lower lobe nodules in 10 cases, right middle lobe nodules in 7 cases and at hilar region in 4 cases. The size of the nodules ranged from 1.5 to 2.0 cm, average size was 5.4 cm. The depth from the skin to the nearest part of the nodule was 2.5 to 12 cm, average distance was 5.7 cm.

Anterior approach of PTNB was done in 58 cases (53.2 percents), posterior approach was performed in 42 cases (38.5 percents) and lateral approach in 9 cases (8.3 percents). The method used for localization was fluoroscopy in 96 cases (88 percents), ultrasonography in 11 cases (10 percents) and X-ray computed tomography in 2 cases (2 percents).

Spinal needles were used in 82 patients (75.2 percents), cutting needle e.g. Franseen (Cook, Australia) or True-cut (Cook, Australia) in 18 cases (16.5 percents) and aspiration needle, e.g. Chiba needle (Cook, Australia) in 6 case (7.3 percents). More than half of the needles (55.5 percents), were re-used at least once. 21-G needles were used in 39 patients (35.8 percents), 20-G size in 25 cases (23 percents), 18-G needles in 22 cases (20.2 percents), 23-G size in 18 cases (16.5 percents), 22-G size in 5 cases (4.6 percents).

The puncture was performed only once in 65 cases (58.7 percents), twice in 40 cases (37.6 percents) and thrice in 4 cases (3.7 percents).

Complications were seen in 26 patients (24 percents) including pain at the sites of puncture in 9 cases (8.3 percents), hemoptysis in 7 cases (6.4 percents), non-blood stained cough in 6 cases (5.5 percents) and other problems in 4 cases. Immediate pneumothorax was seen in 4 cases with average degree of 7.2 percents of the pleural space. Delayed 4 hrs-pneumothorax was seen in 4 cases with average volume of 16.7 percents of that side of pleural space. One case showed pneumothorax in 48 hours post PTNB. Total cases of pneumothorax were 9 cases (8.26 percents) with range of percentage of pneumothorax from 5 to 50 (average 20) of the pleural space volume. Intercostal drainage was performed in 4 patients who had more than 30 percents pneumothorax or had tension pneumothorax which was seen in 3.7 percents of the total cases (44.4 percents of the whole cases of pneumothorax). The duration of retained ICD was 5-7 days, (average 6.2 days).

The diagnosis could be obtained from cytology, gram stain and culture in 86 cases (78.9 percents). In 23 cases, the tissue was inadequate or malignant cells were not seen. Cancer was seen in 67 cases (78 percents), infectious process in 19 cases (22 percents). Squamous cell carcinoma predominated in cancer group and was seen in 25 cases (37.3 percents of all cancer patients). Other cell types were listed in the table 1.

In the patients with infection, bacteria was shown in 8 cases (42 percents), tuberculosis in 7 cases, fungus in 1 case and unidentified specific type of infection in 3 cases.

Table 1. The result of cytology in 67 patients.

Results of cytology	No. of patients	percents of patients
Squamous cell carcinoma	25	37.3
Non small cell carcinoma	11	16.4
Positive for malignancy	8	12
Adenocarcinoma	6	8.9
Large cell carcinoma	6	8.9
Metastasis	5	7.5
Small cell carcinoma	4	6
Others	2	3
Total	67	100.00

DISCUSSION

High diagnostic yield (more than 85 percents) of the PTNB was seen in the report from abroad (1,6). This is probably due to the combined factors e.g. modern diagnostic machine, and needle (7,8), repeated study was obtained in one setting with immediate cytologic interpretation in case of inadequate specimen (9).

Lower diagnostic yield in our series (79 percents) was probably secondary to the following reasons: 1) spinal needle, though easy to obtain and cheap, was not design for cutting or sucking the tissue and the size of the internal lumen was smaller than other types of needle; besides they were used more than once 2) the specimen obtained was not examined immediately. Comparing with the diagnostic yields from other reports which had similar inferiority showed the same results (9,10).

The incidence of hemoptysis was similar to the report of others (5). The incidence of pneumothorax in our series was lower (8.3 percents) than from other reports (1) which appeared to be 30 percents. The reason behind this was probably less needle puncture (average 1.4 times) than that reported by Austin (9) which had more repetition of the puncture owing to immediate cytology interpretation.

REFERENCES

1. Fraser RS, Pare JAP, Fraser RG, Pare PD. Methods of roentgenologic and pathologic investigation in Synopsis of Disease of the chest. 2nd Ed. Philadelphia: Saunders: 1994; 132-133.
2. Thammakumpee G. Transthoracic needle aspiration biopsy of lung lesions in Songklanagarind Hospital. Songklanagarind Medical Journal 1992; 10: 219-223.
3. Sirivanichai C. Ultrasound-guided biopsy of thoracic tumors. Presented in the 32th Annual Meeting of Thai Radiological Society of Thailand. 26-28 Jan 1995, Bangkok.
4. Chonnmitri I. Fine needle aspiration biopsy of lung lesions. J Med Assoc Thai 1993; 76: 394-398.
5. The American Thoracic Society. Guideline for percutaneous transthoracic needle biopsy. Am Rev Respi Dis 1989; 140: 255.
6. Perlmut LM, Johrnston WW, Dunnick NR. Percutaneous transthoracic needle aspiration: A review. AJR 1989; 152: 451-455.
7. Zavala DC, Schoel JE. Ultrathin needle aspiration of the lung in infectious and malignant disease. Am Rev Respi Dis 1981; 123: 125.
8. Yazdi HM, Macdonald LL, Hickey NM. Thoracic fine needle aspiration biopsy versus fine needle cutting biopsy: a comparative study of 40 patients. Acta Cyto 1988; 32: 635.
9. Austin JH, Cohen MB. Value of having a cytopathologist present during percutaneous fine-needle aspiration biopsy of lung: report of 55 cancer patients and metaanalysis of the literature. AJR 1993; 160: 175-177.
10. Stevens JM, Jackman RJ. Outpatient needle biopsy of the lung: its safety and utility, Radiology 1984; 134: 301-304.
11. Fish GD, Stanley JH, Scott Miller K, et al. Postbiopsy pneumothorax: estimating the risk by chest radiography and pulmonary function tests. AJR 1988; 150: 71-74.
12. Khouri NF, Stitik, Erozan YS, et al. Transthoracic needle aspiration biopsy of benign and malignant lung lesions. AJR 1985; 144: 281-288.

EMBOLIZATION OF A DURAL SINUS FISTULA BY INTRAOPERATIVE INJECTION WITH N-BUTYL CYANO ACRYLATE (NBCA)

Sirintara PONGPECH[1], Suthisak SUTHIPONCHAI[2],

SUMMARY

A patient presented with multiple episodes of intracranial hemorrhage from a dural arterio-venous fistula (DAVF) involving the Rt transverse sinus. The sinus was totally occluded at the sigmoid-jugular junction with narrowing of the left side venous drainage; leading to the venous retrograde flow into the cortical veins. Attempts to transarterial superselective embolization with NBCA were performed. The branches of feeders were only slightly decreased. Transjugular approach could not be done due to the occlusion of both side jugular bulbs. The surgical small craniotomy at Rt transverse sinus was performed to avoid the risks of the sinus exposure. Direct puncture with the technique of guide wire were followed by catheterization deep into the right sigmoid junction for injection of the NBCA. The torcula was firmedly compressed to avoid the migration of glue into the contralateral side sinus. The complete cure of the dural fistula and improvement of the clinical manifestation were achieved after the procedure.

CASE REPORT

A 26-year-old man presented with multiple episodes of intraparenchymal hemorrhage at posterior occipital cortex and subarachnoid hemorrhage (Fig. 1 a-b). Each episode caused coma with worsening of the neurological deficits.

Angiographic study revealed multiple enlarged dural feeders from the right external carotid artery (Fig. 2 a) and tentorial branch from the right internal carotid artery. These feeders opend into the DAVF at right transverse sinus with totally occlusion of the right sigmoid-jugular junction. The opposite jugular was narrow at the same level (Fig. 3 a-b). Venous drainage of the DAVF was retrogradely filled into the superior sagittal sinus and straight sinus with multiple dilated cortical veins (Fig. 2 b).

Several sessions of superselective transarterial NBCA embolization did not achieve occlusion of the fistula (Fig. 4 a-c). In addition, it could not prevent intracranial hemorrhages with progressive worsening of the neurological symptoms.

Therefore, we have made a decision to perform the intraoperative occlusion with NBCA via direct puncture after surgical small craniotomy. After the outlining of the right transverse sinus was seen; 16 G cathlon needle was used to puncture into the sinus from the most medial part. After that, the 032 Terumo guide wire was inserted and short cut tapering end 4F catheter was followed (Fig. 5). As the tip reached the spontaneous occluded right sigmoid-jugular junction; manual compression to completely control the venous flow at the right side torcula was successful (confirmed by fluoroscopic contrast testing). The total amount of 3.5 ml. pure NBCA was injected to fill the whole right transverse sinus (Fig. 6 a,b). The 4F catheter was rapidly withdrawn before polymerization occurred. The manual control was last within a few minutes. No active bleeding or immediate complications

[1] Department of Radiology, Ramathibodi Hospital, Rama 6 Street, BKK 10400, THAILAND.
[2] Department of Radiology, Siriraj Hospital, BKK.

were observed. The surgical closure of the craniotomy was done.

Clinical improvement after the procedure was continuously observed and follow up 2 weeks angiogram was performed which showed the complete closure of the DAVF with improvement of the venous congestion (Fig. 7 a-c).

(a) (b)

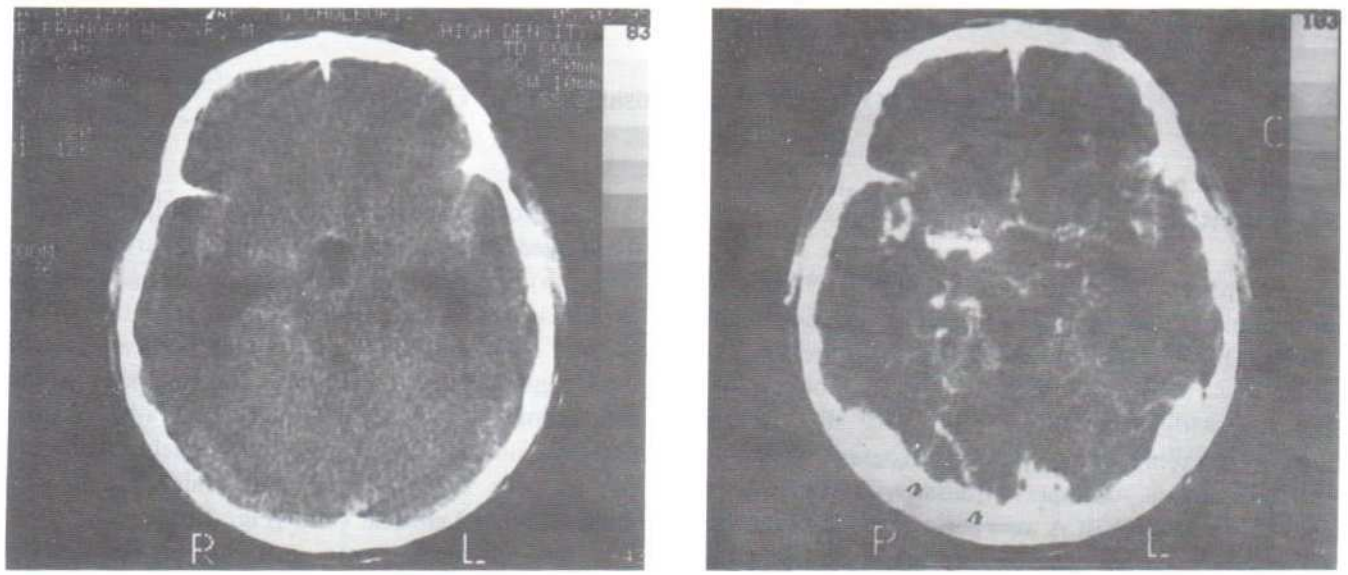

Fig. 1 (a,b) NCCT (a) and CECT (b) showed subarachnoid hemorrhage, hydrocephalus and diffuse abnormal enhanced vessels.

(a) (b)

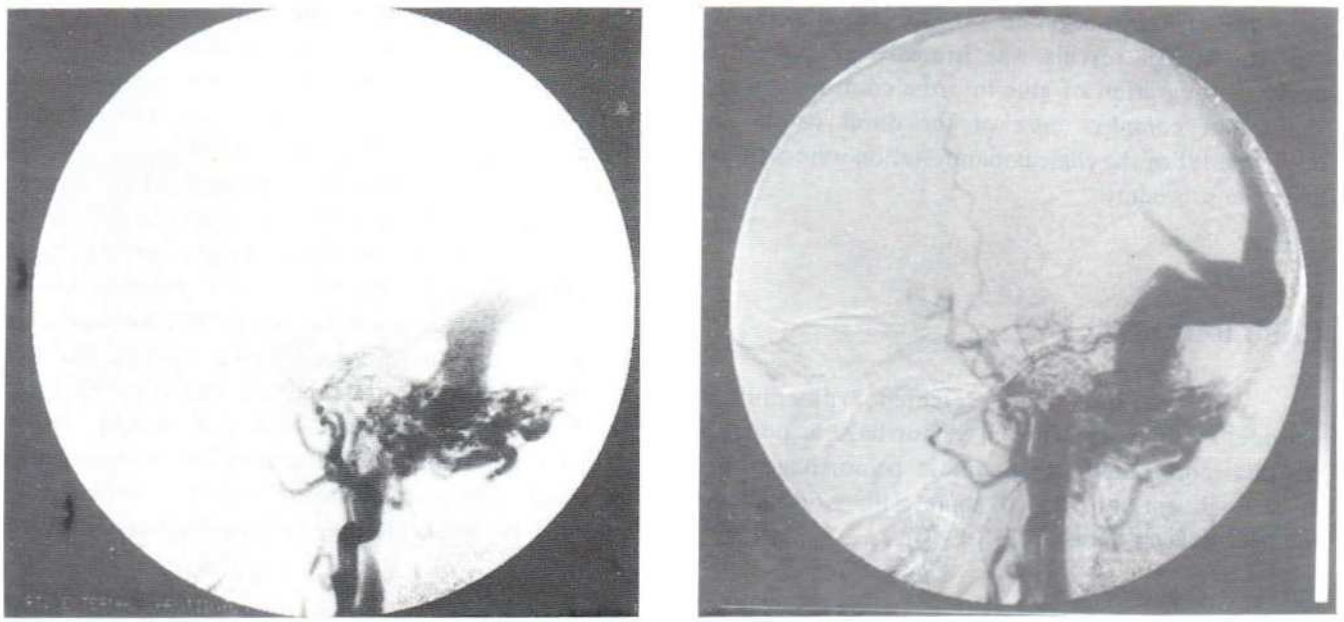

Fig. 2 (a,b) Right external carotid angiogram in lateral view in arterial phase (a), venous phase (b), showed multiple dural feeders opening into the right transverse sinus, narrowing of the jugular bulb and retrograde venous drainage (Djindjian classification type a + b).

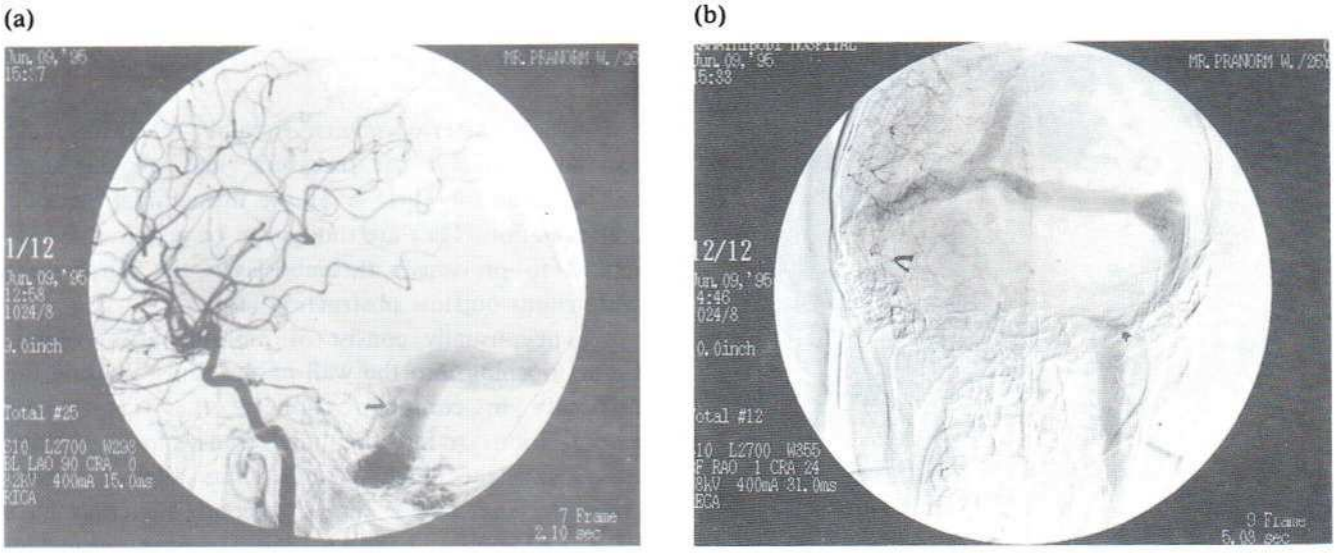

Fig. 3 (a-b) Post transarterial embolization control angiogram, RICA series showed a tentorial branch feeding the DAVF (arrow) (a) and total occlusion of right sigmoid sinus (arrow) with marked narrowing of the left side (arrows) (b).

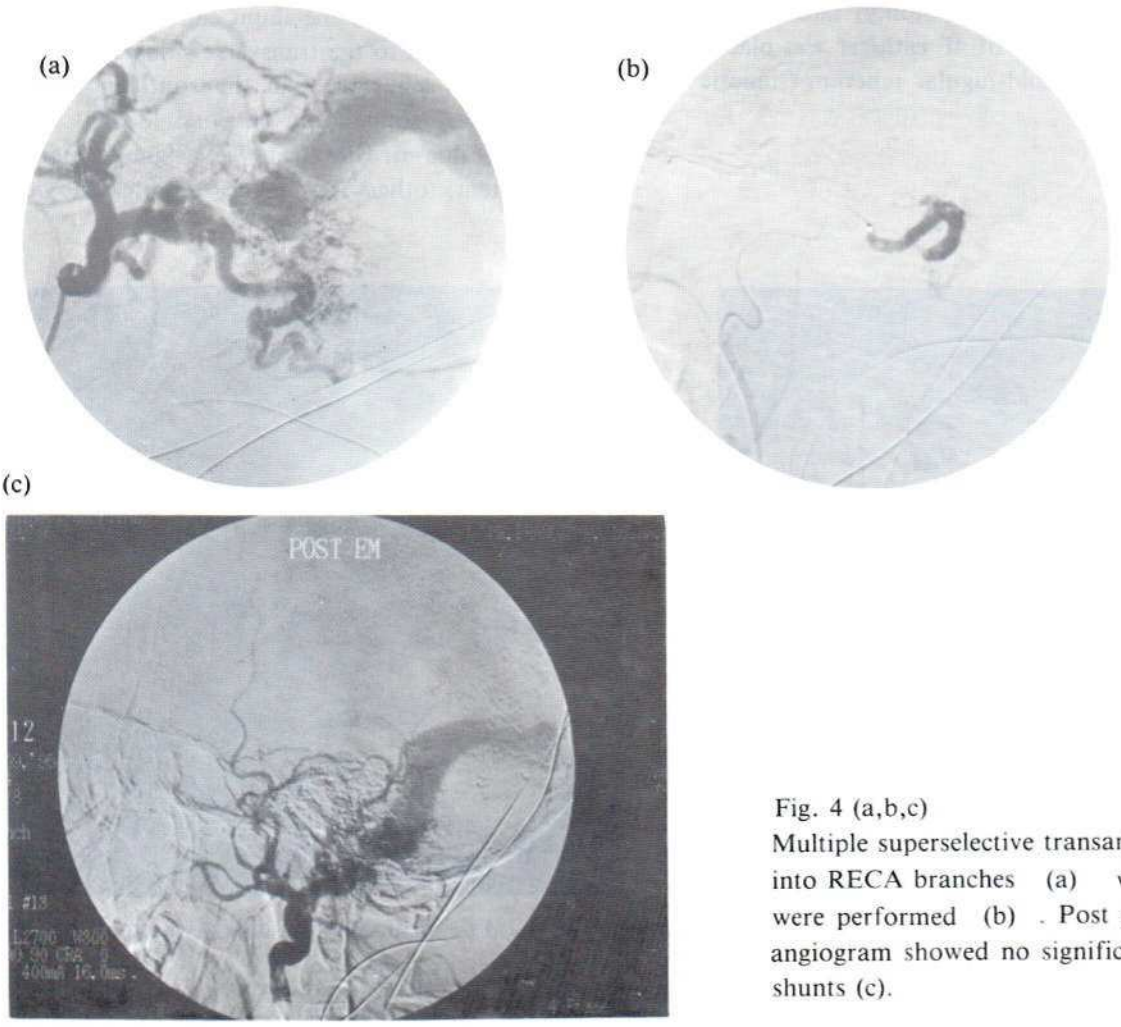

Fig. 4 (a,b,c)
Multiple superselective transarterial catheterization into RECA branches (a) with NBCA injection were performed (b) . Post embolization control angiogram showed no significant changes of the shunts (c).

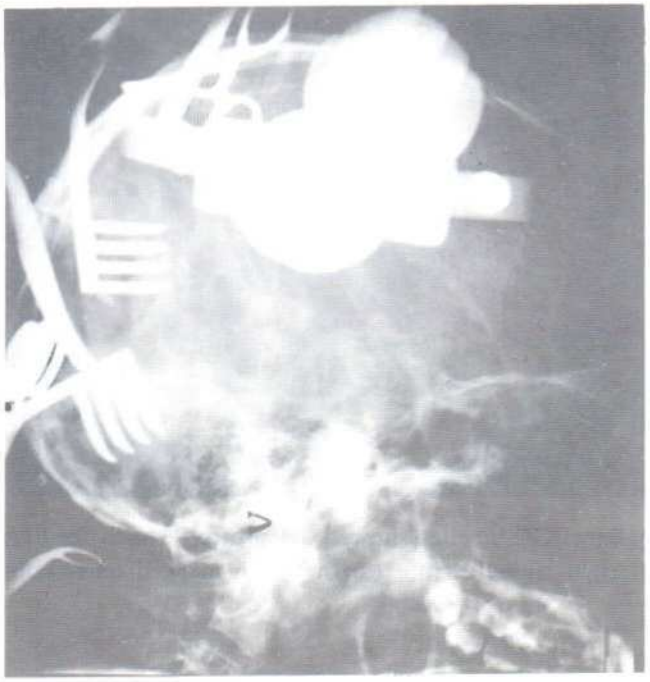

Fig. 5 Intraperative (small craniotomy) lateral skull film showed the tip of 4F catheter was placed at the right sigmoid-jugular junction (stenotic point;arrow)

DISCUSSION

Dural arterio-venous fistulas (DAVF) most commonly involve the transverse and sigmoid sinus and account for 10-15% of the intracranial vascular malformation. They are thought to be acquired lesions related to previously thrombosis of the dural sinus and venous outflow obstruction (4).

They usually consist of multiple arteriovenous shunts opening into the wall of the sinus; causing the difficulty in complete cure by the transarterial embolization. On the other hand, transvenous approach to occlude the single venous sinus allows a more complete cure. Many kind of embolic materials have been used such as balloons, coils, or even permanent liquid substances (1,2).

There were also some reports on the direct puncture of the enlarge arterial feeders (i.e. occipital arteries) with good results (3). Compression of the occipital artery was claimed to cause clinical cure up to 20% (5). However, when the sinus is occluded, transjugular approach to the shunt can be impossible. Percutaneous access to the transverse sinus by passing the contralateral sinus through the confluence sinus to the thrombose sinus could be possible only when at least one side of the transverse-sigmoid-jugular sinus is patent, otherwise, access requires surgical approach.

(a)

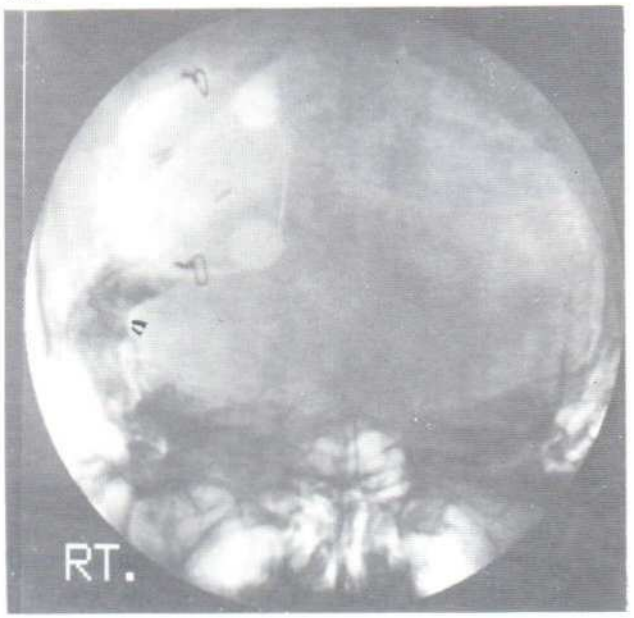

(b)

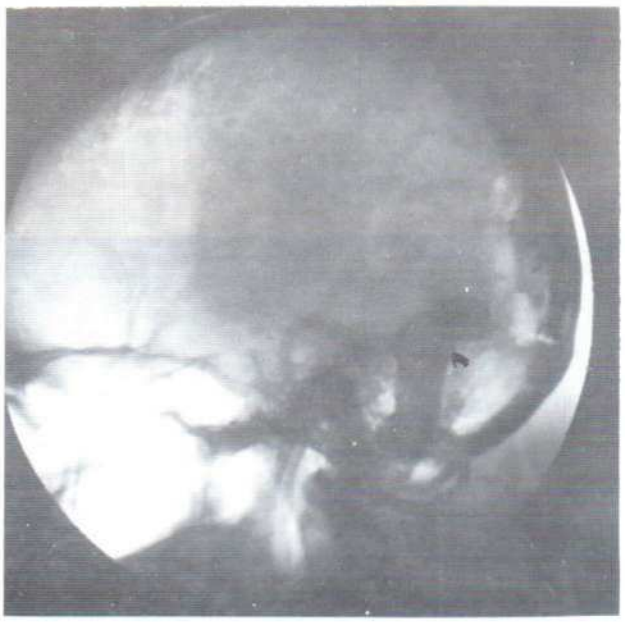

Fig. 6 (a,b) AP and lateral skull film after the procedure showed good deposition of the NBCA (opaque density: arrows) in the whole Right transrerse sinus.

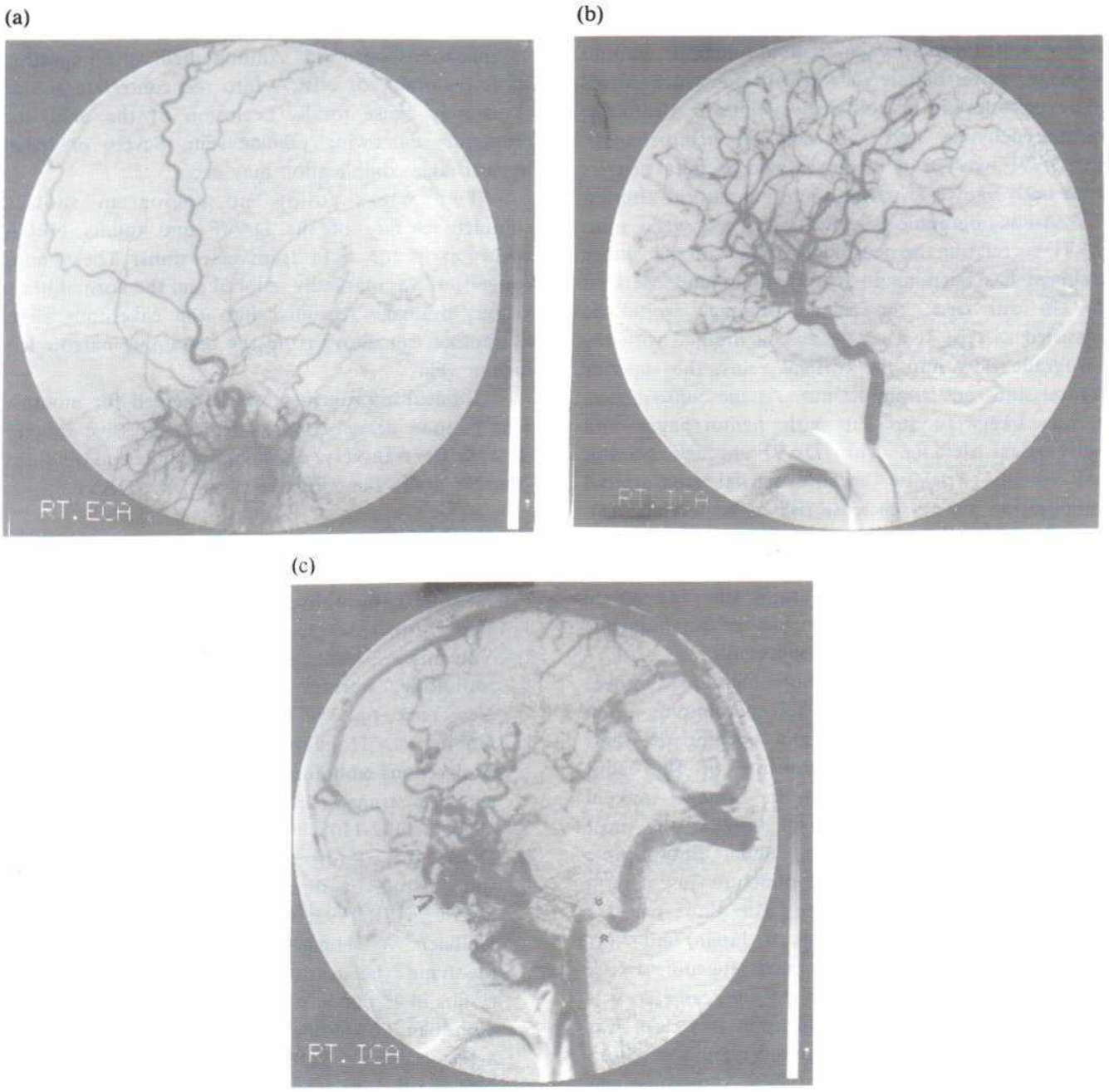

Fig. 7 (a,b,c) Follow up 2 weeks angiogram RECA showed complete closure of the shunts (a); no more tentorial branch of the RICA was observed (b). The visualized transverse sinus (c) was the contralateral side which showed narrowing of the left jugular bulb (double arrow); venous recruited via cavernous sinus (arrow).

In this case, DAVF was located on the right transverse sinus which was totally thrombosed distal to the shunts (at the jugular-sigmoid junction). Venous drainage was retrograde via cortical veins which caused many episodes of neurological symptoms (from the intraparenchymal and subarachnoid hemorrhages). The DAVF was fed by meningeal and occipital arteries from both right external and internal carotid arteries.

An angiographic classification of transverse sinus DAVF correlating the neurological risk with the venous drainage has been made by Djindjian and Merland (6). In our case, the fistula drainage would be classified as type II a+b because it drained with the retrograde flow into the cortical veins, the superior sagittal sinus and straight sinus. As the consequence, it was likely to present with hemorrhages and neurological deficits. This DAVF needed prompt and complete closure because partial transarterial embolization did not decrease risk of hemorrhage (1).

Transvenous approach from femoral vein passing through both jugular bulbs would also be impossible due to the total occlusion of right side and severe narrowing of the left side, even idea of percutaneous jugular puncture would not be successful.

Because of all the restrictions mentioned above, the intraoperative small burr hole craniotomy upon the right transverse sinus without opening the dura was performed. After the outline of the right transverse sinus was visualized, the spongel manual compression in order to control flow at the most medial part could be obtained under fluoroscopic contrast injection test. Direct puncture just lateral to the control point was made. The short cut 032 Terumo guide wire (Terumo, Tokyo, Japan) and short cut tapering 4F catheter (Nycomed, Ingenor, Paris, France) were chosen. The tip of the catheter was placed as distal as possible which, in this case, was at the occlusion of the right sigmoid-jugular junction. About 3.5 ml. of almost pure NBCA mixture was injected to fill the whole right transverse sinus and the catheter was rapidly pulled out. No immediate complications occurred. Among them, the migration of few amount of NBCA into the contralateral side sinus may cause totally occlusion of the only one remaining narrowing jugular vein. Severe or lethal hemorrhagic complication may occur.

Two weeks follow up angiogram showed complete closure of the DAVF and totally NBCA occlusion in the right transverse sinus. The venous congestion was markedly reduced and the normal brain venous drainage recruited into the cavernous sinus as another exit above from the remaining narrow left jugular vein.

Clinical improvement was observed for months. This method decreased risks from aggressive surgery to resect the transverse and sigmoid sinus and obtained good results in the complete cure of the DAVF.

REFERENCES

1. Berentein A., Lasjaunias P., (1992), Surgical Neuro-angiography, Vol. 2, Springer-Verlag, Berlin, pp. 175-233.
2. Valvanis A., et al., (1993), Interventional Neuro-radiology, Springer-Verlag, Berlin Heidelberg New York, pp. 35-54.
3. Gobin V., Houdart E., et al., Percutaneous transvenous embolization through the thrombosed sinus in transverse sinus dural fistula, AJNR 1993;14:1102-1105.
4. Gensberg S., Radford R., Embolization of a dural sinus fistula by direct puncture of the occipital arteries, AJR 1993;160:1265-1266.
5. Halbach VV., Higashida RT., et al. Dural fistulas involving the transverse and sigmoid sinuses: results in 28 patients. Radiology 1987;163:443-447.
6. Djindjian R., Merland JJ., Theron J. Superselective arteriography of the external carotid artery. New York, NY. Springer-Verlag. 1977;606-628.

BENIGN LOCALIZED FIBROUS PLEURAL MESOTHELIOMA IN A PATIENT WITH HYPOGLYCEMIC SYMPTOM

Sopon KUMPOLPUNTH[1], Patchrin PEKANAN[1],
Wiwatana THANOMKIAT[2], Thitiporn RANGSITPOL[1,3]

ABSTRACT

A case of localized fibrous pleural mesothelioma in a 55 year-old male patient with hypoglycemic sympotoms was presented. The patient had also clubbed fingers. A large mass occupied 1/2 to 2/3 of right hemithorax was shown by plain film. An isoechoic mass to the liver was seen by ultrasonography with low echoic areas. A well defined border mass with isodensity to the liver with areas of low density was observed by CT scan. Ultrasonography helped separating the mass from the normal liver. Surgery was performed with easiness and the tumor was totally removed with the disappearance of the hypoglycemic symptoms.

INTRODUCTION

Pleural mesotheliomas was first described by Lieutaud in 1767 (1). It was classified into diffuse and localized mesotheliomas by Klemperer and Rabin (2,3), according to the gross, microscopic and prognostic viewpoints. The diffuse type is better known because of its dramatic gross appearance, its rapidly fatal course and its induction by asbestos (4-6). Localized mesotheliomas, in contrast, are usually purely fibrous and carry a good prognosis (7,8). It has received a variety of names, including fibrous mesothelioma, benign mesothelioma, localized mesothelioma, subpleural fibroma, and localized fibrous tumor of the pleura (4).

We present a case of benign fibrous pleural mesothelioma in a patient with hypoglycemic symptoms. Images are illustrated by plain film, ultrasonography and CT scan.

CASE REPORT

A 55 year-old male farmer from Bureeram Province, in the Northeastern part of Thailand, presented to us with seizure 2 days prior to the admission. His problem began 3 months ago; he was easily tired and had weight loss. One and a half months prior to the admission, he had a behavioural change; having been aggressive only in the morning every day. He, later, developed seizure and finally status epilepticus. He was found to have decreased blood sugar at a local hospital. He smoked 10 cigarettes per day for 30 years and was a regular alcoholic drinker. The positive physical examination findings were hepatomegaly, clubbing of fingers, chachetic, absent Babinskin's sign. His serum blood sugar was 20 mg/dl, calcium 8 mg/dl, and a normal serum insulin level.

[1] Department of Radiology, Ramathibodi Hospital, Rama 6 Street, Bangkok 10400, Thailand.
[2] Department of Radiology, Prince of Songkla University Hospital, Haadyai, Songkla, Thailand.
[3] Department of Radiology, Phra Pinklao Hospital, Bangkok.

Plain chest film in AP and lateral views showed a large intrathoracic mass at the lower half of the right hemithorax (Fig. 1). Ultrasonography of the right upper quadrant showed a solid mass at right lower hemithorax and a normal liver (Fig. 2). CT scan showed a large well defined border solid mass at right lower hemithorax without adjacent organs invasion; multiple small necrotic areas was noted within the mass (Fig. 3).

The tumor from the right lower hemithorax was removed surgically and totally. There was some adhesion to the right hemidiaphragm. The colour of the mass was white with necrotic areas. Histology revealed a benign fibrous mesothelioma.

The hypoglycemic symptoms and seizure disappeared after tumor removal.

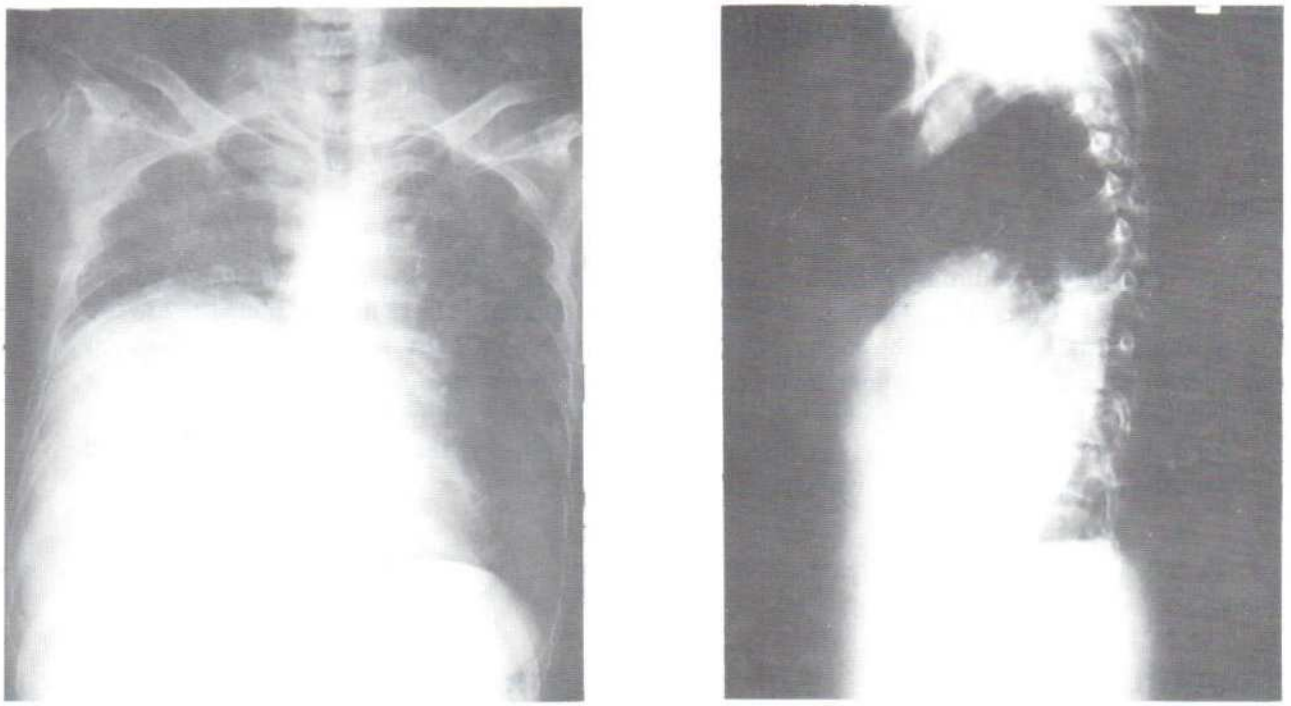

Fig. 1 Plain film of the chest in AP and lateral views showed the appearance of elevated right hemidiaphragm VS a large mass at the lower half to the hemithorax, obliterating right hemidiaphragm.

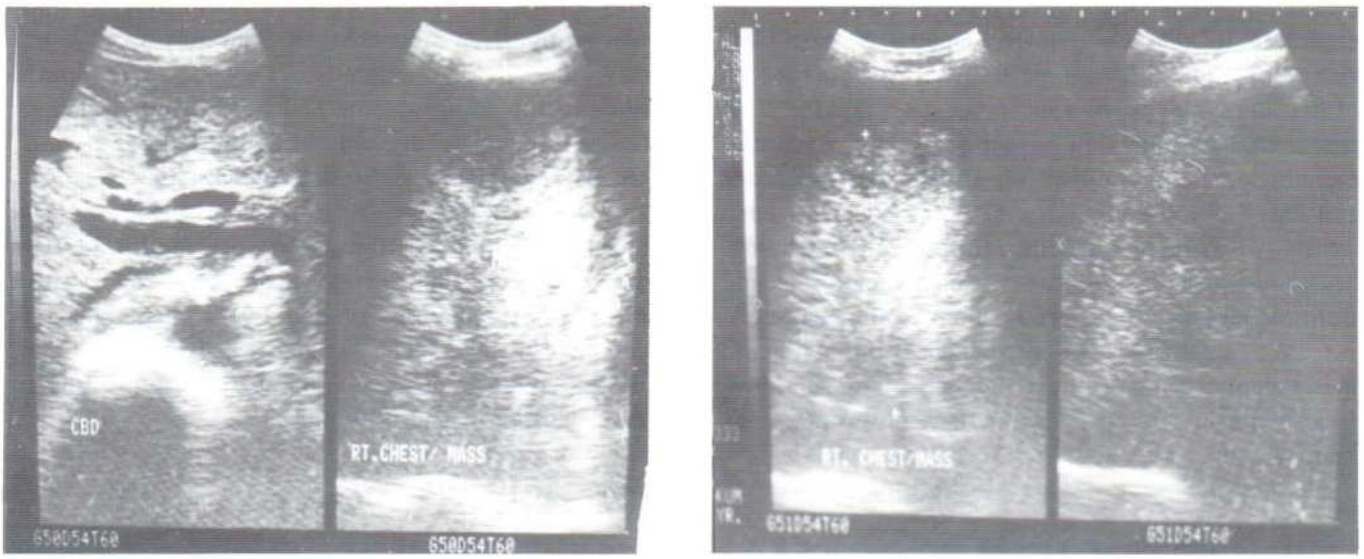

Fig. 2 Ultrasonography in the region of the mass revealed a well defined border mass with iso to slightly hyperechoic to the liver parenchyma and there were areas of low echo. The liver was normal.

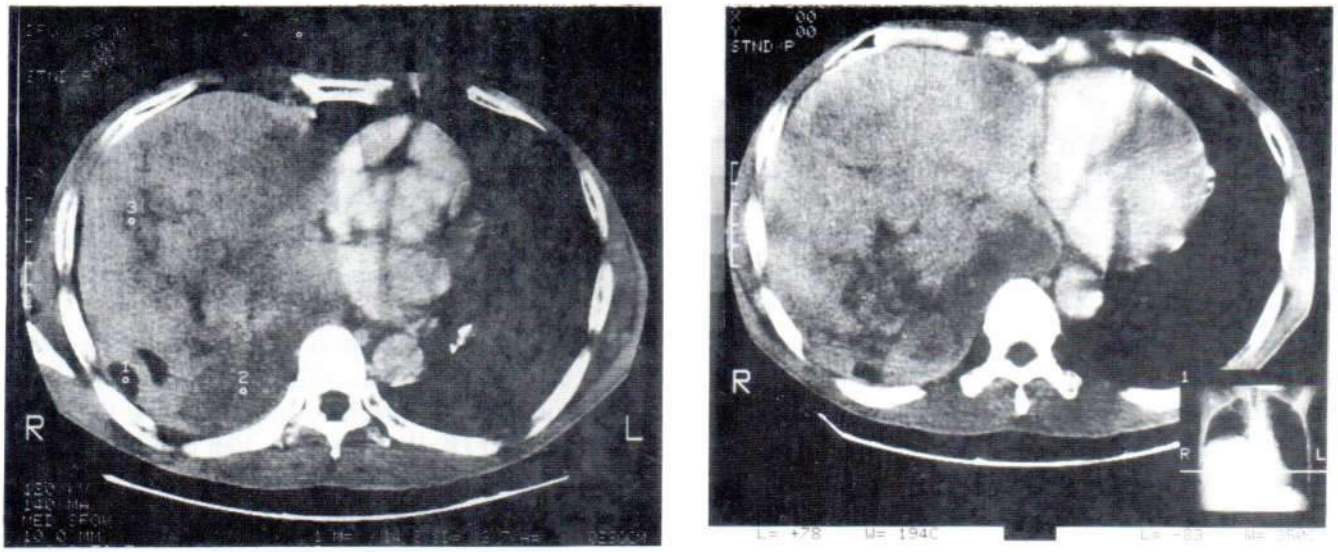

Fig. 3 I.V. contrast axial CT scan of the chest showed a well defined border mass with isodensity to mildly hypodensity to the adjacent heart and aorta. Multiple small low density areas were noted.

DISCUSSION

Solitary fibrous tumors of pleura achieved a classic clinical and pathologic description: a large pedunculated mass attached by a narrow pedicle to the visceral pleura, in an asymptomatic individual who occasionally had hypoglycemia or osteoarthropathy (7,9-13). A minority of localized fibrous tumors of pleura were intrapulmonary lesions (14-15).

The localized fibrous tumors of the pleura occured equally in both sexes, most commonly in the sixth to seventh decades of life. Presenting symptoms included chest pain, dyspnea, and cough; they were observed in three-fourths of patients with a malignant tumor. One in every four of these patients had hypoglycemia, clubbed digits or pleural effusion. Two-thirds of the tumors were attached to visceral pleura, often by a pedicle. The rest arose from the parietal pleura of the chest wall, diaphragm, or mediastinum. Neoplasms in these atypical sites, together with fissural lesions and tumors "inverted" into peripheral lung, were more often malignant. Most neoplasms measured 5-10 cm and weighed 100-400 g. Microscopically, the "patternless pattern" or hemangiopericytic type, was seen in the majority of cases, and mixed patterns were seen in nearly 40% of tumors. All of the benign and 45% of the malignant tumors were cured by simple excision. Patients surgically cured of a malignant neoplasm had pedunculated or well circumscribed lesions. However, 55% of patients with malignant tumors succumbed to their disease secondary to invasion, recurrence, or metastasis. Resectability is the single most important indication of clinical outcome. No tumor expressed epithelial differentiation, either immunohistochemically or ultrastructurally; therefore, England (17) favored the term "localized fibrous tumor" of pleura instead of localized mesothelioma.

Most localized benign fibrous pleural mesothelioma were discovered incidentally or routine chest radiographs (17-20). They can occasionally attain such a large size that they cause considerable opacification of a hemithorax in plain radiograph. More often they appear as solitary, often lobulated, well circumscribed, non calcified soft-tissue masses, either in the periphery of the hemithorax abutting a pleural surface or related to an interlobar fissure. They are often elongated and roughly lenticular, with the greatest dimension in the longitudinal plane. The surface adjacent to the chest wall may be relatively flatter than that abutting the lung parenchyma. Benign mesotheliomas often arise from the visceral pleura and are attached to the pleural surface by a pedicle. In such instances, they project freely into the pleural space, and changes in position and shape can be observed on inspiration and expiration radiographs and/or fluoroscopy (14,21,22). Pleural lesions form obtuse angles with the chest wall (23,24) but a gradually tapering interface of mass and chest wall to be a more reliable sign of pleural origin (17,18).

CT scan has several advantages by showing (1) displacement of adjacent lung parenchyma with

compressive atelectasis and bowing of the bronchi and pulmonary vessels around the mass, (2) a smoothly tapering margin at the junction of the mass with the pleura, (3) in pedunculated lesions, CT can exhibit changes in location and shape in the supine and prone positions, similar to changes observed on fluoroscopy (25), (4) with contrast enhancement, CT scan differentiate a fibrous mesothelioma abutting the mediastinum from an aortic aneurysm. The absence of fat excludes a diaphragmatic herniation that might contain omentum or gastrointestinal viscera, or a pleural lipoma, (5) CT can demonstrate invasion of the chest wall or infradiaphragmatic structures, a rare feature of fibrous mesothelioma.

Ultrasonography may help identify the diaphragm and its location with respect to the mass, when a large mesothelioma fills the inferior hemithorax and CT might not delineate the diaphragmatic interface (26).

Selective inferior phrenic, intercostal, and internal mammary arteriography may localize the mass by determining its blood supply and demonstrate large vascular pedicles and possible sites of vascular adhesion to the diaphragm or chest wall, which can be potential sites of bleeding at surgery (27).

A definitive diagnosis cannot be established by either percutaneous needle aspiration biopsy or cytology from pleural fluid (28). Thoracotomy is necessary for diagnosis, and wide local resection is the treatment of choice (29).

REFERENCES

1. Robertson HE. Endothelioma of the pleura. J Cancer Res 1924; 8: 317-375.
2. Klempere P, Rabin CB. Primary neoplasms of the pleura. A report of five cases. Arch Pathol 1937; 11: 385-412.
3. Shabanah FH, Sayegh SF. Solitary (localized) pleural mesothelioma. Chest 1971; 60: 558-563.
4. Briselli M, Mark EJ, Dickerson R. Solitary fibrous tumors of the pleura. Cancer 1981; 47: 2678-2689.
5. Kucuksu N, Thomas W, Exdinli EX. Chemotherapy of malignant diffuse mesothelioma. Cancer 1976; 37: 1265-1274.
6. Borow M, Conston A, livornese L, Schalet N. Mesothelioma following exposure to asbestos: A review of 72 cases. Chest 1973; 64: 641-646.
7. Scharifker D, Kaneko M. Localized fibrous "mesothelioma" of pleura (Submesothelial fibroma) A clinicopathologic study of 18 cases. Cancer 1979; 43: 627-635.
8. Benoit HW, Ackerman LV. Solitary fibrous mesotheliomas. J Thor Surg 1953; 28: 346-357.
9. Yousem SA, Flynn SD. Intrapulmonary localized fibrous tumor. Am J Clin Pathol 1988; 89: 365-369.
10. Briselli M, Mark EJ, Dickerson GR. Solitary fibrous tumors of pleura: eight new cases and review of 360 cases in the literature. Cancer 1981; 47: 2678-2689.
11. Dalton WT, Zolliker AS, McCaughey WTE, Jacques J, Kannerstein M. Localized primary tumors of the pleura. Cancer 1979; 44: 1465-1475.
12. Janssen JP, Wagennar SS, Van Den Bosch JMM, Vanderschueren RGJRA, Planteydt HT. Benign localized mesothelioma of the pleura. Histopathology 1985; 9: 309-313.
13. McCaughey WTE. Primary tumors of pleura. J Pathol Bac 1959; 76: 517-529.
14. Stout AP, Himadi GM. Solitary (localized) mesothelioma of the pleura. Ann Surg 1951; 133: 50-64.
15. Forter EA, Ackerman LV. Localized mesotheliomas of the pleura. Am J Clin Pathol 1960; 34: 349-365.
16. England DM, Hochholzer L, McCarthy MJ. Localized benign and malignant fibrous tumors of the pleura. Am J Surg Pathol 1989; 13: 640-658.
17. Dedrick CG, McLoud TC, Shepard JO, Shipley RT. Computed tomography of localized pleural mesotheolioma. AJR 1985; 144: 275-280.
18. Theros EG, Feigin DS. Pleural tumors and pulmonary tumors: differential diagnosis. Semin Roentgenol 1977; 12: 239-247.
19. Okike N, Bernatz P, Woolner LB. Localized mesothelioma of the pleura: benign and malignant variants. J Thorac Cardiovasc Surg 1978; 75: 363-370.
20. Taryle D, Lakshminarayan S, Sahn SA. Pleural mesotheliomas: an analysis of 18 cases and review of the literature. Medicine 1976; 55: 153-162.
21. Clagett OT, McDonald JR, Schmidt HW. Localized fibrous mesothelioma of the pleura. J Thorac Surg 1952; 24: 213-230.
22. Berne AS, Heitzman ER. The roentgenologic signs of pedunculated pleural tumors. AJR 1962; 87: 892-895.
23. Fraser RG, Pare JAP. Diagnosis of diseases of the chest, 2d ed vol 1. Philadelphia: Saunders, 1977: 591.
24. Hutchinson WB, Friedberg MJ. Intrathoracic mesothelioma. Radiology 1963; 80: 937-945.

25. Weisbrod GL, Yee AC. Computed tomographic diagnosis of a pedunculated fibrous mesothelioma. J Can Assoc Radiol 1983; 34: 147-148.
26. Doust BD, Baum JK, Maklad NF, Doust VL. Ultrasonic evaluation of pleural opacities. Radiology 1975; 114: 135-140.
27. Hahn PF, Novelline RA, Mark EJ. Arteriography in the localization of massive pleural tumors. AJR 1982; 139: 814-817.
28. Ratzer ER, Pool JL, Melamed MR. Pleural mesotheliomas. AJR 1967; 99: 863-880.
29. McCormack PM, Nagasaki F, Hilaris BS, Martini N. Surgical treatment of pleural mesothelioma. J Thorac Cardiovasc Surg 1982; 84: 834-842.

CYSTIC NEOPLASMS OF THE PANCREAS: CT AND SONOGRAPHY

Janjira JATCHAVALA[1], Sirintara PONGPECH[1],
Patchrin PEKANAN[1], Ratanaporn PORNKUL[1], Churirat KULARBKAEW[2].

ABSTRACT

Cystic neoplasms of the pancreas were pathologically divided into two major groups: microcystic adenomas and mucinous cystic neoplasms. Early diagnosis and differentiation from other pancreatic lesions were essential for appropriate management. Two cases of mucinous cystadenomas, one case of mucinous cystadenocarcinoma and one case of microcystic cystadenoma were presented and the sonographic and computed tomographic features were compared. The differential diagnosis were discussed.

Cystic neoplasms of the pancreas are relatively rare ; accounting for 5 to 15% of pancreatic cystic lesions and less than 5% of pancreatic tumors (1). Pancreatic cystic neoplasms are mainly classified into two categories, microcystic adenoma and mucinous cystic neoplasm (2,3). The mucinous cystic neoplams are subdivided into mucinous (macrocystic) cystadenoma and mucinous (macrocystic) cystadenocarcinoma. Preoperative diagnosis is important because microcystic cystadenoma is benign, thus asymptomatic case does not usually require surgical resection. Mucinous cystadenoma is potentially or overtly malignant.

We presented 4 cases of cystic neoplasms, including two mucinous cystadenomas, one mucinous cystadenocarcinoma and one microcystic cystadenoma. The purpose was to illustrate sonographic and computed tomographic findings of these tumors and assess the advantage of each modality. The differential diagnosis of the tumors from other pancreatic lesions were discussed.

CASE REPORTS

CASE 1.

A 18 year-old female presented with left upper abdominal pain radiating to left shoulder and back for 8 months. There was nausea without vomiting and no history of trauma. Upper G.I. series revealed a retrogastric mass (Fig. 1A). Sonogram showed a large cystic mass located in the tail of pancreas with thin septae throughout the mass, measuring $5 \times 5 \times 6$ cm. (Fig. 1B). CT scan showed a well defined mass with characteristic Hounsfied units in the range of water (Fig. 1C,D). The septations noted on sonography were difficult to appreciate. At surgery, the mass was removed along with the spleen. Gross specimen showed an irregular cavity about $4 \times 3 \times 3$ cm. in size, containing multiloculated thin-walled cysts about 2.5 cm. in diameter. The diagnosis was mucinous cystadenoma.

[1] Department of Radiology, Ramathibodi Hospital, Rama 6 Street, Bangkok 10400, Thailand.
[2] Department of Pathology, Srinagarin Hospital, Khon Kaen, Thailand.

CASE 2

A 32 year-old female presented with abdominal mass and dyspepsia for 2 months. An approximately 4 cm. in diameter, movable mass at mid epigastrium was noted on physical examination. Sonogram revealed a low echoic mass about 6 cm, in diameter at tail of pancreas with internal septations and slightly smooth thick wall (Fig. 2A). CT scan showed a cystic mass located between body and tail of pancreas, measuring 5×4 cm. There was pressure effect to inferior surface of left lobe liver (Fig. 2B,C). No lymphadenopathy or evidence of pancreatic tail atrophy was noted. At surgery, a well circumscribed cyst was found at the tial of pancreas. Distal pancreatectomy and splenectomy was performed. Gross specimen showed a multiloculated cyst about 4 cm. in largest diameter at posterior aspect of proximal part of pancreatic body. The inner surface of the wall was irregular with small areas of golden yellow soft tissue. Histology indicated mucinous cystadenoma.

CASE 3

A 40 year-old female presented with a movable, and tender left upper quadrant mass. It was progressively enlarged for 7 months. An IVP study showed a retroperitoneal mass displacing left kidney inferomedially (Fig. 3A). Sonogram revealed a large cystic mass in the tail of pancreas containing fine and homogeneous internal echoes (Fig. 3B). CT scan showed a well-circumscribed cystic mass, size about $10 \times 10 \times 9$ cm. Small mural projection was seen in the superior aspect of the mass (Fig. 3C,D). The patient underwent distal pancreatectomy and splenectomy. A cystic mass was found about 20-25 cm. in diameter. It contained chocolate-like content and papillary growth from its wall. The histology was mucinous cystadenocarcinoma.

CASE 4

A 75 year-old female, known case of Parkinsonism, presented with left upper abdominal

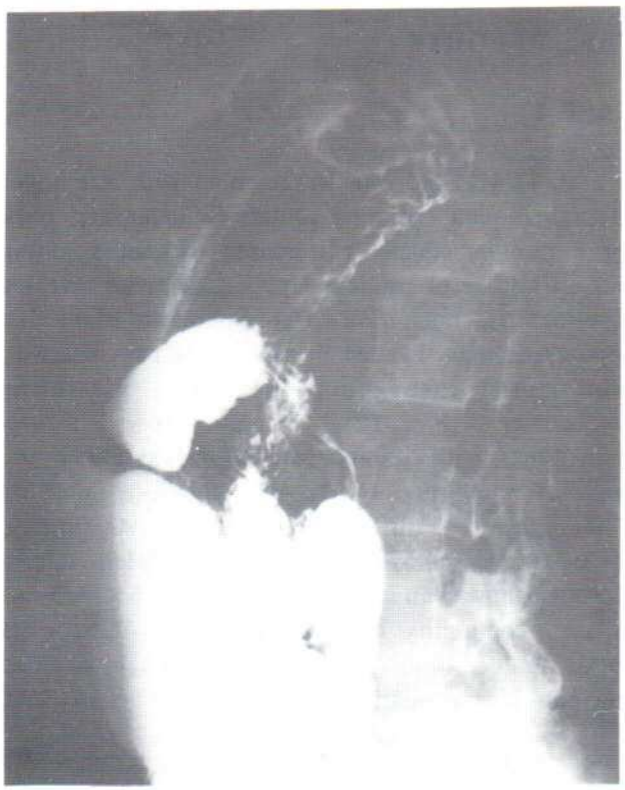

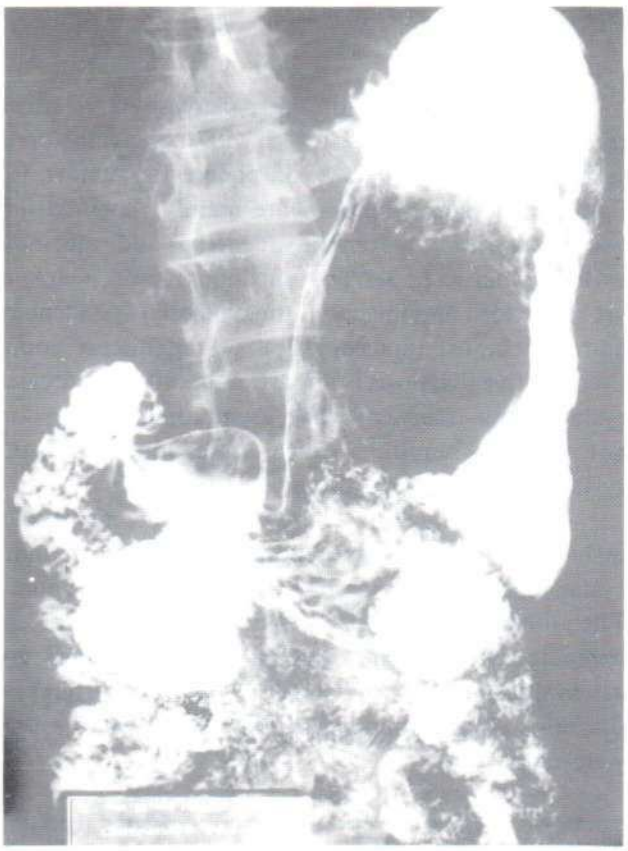

Fig. 1A Case 1 Mucinous cystadenoma. Upper GI series showed a large retrogastric mass.

mass for 6 months. She had weight loss and low grade fever. Sonogram revealed a large mixed echogenic solid mass about 9 cm. in diameter, located at an anteromedial aspect to left kidney and likely to continue with the tail of pancreas (Fig. 4A). Non-contrast CT scan showed a large, lobulated cystic mass about $8 \times 9 \times 6$ cm in size. with foci of central calcification. Contrast study demonstrated enhanced septations and rim enhancement. The origin could not be definitely determined, it might arise from the anterior pararenal space involving pancreatic tail and body, or mainly from the pancreas itself. The mass displaced the posterior wall of the stomach upward and the transverse colon downward (Fig. 4B,C). Gastroscope was normal. At surgery, there was a retroperitoneal mass about 15 cm. in diameter situated posterior to the lesser sac, adhering to the tail of pancreas. Distal pancreatectomy was performed. Gross specimen showed a large, multiloculated cystic mass, measuring $11 \times 8 \times 9$ cm. There were numerous small cysts separated by fibrous strands. The histologically verified a serous (microcystic) cystadenoma.

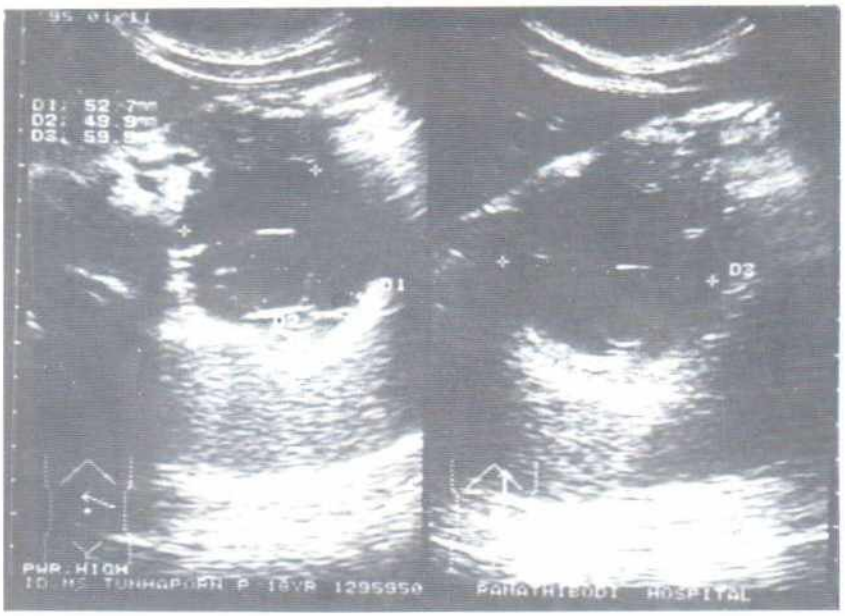

Fig. 1B Case 1 Ultrasound showed a large cystic mass located in the tail of pancreas with thin septae throughout the mass.

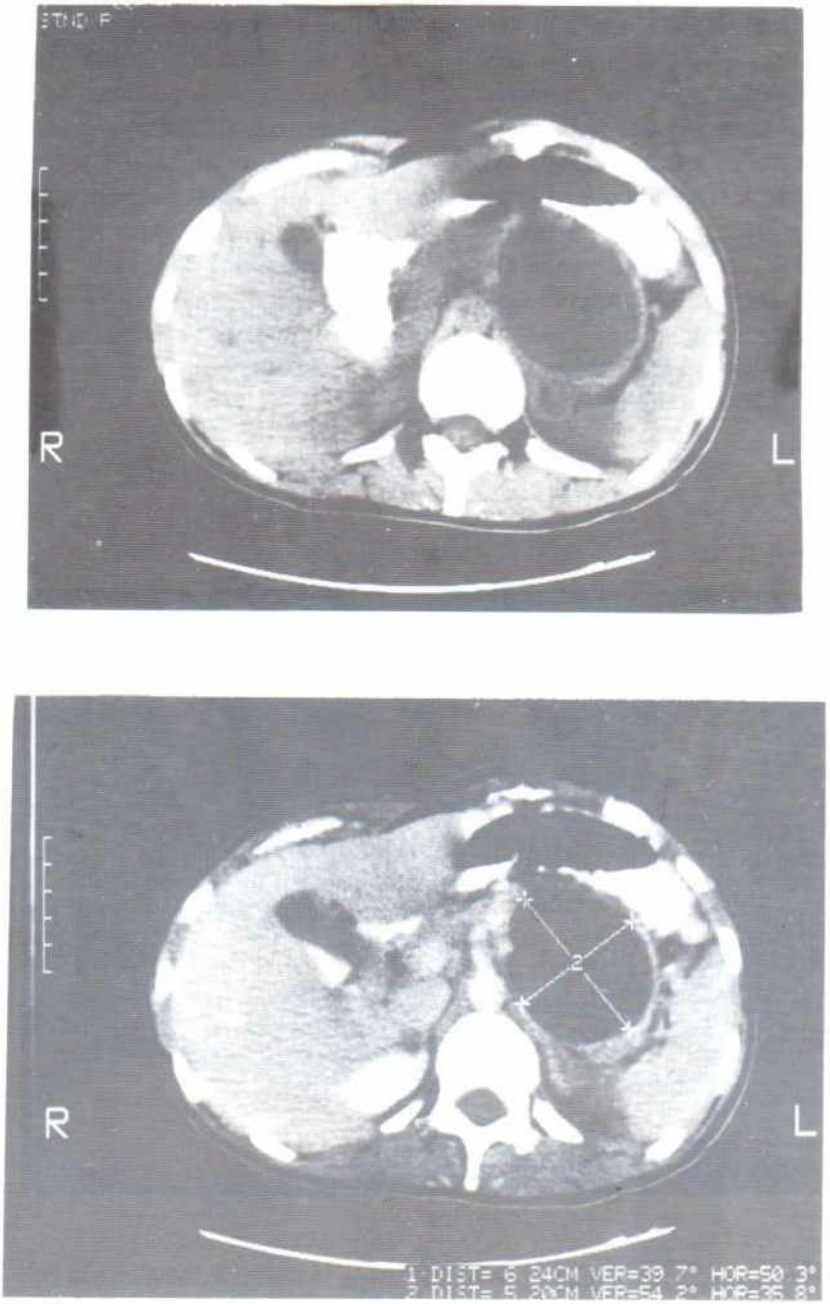

Fig. 1 C,D Case 1

C. Non-contrast CT scan showed a cystic mass at tail of pancreas

D. Contrast scan showed slightly enhanced wall, the septations were difficult to identify

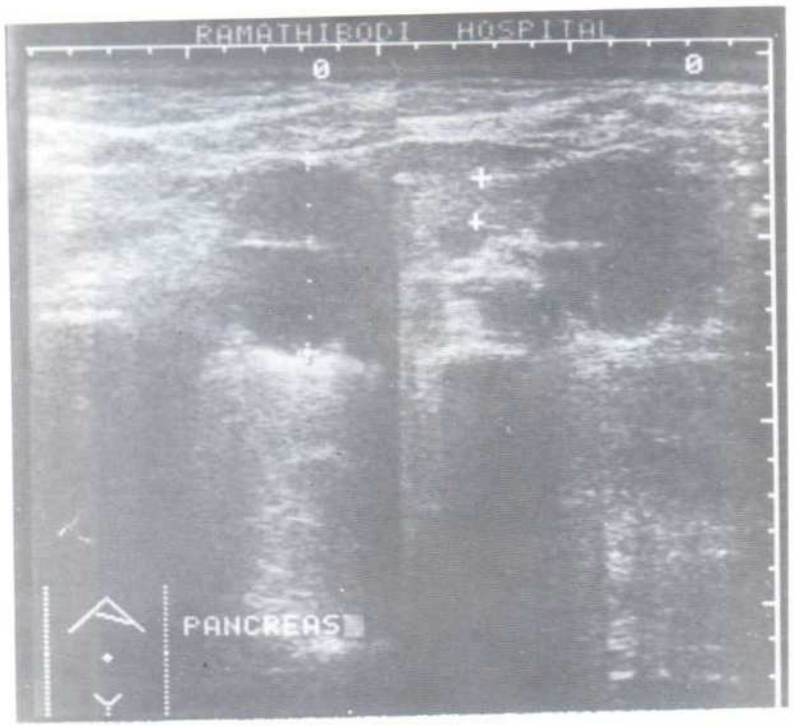

Fig. 2A Case 2 Mucinous cystadenoma
Sonogram showed a low echoic mass at the tail of pancreas with internal septations and slightly smooth thick wall.

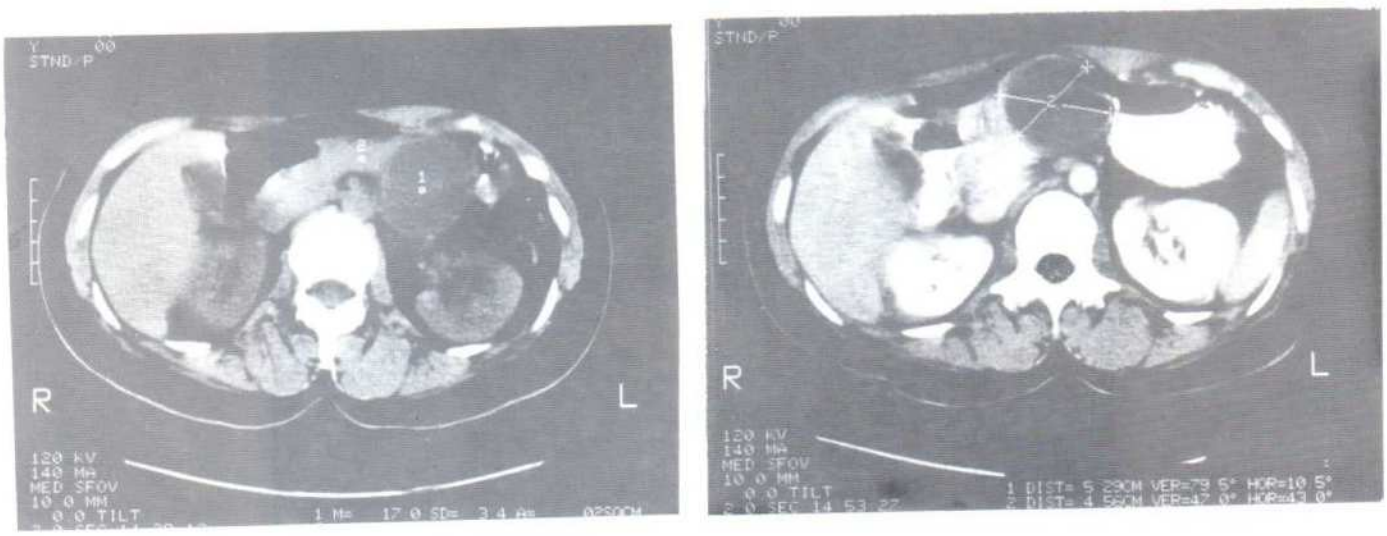

Fig. 2 B,C Case 2. B. Non-contrast CT scan showed a well defined cystic mass located between body and tail of pancreas.
C. Contrast study showed slightly enhanced wall. Septations was not seen.

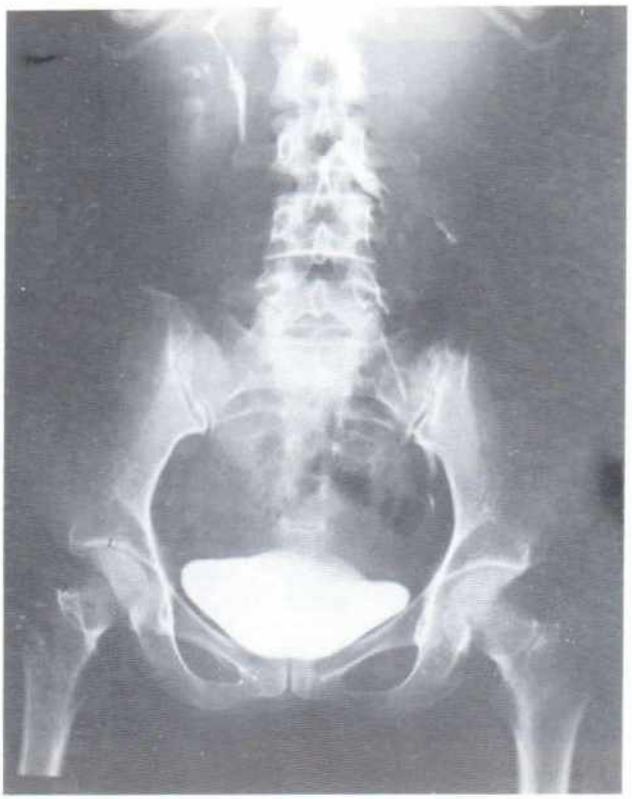

Fgi. 3A. Case 3. Mucinous cystadenocarcinoma IVP showed a large retroperitoneal mass displacing left kidney inferomedially.

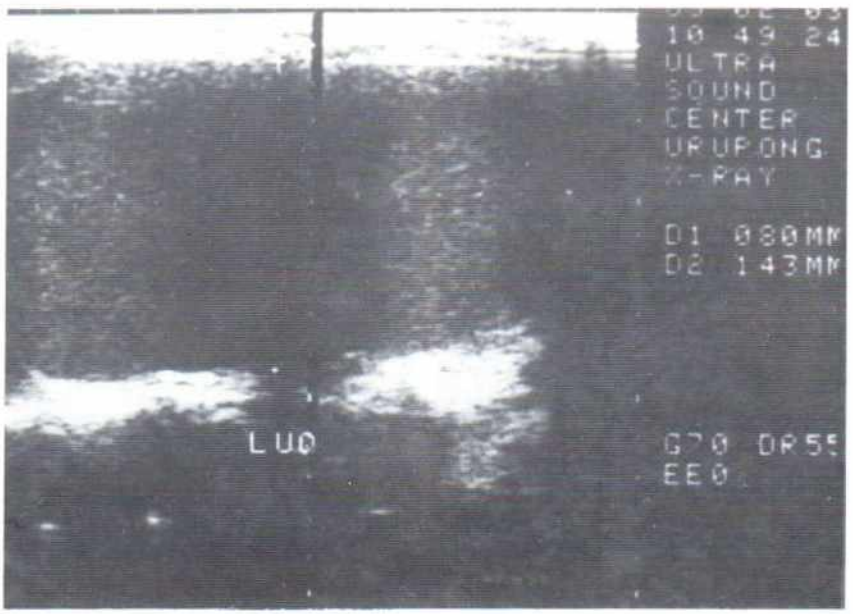

Fig. 3B Case 3. Sonogram showed a large cystic mass in the area of pancreatic tail. Homogeneous internal echoes were demonstrated.

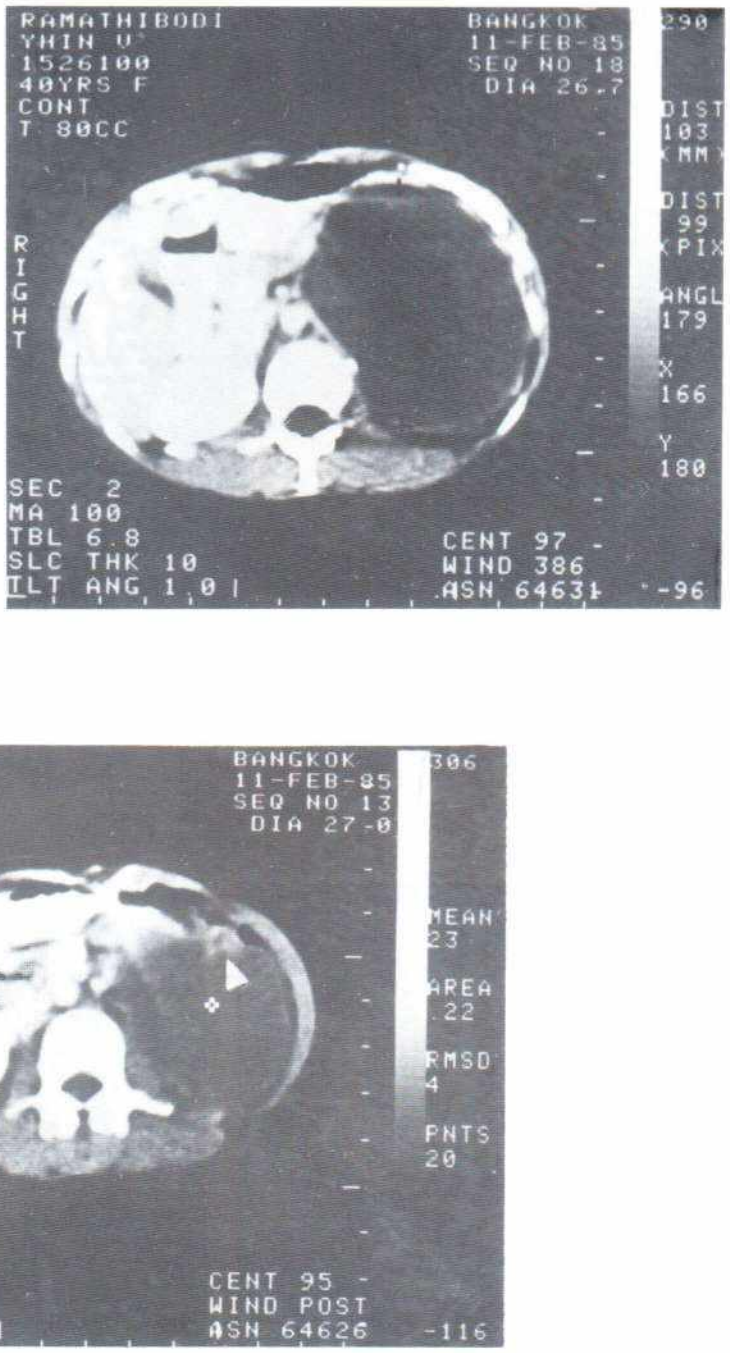

Fig. 3 C,D Case 3. Contrast study showed a cystic mass at the tail of pancreas. Small mural projection was seen at superior wall of the mass (arrowhead).

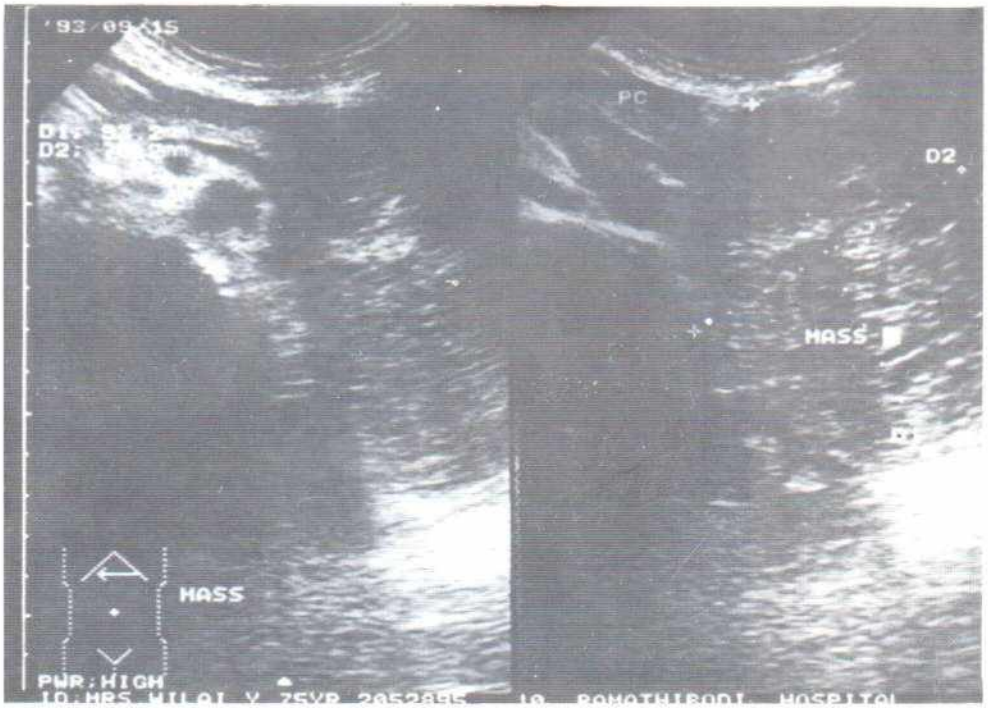

Fig. 4A Case 4 Microcystic cystadenoma.
A sonogram revealed a large mixed echogenic solid echo mass.

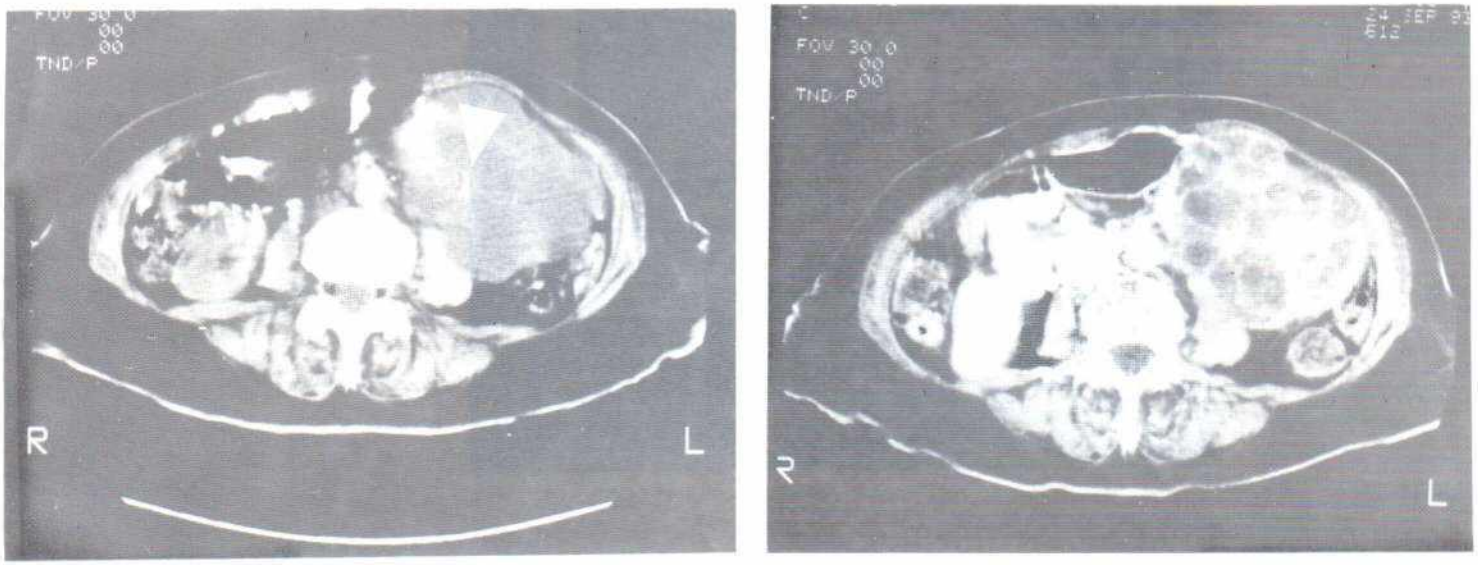

Fig. 4 B,C Case 4. B. Non-contrast study showed a large, lobulated cystic mass with foci of central calcification (arrow head)
C. Contrast study demonstrated enhanced septations and rim enhancement.

DISCUSSION

Compagno and Oertel classified the cystic pancreatic neoplasms into two groups; microcystic adenomas and mucinous cystic neoplasms, which include mucinous cystadenoma and mucinous cystadenocarcinoma (2,3).

The mucinous cystadenoma or cystadenocarcinoma typically was a smooth surfaced mass that was either unilocular or multilocular cysts more than 2 cm. in diameter and usually had dense fibrous walls with papillary projections. Their walls and septa sometimes had small calcification. The tumor prevailed in middle aged woman (average age 48 yrs., sex ratio 6:1) and located most frequently in the body and tail of pancreas (4-6). The lesion has a significant malignant potential. Surgical excision was the therapy of choice.

The microcystic adenomas typically had multiple (usually more than 6), small (usually less than 3 cm. in diameter) cysts. The tumor may contain a central stellate scar, sometimes associated with calcification (40% of cases) which was not seen in mucinous cystic neoplasm. The cysts contained glycogen-rich fluid. There was a 1.5:1 female predominance and occured in elderly patient (average 68 years). The tumor could originate from any location in the pancreas. (4-6). In asymptomatic patient, surgery may not be required.

The CT and sonographic appearance of the cystic neoplasms can be explained on the basis of the primary morphologic difference in these tumors.

In two cases of mucinous cystadenomas, the sonogram showed classic anechoic cysts with enhanced through transmission and internal septations. CT scan showed a well circumscribed water density mass. The internal septa were faintly seen in case 1 and was not seen in case 2. Thus sonogram was better than CT scan in demonstration of septations. In case 3, mucinous cystadenocarcinoma, sonogram showed a cystic mass with internal echoes which may represent debris or hemorrhage. Mural projection was demonstrated by CT scan. CT scan in most cystadenocarcinomas were usually similar to that of mucinous cystadenomas except when invasion to adjacent organs or distant metastases was present. (5,7).

In the case of microcystic cystadenoma, sonogram showed a large mixed echogenic solid appearing mass at the tail of pancreas. The explanation for solid appearance of this tumor was not clear, may be due to the extremely small size of the cysts (4). CT scan could obviously demonstrate calcification in the central stellate scar. The septa were markedly enhanced in contrast enhanced CT images, giving a honeycomb appearance.

A common differential diagnosis in these patients was pancreatitis with pseudocyst formation. Pseudocysts were unilocular, rounded masses whose wall was uniform in width and frequently located outside the pancreas and be found in patients with clinical and laboratory evidence of pancreatitis (8,9). Atypical pseudocysts containing hemorrhage and/or debris or those with septa or irregular wall might be difficult to distinguish from cystic tumor by sonogram (10). CT scan might be helpful by virtue of contrast enhanced solid portion of the tumor (11).

Pseudocysts or retention cysts might be found in associated with pancreatic cancer, they could simulate a cystic neoplasm (12). These cysts usually located between the solid tumor and the tail of pancreas. CT scan may show a solid mass consistent with pancreatic cancer and/or dilatation of the proximal pancratic duct. The presence of septa or daughter cysts along the wall of a large cyst favored cystadenocarcinoma.

Some solid pancreatic cancers may show areas of very low density caused by tumor necrosis (13). The low density areas were usually irregular in shape and small in size, in comparison with the solid portion of tumor.

Islet-cell carcinomas and leiomyosarcomas of adjacent organs which had undergone central necrosis may appear as a unilocular or multilocular cysts with thickened wall (14), but the degree of contrast enhancement of these tumors may be greater than that of cystic pancreatic neoplasms.

The rare cystic tumors such as congenital cyst and lymphangioma might be unilocular or multilocular occuring in infant (15). Patients with von Hippel-Lindau disease had multiple small pancreatic cysts along with an increased incidence of pancreatic carcinoma (16). Cystic lymphangioma of the pancreas was very rare. It was a benign tumor origination from lymphatic vessels. CT scan revealed a cystic, multiloculated mass which was indistinguishable from pancreatic cystadenoma (17).

In conclusion, a correct preoperative diagnosis of cystic pancreatic neoplasm should be possible by a combination of the sonogram and CT scan. Knowledge of their radiologic and pathologic features, analysis of the number and size of cysts, could successfully subtype the tumors into benign microcystic adenomas or potentially malignant mucinous cystadenomas or cystadenocarcinomas.

REFERENCE

1. Cubilla LA, Fitzgerald PJ : Classification of pancreatic cancer (nonendocrine). Mayo clin Proc 1979;54:449-458.
2. Compagno J, Oertel JE : Microcystic adenomas of the pancreas (glycogen-rich cystadenomas) A clinico-pathologic study of 34 cases. Am J Clin Pathol 1978;69:289-298.
3. Compagno J, Oertel JE : Mucinous Cystic Neoplasms of the pancreas with overt and latent malignancy (cystadenocarcinoma and cystadenoma). Am J Clin Pathol 1978;69:573-580.
4. Wolfman NT, Ramquist NA, karstaedt N, Hopkins MB. Cystic neoplasms of the pancreas: CT and sonography. AJR 1982;138:37-41.
5. Itai Y, Moss AA, Ohtomo K. Computed tomography of cystadenoma and cystadenocarcinoma of the pancreas. Radiology 1982;145: 419-425.
6. Frideman AC, Lichtenstein JE, Dachman AH. Cystic neoplasms of the pancreas: radiologic-pathologic correlation. Radiology 1983;149:45-50.
7. Johnson CD, Stephen HD, Charboneau JW. Cystic pancreatic tumors : CT and Sonographic Assessment. AJR 1988;151:113-1138.
8. Becker WF, Welsh RA, Pratt HS. Cystadenoma and cystadenocarcinoma of the pancreas. Ann Surg 1965;161:845-860.
9. De Santos LA, Bernardino ME, Paulus DD, Martin RE. Computed tomography of cystadenoma of pancreas. J Computed Assist Tomogr 1978;2:222-225.
10. Laing FC, Gooding GAW, Brown T, Leopold GR. Atypical pseudocysts of the pancreas: an ultrasonographic evaluation. JCU 1979;7:27-33.
11. Araki T, Ohtomo K, Itai Y, Lio M. Demonstration of septa in cystic lesions : comparison study of computed tomography and ultrasound. Clin Radio 1982;33:325-329.
12. Itai Y, Moss AA, Goldberg HI. Pancreatic cysts caused by carcinoma of the pancreas : a pitfall in the diagnosis of the pancreatic carcinoma. J Comput Assist Tomogr 1982;6:(4):772-776.
13. Kaplan JO, Ishifoff MB, Barkin J, Livingstone AS. Necrotic carcinoma of the pancreas: "the pseudo-pseudocyst". J Comput Assist Tomogr 1980;4:166-167.
14. Gold J, Rosenfield AT, Sostman D, Burrell M, Taylor KJW. Nonfunctioning islet cell tumors of the pancreas : radiographic and ultrasonographic appearances in two cases. AJR 1978; 131:715-717.
15. Mares AJ Hirsch M. Congenital cysts of the head of pancreas. J Pediatr Surg 1977;12:547-552.
16. Fill HL, Lamiell JM, Polk NO. The radiographic manifestation of von Hippel-Lindau disease. Radiology 1979;133:289-295.
17. Ignazio P, Emanuele S, Michele G, et al. Cystic Lymphangioma of the pancreas: CT Demonstration. J Comput Assist Tomogr 1985;9:209-213.

In Touch with Tomorrow

TOSHIBA

GLOBAL IMAGING ▪ MEDICAL SYSTEMS

Diagnostic Nuclear Medicine Systems

GCA-7100A/DI

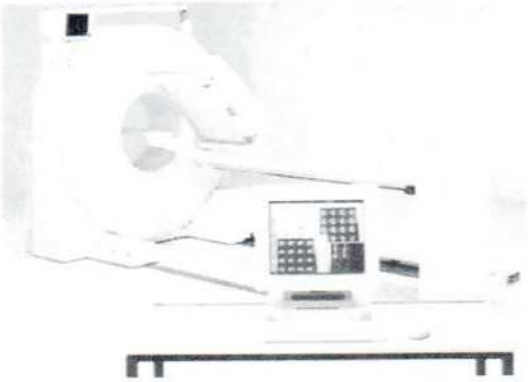

Dedicated to Progress in Health and Human Welfare

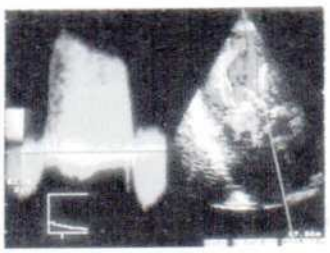

Power*vision*™

Diagnostic Ultrasound Systems

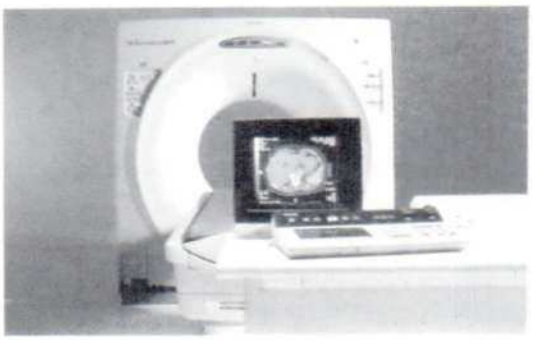

X-Ray Computed Tomography Systems

*X*vision GX

FLEX ART™

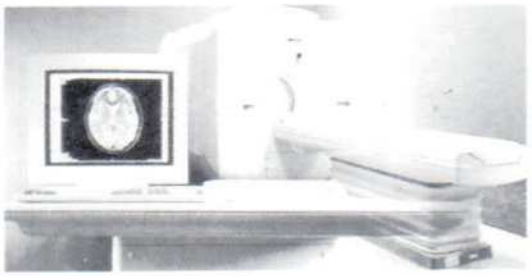

Magnetic Resonance Imaging Systems

CMC BIOTECH

CMC BIOTECH CO., LTD.

1433 Soi 3/3 Muban Town-in-Town Ladphrao 94 Road, Bangkapi Bangkok 10310 Tel. 530-4995-6, 559-3261-2 Fax. (662) 539-6903

North Eastern Branch :

301/155 Muban Khon Kaen Villa, Mittrapab Road, Amphur Muang Khon Kaen 40000 Tel. (043) 246210, 244729, Handphone 01-9283082 Pagephone 151, 152 call 341787

Southern Branch :

306 Prachayindee Road, Khorhing, Haadyai Songkhla 90110 Tel. (074) 356259, Handphone 01-9359703 Pagephone 151, 152 call 341790